

# Micromotion and fluid flow around cementless femoral components in total hip arthroplasty

THÈSE N° 7400 (2016)

PRÉSENTÉE LE 19 DÉCEMBRE 2016

À LA FACULTÉ DES SCIENCES ET TECHNIQUES DE L'INGÉNIEUR  
LABORATOIRE DE BIOMÉCANIQUE EN ORTHOPÉDIE  
PROGRAMME DOCTORAL EN MÉCANIQUE

ÉCOLE POLYTECHNIQUE FÉDÉRALE DE LAUSANNE

POUR L'OBTENTION DU GRADE DE DOCTEUR ÈS SCIENCES

PAR

Valérie Hélène Emilie Malfroy Camine

acceptée sur proposition du jury:

Prof. L. Laloui, président du jury  
Prof. D. Pioletti, Dr A. Terrier, directeurs de thèse  
Prof. N. Verdonschot, rapporteur  
Prof. Ph. Büchler, rapporteur  
Prof. S. Sakar, rapporteur



ÉCOLE POLYTECHNIQUE  
FÉDÉRALE DE LAUSANNE

Suisse  
2016



“Life is not easy for any of us. But what of that? We must have perseverance and above all confidence in ourselves. We must believe that we are gifted for something, and that this thing, at whatever cost, must be attained.”

- Marie Skłodowska-Curie





# Acknowledgements

First and foremost I would like to express my deepest gratitude to my thesis advisors Dr. Alexandre Terrier and Prof. Dominique Pioletti for their valuable guidance. The door of their office was always open whenever I ran into a trouble spot or had a question about my research. They consistently allowed this thesis to be my own work, but definitely provided me with the tools that I needed to steer in the right direction.

I would like to thank the rest of my thesis committee, Prof. Lyesse Laloui, Prof. Selman Sakar, Prof. Nico Verdonshot, and Prof. Philippe Büchler, for their insightful comments and suggestions, but also for letting my defence be an enjoyable moment.

The clinical aspects of this thesis were supervised by Dr. Hannes Rüdiger. He performed all the surgeries, arranged the collaborations with industrial partners and brought countless brilliant ideas and valuable comments about this research project. I'm very grateful to him for sharing his knowledge of the clinical world, and for always finding the time to answer my questions.

My sincere thanks goes to Prof. Gallaire, Dr. Martin Broome, and Dr. Joël Cugnoni, who reviewed my thesis proposal and made extremely valuable comments.

I highly acknowledge the EPFL, the Swiss National Science Foundation and the Swisslife Jubiläumsstiftung: without their financial support, this research wouldn't have been possible. I would also like to thank DePuy Synthes, who graciously offered the implants used in this study, along with the CAD files and the instrumentation set for implantation. I am grateful to Hughes Cadas from the Plateforme for Morphology Teaching at the Medical School (UNIL-CHUV) for providing the fixed cadaveric femurs that I used to develop the experimental setup described in Chapter 2. A big thanks also goes to Alejandro Dominguez from the Centre Universitaire Romand de Médecine Légale (UNIL-CHUV), for the help with the numerous CT-scans of the cadaveric femurs.

A very special thanks goes to the whole team of the mechanics workshop (ATME) for their support, for coffee breaks, and for precisely machining pieces for my setups: your work is invaluable. I am indebted in particular to Marc Jeanneret, for teaching me everything starting from technical drawing, and for always being available to help me when I broke a piece. If this project is a success, it's certainly thanks to you, and your love of a job well done. I don't think I will ever be able to tighten a screw without thinking of you and your wise advices: thank you for everything. A big thanks also to the team of the SV-Workshop for always being available to help me replace missing screws.

I thank Virginie Kokocinski, for dealing perfectly with all the administrative paperworks so I could focus on my research instead, and for her permanent smile and kindness. It was a real pleasure to work with you.

I owe a lot to the people who shared their knowledge and suggestions with me. I am forever indebted to Ulrike Kettenberger, for teaching me all she knew about micro-CT scanning, and for being my main intellectual sparring partner in this lab. She offered countless successful suggestions, insightful comments, and certainly helped me to bring this project to the best outcome possible. Thank you also for your support in tough moments. I'd also like to thank Miguel Gortchacow, Xabier Larrea, Philippe Abdel-Sayed, Salim Darwiche, and Arne Vogel, who offered insightful advices, comments, and suggestions on how to navigate this PhD journey, especially during the preparation of my thesis proposal. Finally, I'd like to thank Christoph Engelhardt, who mentored me during my master project at LBO, for being always here to share his knowledge in numerical modeling and for providing a great IT infrastructure to this lab.

I thank my fellow labmates for the stimulating discussions, and for all the fun we have had in the last five years. Thank you to: Patricia Scheuber, Sandra Jaccoud, Adeliya Latypova, Mohammadreza Nassajian, Jérôme Hollenstein, Anthony Groguz, Julien Ston, Tanja Hausherr, Francesc Levrero, Azadeh Khoushabi, Andreas Schmocker, Valérie Parvex, Caroline Fernandes, Antoine Dewarrat, Maïka Guillemin, Raphaël Obrist, Naser Nasrollahzadeh Mamaghani, Jens Antons, Yasmine Meharzi, Davide Cuttica, Claire Delabarde and Peyman Karami.

A special thanks goes to my students: Valérie Parvex, Sandra Gribi, Louis Clavel, Denis Stauffer, Maider Gisasola, Madge Martin and Céline Wyss. You were all a great source of inspiration, and your projects contributed to make this thesis successful.

Thank you to Caroline Baer and Thomas Foetisch, my friends fellow PhD students at EPFL, for the coffee breaks or lunch breaks where we shared the ups and downs of the daily PhD

life. A huge thanks to Romain Lauper and Stéphanie Cherbuin, for regularly reminding me that life is also great outside of academia. Thank you also to Gwennaëlle Monnot, for her support in the last weeks of the PhD: you made me smile and gave me the courage I needed to complete the writing.

A huge thanks to my friends and family for all the fun times we shared. Your encouragement and support carried me through this journey.

I must express my very profound gratitude to my parents for providing me with unfailing support and continuous encouragement throughout the process of researching and writing this thesis. Words cannot express how grateful I am for your education and all of the sacrifices that you've made on my behalf. This accomplishment would not have been possible without you. Thank you.

Finally, I would like to express my deepest gratitude to Christian Mounir. Thank you for being my partner, with shared risks and profits, and for sailing with me through both PhD and life journeys. Thank you for understanding the late nights and weekends working, for supporting me during the intense last months of thesis writing, and for your constant trust, patience and love through high tide and low tide.



# Résumé

L'arthroplastie totale de la hanche est une opération qui permet de soulager efficacement les douleurs et de restaurer la mobilité de l'articulation chez les patients souffrant d'arthrose sévère. Cependant, malgré les récentes avancées techniques dans le développement des implants non-cimentés, entre 5% et 10% des tiges fémorales sont révisées dans les 15 ans qui suivent l'implantation. Les opérations de révision des prothèses de hanche offrent des résultats moins convaincants, et sont associées à des séjours hospitaliers plus longs que les arthroplasties primaires. La principale cause de révision des tiges fémorales non-cimentées est le descellement aseptique de la prothèse. Les mécanismes qui conduisent à cette situation complexes, mais il est généralement reconnu que l'environnement mécanique initial joue un rôle critique. En particulier, les micro-mouvements et l'écoulement de fluide à l'interface os-implant ont été directement reliés au descellement aseptique. Dans cette thèse, ces deux aspects ont été estimés localement à l'aide de méthodes expérimentales et numériques.

Tout d'abord, une technique pour mesurer les micro-mouvements locaux autour des tiges fémorales en métal a été développée. Cette technique se base sur l'imagerie microtomographique (micro-CT) de marqueurs radio-opaques, et s'est révélée très fiable. La première cartographie des micro-mouvements autour d'une tige fémorale non-cimentée a pu être générée. Cette technique offre des perspectives prometteuses dans le domaine des tests pré-cliniques d'implants, et ouvre la voie vers la validation d'outils de planification pré-opératoires spécifiques au patient.

Par la suite, cette technique a été utilisée pour comparer la stabilité initiale de tiges fémorales avec ou sans collerette. Les micro-mouvements locaux ont été mesurés dans deux groupes de fémurs cadavériques implantés avec l'une ou l'autre version de la tige. Nous n'avons pas trouvé de différence significative de stabilité primaire entre des tiges fémorales avec ou sans collerette.

Enfin, un modèle poroélastique de l'interface os-implant autour d'une tige fémorale a été

développé. Le modèle simulait les mouvements de fluide dus aux micro-mouvements de la tige, à partir de mesures locales des micro-mouvements obtenues avec la technique basée sur l'imagerie micro-CT développée précédemment. Le modèle a permis d'obtenir la distribution des vitesses du fluide dans le tissu de granulation et dans l'os autour de l'implant. Nous avons pu en déduire la gamme des contraintes de cisaillement auxquelles les cellules situées dans ces tissus sont soumises. Ces résultats pourraient être utilisés pour tenter de relier les stimuli mécaniques imposés aux cellules dans l'espace os-implant à la réponse cellulaire observée *in vitro* en présence d'écoulement de fluide.

En raison du vieillissement de la population et de l'augmentation continue des arthroplasties chez les jeunes patients, l'amélioration de la survie à long terme des implants non-cimentés est devenue un enjeu majeur du domaine de l'orthopédie. Cette thèse propose des outils qui peuvent mener à un prolongement de la durée de vie des implants, ainsi qu'à une meilleure connaissance des mécanismes à l'origine du descellement aseptique, réduisant d'autant la nécessité de recourir à des révisions couteuses.

Mots-clés: arthroplastie de la hanche; tiges fémorales non-cimentées; micro-mouvements; écoulement de fluide; interface os-implant

# Abstract

Cementless total hip arthroplasty is a highly successful and reliable procedure to restore joint function and reduce pain in patients with severe osteoarthritis. Nevertheless, despite the technical advances over the last decades in the development of cementless implants, between 5 % and 10% of cementless femoral components have been revised at 15-year follow-up. Revision procedures are less successful, require longer hospital stays, and are associated with higher mortality rates than primary procedures. The main cause for revision of cementless femoral components is aseptic loosening. The mechanisms behind aseptic loosening remain unclear, but the initial local mechanical environment is thought to be critical. In particular, both excessive micromotion and fluid flow at the bone-implant interface during early peri-implant healing have been related to aseptic loosening. In this thesis, micromotion was measured *in vitro* and fluid flow was predicted from measured micromotion using numerical modeling. The thesis is divided into three studies.

First, a micro-computed tomography (micro-CT) based technique using radiopaque markers to measure full-field local implant micromotion around metallic cementless stems was developed. The technique was highly reliable, with a bias and repeatability similar to that of linear variable differential transformers (LVDTs), which are the current gold standard for micromotion measurement. It provided the first full-field map of micromotion around a cementless femoral stem. This technique offers promising developments in the area of pre-clinical testing of orthopedic implants, and paves the way towards the validation of patient-specific preoperative planning tools.

Then, the developed micro-CT technique was used to compare the primary stability of the collared and collarless versions of the same cementless femoral stem. Local micromotion was measured in two groups of cadaveric femurs implanted with either version of the stem. We found no significant difference in primary stability between collared and collarless stems for activities of daily living.

Finally, a poroelastic finite element model of the initial bone-implant interface around a cementless stem was developed. The model predicted micromotion-induced fluid flow based on local micromotion determined experimentally with the micro-CT based technique. We obtained the distribution of fluid velocity in the granulation tissue between the implant and bone, and within the bone that surrounds the implant. From fluid velocity, we inferred the range of shear stress experienced by the cells hosted in each tissue. These results offer new prospects to understand the interplay between mechanical and biological aspects that leads to aseptic loosening. Indeed, the mechanical stimuli experienced by cells in the peri-implant space could be related to results obtained *in vitro* with cells cultured in flow chambers.

With the aging population and the continual increase of arthroplasties in young patients, improving the long-term success of cementless implants is becoming a major challenge for the orthopedic community. This thesis proposed tools that can lead to improvements of implants survival, and a better understanding of the mechanisms behind aseptic loosening, reducing the need for implant revisions and their associated social and financial burden.

Keywords: total hip arthroplasty; cementless femoral stems; micromotion; fluid flow; bone-implant interface



# Contents

<b>Acknowledgements</b>	<b>i</b>
<b>Résumé</b>	<b>v</b>
<b>Abstract</b>	<b>vii</b>
<b>List of figures</b>	<b>xi</b>
<b>List of tables</b>	<b>xiii</b>
<b>1 Introduction</b>	<b>1</b>
<b>2 Full-field micromotion measurement around cementless femoral stems</b>	<b>23</b>
<b>3 The effects of a collar on the primary stability of cementless femoral stems</b>	<b>41</b>
<b>4 Micromotion-induced fluid flow around a cementless femoral stem</b>	<b>57</b>
<b>5 Conclusions and perspectives</b>	<b>77</b>
<b>A Supplementary material to Chapter 2</b>	<b>87</b>
<b>B Supplementary material to Chapter 3</b>	<b>89</b>
<b>C Supplementary material to Chapter 4</b>	<b>91</b>
<b>D Bibliography</b>	<b>97</b>
<b>E Curriculum Vitae</b>	<b>111</b>



# List of Figures

1.1	Total hip replacement procedure . . . . .	2
1.2	Temporal changes in percentages of each fixation method used in primary hip arthroplasties . . . . .	3
1.3	The four stages of bone healing around cementless implants . . . . .	5
1.4	Summary of proposed causes for aseptic loosening of cementless implants . . .	7
2.1	Experimental setup . . . . .	27
2.2	Image processing and micromotion computation . . . . .	29
2.3	Bias and repeatability estimation protocols . . . . .	30
2.4	Normal, tangential, and absolute micromotion measured around a cementless femoral stem . . . . .	32
2.5	Distribution of normal, tangential, and absolute micromotion in compression and torsion by zone of the femoral stem . . . . .	34
3.1	Collarless and collared versions of the straight cementless femoral stem . . . .	45
3.2	Loading devices designed to fit inside the micro-CT scanner . . . . .	46
3.3	Subsidence and micromotion computation . . . . .	47
3.4	Subsidence of collarless and collared stems . . . . .	48

3.5	Sample distribution of absolute micromotion around one collarless stem and one collared stem . . . . .	50
3.6	Distribution of absolute, normal, and tangential micromotion in compression by Gruen zone around collarless and collared stems . . . . .	51
3.7	Distribution of absolute, normal, and tangential micromotion in torsion by Gruen zone around collarless and collared stems . . . . .	52
4.1	Geometry of the idealized model . . . . .	62
4.2	Assembly of geometry for the 2D representative transverse sections and the simplified 3D model . . . . .	64
4.3	Distribution of micromotion-induced interstitial fluid absolute velocities at representative transverse sections of the bone-implant interface . . . . .	67
4.4	Distribution of micromotion-induced interstitial fluid velocities in the granulation tissue and trabecular bone around a simplified cementless femoral stem . . . . .	69
A.1	Gap measured around the cementless femoral stem . . . . .	88
C.1	Distribution of implant micromotion measured experimentally and used as boundary conditions . . . . .	95

# List of Tables

2.1	Reliability assessment of Micro-CT based measurement of micromotion . . .	31
2.2	Minimum, maximum, and median micromotion along the different anatomical axis for compression and torsion . . . . .	33
4.1	Sensitivity study: full-factorial design factors and levels . . . . .	61
4.2	Poroelastic material properties used in the model . . . . .	62
4.3	ANOVA for the full factorial design . . . . .	66
B.1	Donor information . . . . .	90
C.1	Number of mesh elements and degrees of freedom (DOF) for each model . . .	94



# Chapter 1

## Introduction



## Total hip arthroplasty

Total hip arthroplasty (THA) is a very successful treatment option for patients suffering from severe osteoarthritis (Learmonth et al., 2007). The degenerated articular surfaces are replaced by a femoral and an acetabular components (Fig. 1.1), reducing hip pain significantly and restoring joint function (Ethgen et al., 2004). The femoral component is generally composed of a metallic femoral stem fitted with a metallic or ceramic femoral head, while the acetabular component is commonly made of a metallic shell associated with a polyethylene, metal or ceramic liner. With the ageing population, the number of hip arthroplasties is increasing regularly every year, reaching a total of 655'000 in 2011 in OECD countries, which represents 210 procedures per 100'000 inhabitants (Pabinger et al., 2014).

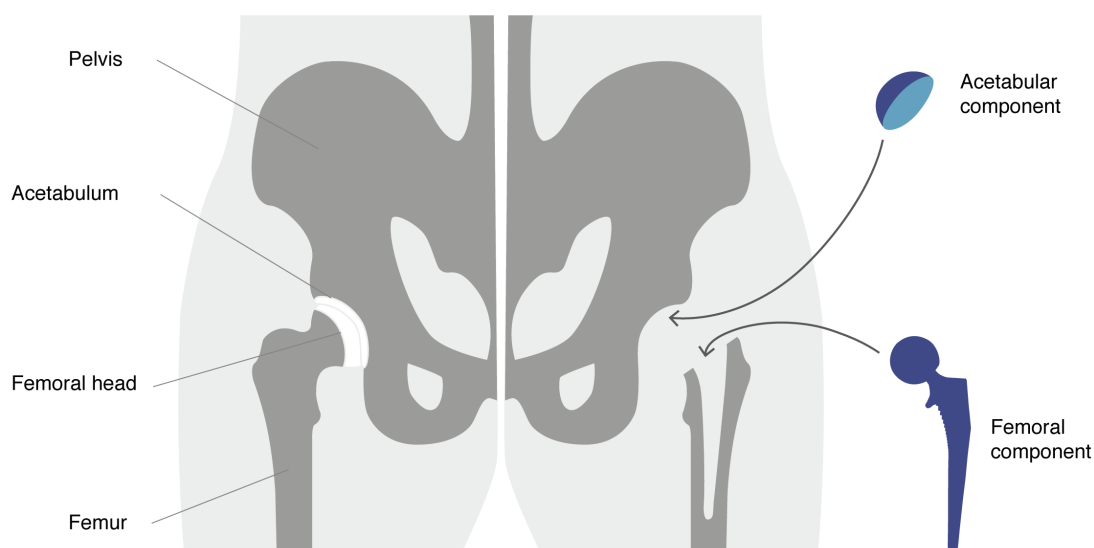


**Figure 1.1:** Total hip replacement procedure - The femoral head is resected and the medullary canal is shaped to fit the femoral component. The damaged cartilage of the acetabulum is removed and replaced by the acetabular cup.

Patients younger than 70 years old are now encountered frequently, accounting for more than half of the patient population. This represents an important change to the initial patient demographics (Pabinger et al., 2014), and a big challenge for the orthopaedics research community. Indeed, younger patients are more active and require earlier revision of their implants (Australian Orthopaedic Association National Joint Replacement Registry, 2015). However, revision procedures have a much lower rate of success: implant failures and complications are more common (Ong et al., 2010), and the associated mortality rates (Issa et al., 2013) and healthcare costs (Vanhegan et al., 2012) are much higher than for primary arthro-



plasties. As a result, the focus of hip arthroplasty research has moved to the enhancement of the long-term success of the primary procedure, especially in the younger and more active patients.

Two types of fixation coexist for both acetabular and femoral components: cemented and cementless. Cemented implants achieve initial fixation by filling the bone-implant gap with a cement layer, while cementless implants are press-fitted in the bone cavity. Cemented approaches were privileged until very recently (Fig. 1.2). The rising number of young patients, active, and highly susceptible to require a revision of their hip implant has changed this paradigm. Indeed, the revision rates are higher with cemented implants in young patients (Australian Orthopaedic Association National Joint Replacement Registry, 2015; Pedersen et al., 2014). Moreover, revisions of cemented implants are excessively complicated, because of the difficulties arising when the surgeon needs to remove the cement mantle. On the other hand, progresses made in the last decades with porous coatings and implant design lead to cementless implants having similar long-term outcomes to those of cemented implants (Hooper et al., 2009; Wyatt et al., 2014). As a consequence, cementless implants are now the preferred type of fixation for young patients (Australian Orthopaedic Association National Joint Replacement Registry, 2015).

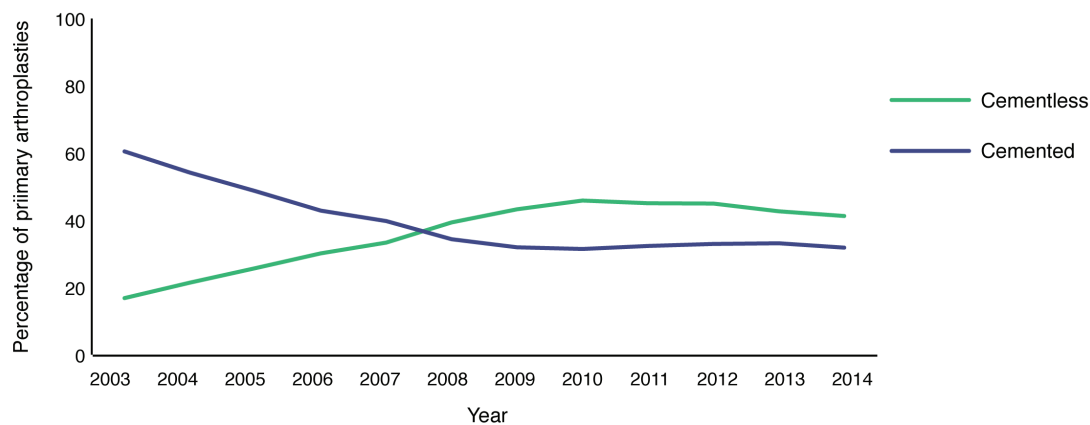


**Figure 1.2:** Temporal changes in percentages of each fixation method used in primary hip arthroplasties (National Joint Registry for England, Wales, Northern Ireland and the Isle of Man, 2015).

Despite all these efforts, the short and long-term survival of cementless implants is limited by aseptic loosening, which is the main cause for revision (Wyatt et al., 2014). The loosening of the bond between the implant and the bone results in pain and disability for the patient, ultimately precipitating the revision of the implant. The conditions that lead to aseptic loosening are multi-factorial and include mechanical and biological causes. The relative contributions

and probable synergistic effects between these elements remain poorly understood. However, multiple studies have shown, that even though aseptic loosening can occur long after the arthroplasty, it is closely linked to the conditions and events that take place during the early phases of peri-implant healing (Kärrholm et al., 1994; Mjöberg, 1994).

## **Bone healing around cementless implants**

The fixation of cementless implants in bone is achieved through osseointegration. The term "osseointegration" designates the direct mechanical interlock that forms between the host bone and the implant surface (Carlsson et al., 1986). Peri-implant healing around cementless implants is an intramembraneous process, where bone is formed directly without going through an intermediate cartilage phase (Davies, 2003; Raghavendra et al., 2005; Terheyden et al., 2011). It can be divided into four stages (Fig. 1.3).

The first stage is the bleeding phase and lasts up to a few hours following implantation. Following the damages to the blood vessels because of the surgical trauma, a hematoma forms around the implant. Blood plasma, leucocytes and platelets are released in the peri-implant space and a protein layer including fibronectin and fibrinogen deposits on the implant surface.

The second stage lasts from a few hours up to a few days and is the inflammatory phase. During this phase, the hematoma coagulates through the action of activated platelets to form a blood clot at the bone-implant interface. The blood clot provides a structural matrix whose main component is fibrin. A number of inflammatory factors are released in the peri-implant space and macrophages are recruited to clean tissue and cell debris.

The proliferative phase lasts from a few days up to several weeks. Following the release of signaling molecules in the peri-implant space, mesenchymal stem cells are recruited and migrate to the fibrin clot. Mesenchymal stem cells (MSCs) are multipotent adult stromal cells that have the ability to differentiate into different cell types, including osteoblasts, chondrocytes or adipocytes (Uccelli et al., 2008). Simultaneously, the process of angiogenesis to generate new blood vessels is initiated, and fibroblasts from the surrounding healthy tissues migrate to the blood clot. These fibroblasts secrete extracellular matrix proteins, and the fibrin clot becomes a new vascularized connective tissue that hosts the MSCs: the granulation tissue. A variety of osteogenic growth factors are released in the granulation tissue, and control the fate of the MSCs toward the osteogenic lineage. The differentiation of MSCs into osteoblasts that synthesize the bone matrix leads to the formation of woven bone at the bone-implant interface. Woven bone is an immature form of bone, in which the collagen

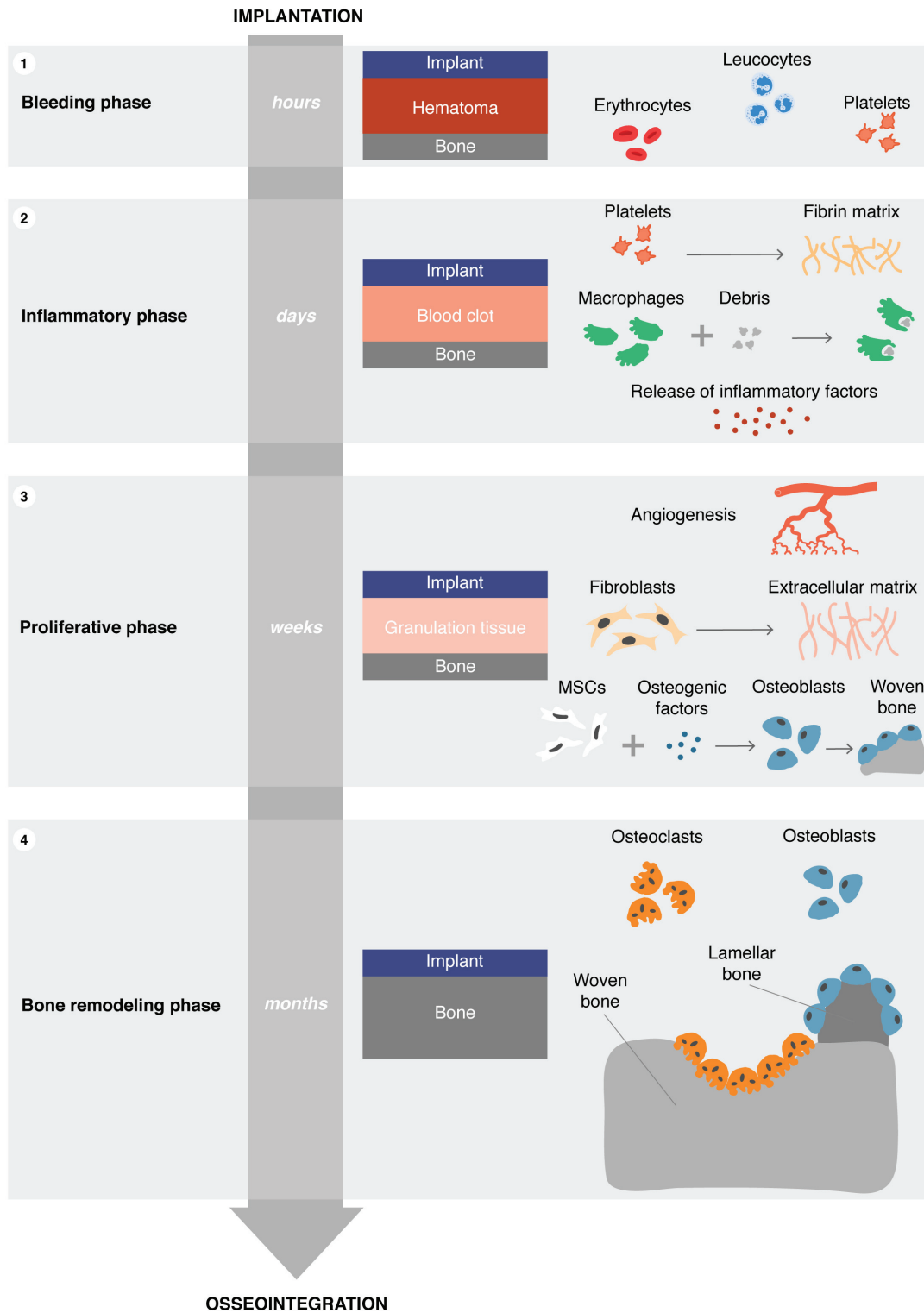


**Figure 1.3:** The four stages of bone healing around cementless implants.

fibers are arranged randomly.

The last stage of cementless peri-implant healing is the bone remodeling phase, which can last up to several months. Bone remodeling is a continuous process through which bone is resorbed by osteoclasts, and new bone is formed by osteoblasts. The bone that forms following remodeling is called lamellar bone, because of the parallel orientation of its collagen fibers. Following Wolff's law (Wolff, 2010), the newly formed bone is oriented to sustain the loads to which the implant is subject. The bone remodeling phase continues until all the woven bone has been replaced with lamellar bone.

### **Aseptic loosening of cementless implants**

Aseptic loosening is a complication of cementless arthroplasties that is defined by the failure of the implant mechanical fixation in the absence of infectious causes. It is characterized by the presence of a fibrous tissue layer at the bone-implant interface, and the subsequent formation of areas of peri-implant osteolysis. The process can occur early, in the absence of initial osseointegration of the implant, as well as several years after the implantation despite the initial osseointegration of the implant (Abu-Amer et al., 2007).

The underlying causes behind aseptic loosening are uncertain. Early implant migration in the year following the arthroplasty was associated with aseptic loosening up to seven years later, suggesting that loosening arises from conditions encountered during the early phases of peri-implant healing (Kärrholm et al., 1994). Multiple theories about the origins of aseptic loosening have been proposed over the years (Fig. 1.4), from biological causes like inflammatory response to wear particles or individual genetic variations, to mechanical causes like excessive implant micromotion or high fluid pressure and flow in the joint space (Sundfeldt et al., 2006).

Wear particles were one of the first proposed explanation for aseptic loosening of implants. It was driven by the observation of an inflammatory response in the tissues surrounding loosened implants, and of polyethylene and metal particles in histological sections of the bone-implant interface (Willert et al., 1996). It is thought that macrophages are recruited to eliminate those wear particles through phagocytosis, and that in the process, they release inflammatory factors. The release of these factors initially triggers the formation of interfacial fibrous tissue, and then activates the recruitment of more macrophages and osteoclasts to the bone-implant interface, contributing to peri-implant osteolysis (Beck et al., 2012; Ollivere et al., 2012). However, the theory has been disputed, since in animal experiments where polyethylene wear particles were injected into the joint space of osseointegrated implants,

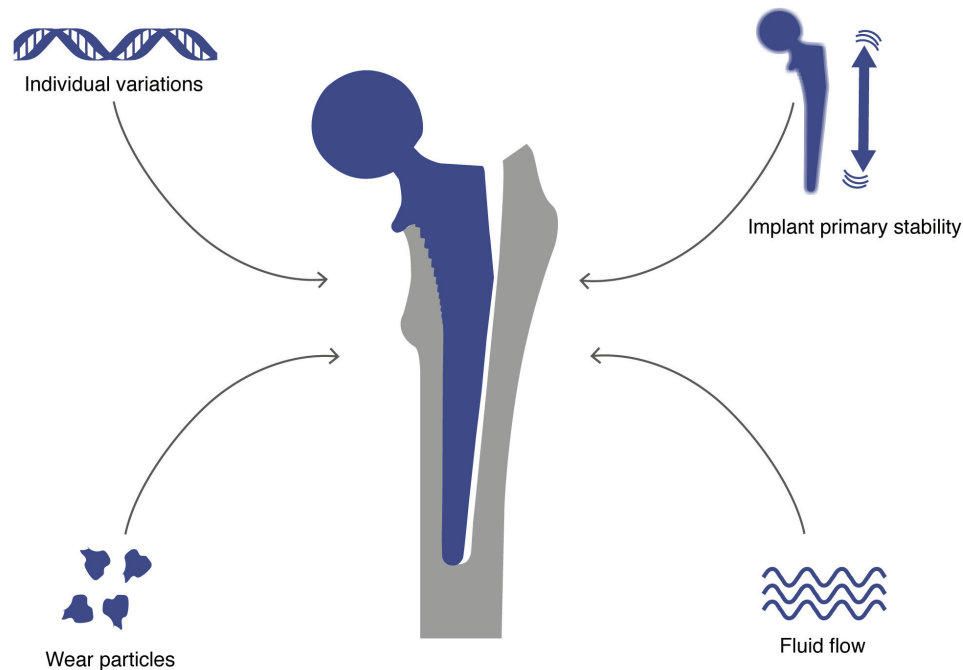


**Figure 1.4:** Summary of proposed causes for aseptic loosening of cementless implants.

no biological or mechanical reactions were observed (Aspenberg et al., 1996; Sundfeldt et al., 2002). Therefore, though wear particles probably participate to aseptic loosening, they do not seem to be sufficient to trigger an inflammatory response and osteolysis (Sundfeldt et al., 2006).

Individual genetic variations were recently proposed to also play a role, especially in the inflammatory response to wear particles. Macrophages from different patients were exposed to polyethylene wear particles, and important variations in the inflammatory response of the macrophages from the different donors were observed (Matthews et al., 2000b; Matthews et al., 2000a).

The primary stability of implants is another element that was identified as a possible cause for aseptic loosening. Primary stability of cementless implants designates the stability of the implant directly after the operation, as opposed to the secondary stability, which describes the stability of the implant after osseointegration is achieved. The primary stability is characterized by the relative motion between the bone and the implant that takes place when the implant is loaded. A study of *postmortem* cementless femoral stem retrievals found that osseointegrated implants experienced peak micromotion of  $40\ \mu\text{m}$ , whereas in one case of failed bone ingrowth, the implant encountered micromotion of  $150\ \mu\text{m}$  (Engh et al., 1992).

Furthermore, in animal experiments where implants were subjected to different levels of micromotion, small levels of micromotion below 40  $\mu\text{m}$  resulted in osseointegration of the implant, while higher level of micromotion lead to the formation of interfacial fibrous tissue and failed bone ingrowth (Jasty et al., 1997; Pilliar et al., 1986; Søballe et al., 1992). Finally, studies that combined implant micromotion with wear particles found out that wear particles alone did not have any effect on osseointegration, but micromotion with or without the presence of wear particles lead to the formation of fibrous tissue. When implant micromotion was stopped, fibrous tissue resorbed and bone ingrowth was observed in the particle-free group but the fibrous tissue persisted in the presence of wear particles (Aspenberg et al., 1996). This study suggests that excessive implant micromotion could initiate the process of aseptic loosening, while wear particles could play a role in the later stages.

Fluid flow and fluid pressure were also proposed to be an important aspect in aseptic loosening (Aspenberg et al., 1998; Nam et al., 2013). The bone and soft tissues that surround the implant are saturated with interstitial fluid. Loading of the implant and associated micromotion leads to the deformation of the tissues surrounding the implant, generating changes in fluid pressure (Hendrix et al., 1983) and fluid flow. Increased fluid pressure was observed in the joint capsule of patients with loosened hip implants (Robertsson et al., 1997). The local application of high fluid pressure at the interface of osseointegrated implants in rabbits lead to local peri-implant osteolysis and aseptic loosening (Vis et al., 1998b; Vis et al., 1998a). In another animal experiment, it was shown that the areas of osteolysis were mainly located around existing bone cavities, where the fluid pressure is lower and the fluid flow higher, hereby suggesting that high fluid flow at the bone-implant interface is a potential explanation for aseptic loosening (Fahlgren et al., 2010). The mechanisms through which fluid flow and fluid pressure could cause osteolysis remain unresolved, but several hypotheses have emerged. One of them is the activation of osteoclasts following the application of fluid pressure: *in vitro* experiments showed that macrophages subject to fluid pressure released inflammatory factors that activate osteoclasts (Ferrier et al., 2000). On the other hand, mesenchymal stem cells have been shown to be responsive to both fluid pressure (Haudenschild et al., 2009; Steward et al., 2014; Wagner et al., 2008) and fluid flow (Arnsdorf et al., 2009b; Arnsdorf et al., 2009a; Govey et al., 2013; Kreke et al., 2005; Sharp et al., 2009). Different levels of fluid flow could affect the osteogenic differentiation of mesenchymal stem cells. Finally, fluid flow could play a role in the transport of wear particles, nutrients, oxygen, waste products or regulatory signals (Donahue et al., 2003; Nam et al., 2013). In particular, flow-induced gradients of morphogens have been proposed to control the differentiation of mesenchymal stem cell (Ambard et al., 2006; Gortchacow et al., 2013; Hemmingsen et al., 2013).

## **Primary stability of cementless femoral stems**

Among the latest efforts to increase the long-term success of total hip arthroplasty, the cementless femoral component has attracted much of the attention. Aseptic loosening is the main cause for revision of cementless femoral components (Wyatt et al., 2014), and a poor primary stability of the stem is directly linked to aseptic loosening (Engh et al., 1992; Jasty et al., 1997; Søballe et al., 1992). For this reason, much research has been conducted to enhance the primary stability of cementless femoral stems.

Most of this research concentrated on two aspects influencing the stem's primary stability: the design of the stem and the surgical technique.

Following the first successful straight cementless stems designs, multiple modifications have been proposed (Khanuja et al., 2011). Anatomical stems were introduced at the beginning of the 1990s, with the idea that a curved design would be better suited to the proximal femoral canal geometry (Noble et al., 1988). More recently, short femoral stems were popularized, in an attempt to propose a more bone-preserving alternative to traditional cementless stems (Feyen et al., 2014). With the rise of personalized medicine, custom-made stems have also been proposed, with the idea that stem designs optimized for the patient's own anatomy could achieve better mechanical stability (Götze et al., 2002). Smaller design modifications were also introduced, such as modular necks, to better replicate the patient's own femoral neck angle or offset and restore its original hip biomechanics (Su et al., 2013), or the addition of a collar, which was thought to help the axial and rotational primary stability of the stem (Mai et al., 2010).

Proposed improvements to the surgical technique include studies on the influence of stem's positioning and bone-implant contact on primary stability, and pre-operative planning. Pre-operative planning ideally would provide optimized stem design and positioning specific to the patient leading to maximal primary stability.

These proposed modifications to the surgical procedure or the stem's design have been investigated by mean of either experimental measurement of stem's micromotion or estimation of the primary stability through finite element modeling.

The current gold standard for the experimental measurement of cementless femoral stems micromotion is the use of linear variable differential transformers (LVDTs). They are generally mounted by drilling a hole through the bone cortex and inserting a pin in the stem to measure 3D relative bone-implant micromotion. LVDTs-based micromotion measurements display

an excellent accuracy in the order of  $1\ \mu\text{m}$ , and their repeatability can be as high as  $2\ \mu\text{m}$  (Østbyhaug et al., 2010). A few simultaneous local measurement points are possible, with a reported maximum of six LVDTs mounted simultaneously at different locations around the stem (Bieger et al., 2012; Britton et al., 2004; Fottner et al., 2011; Kassi et al., 2005; Østbyhaug et al., 2010). LVDTs have been used successfully for the pre-clinical testing of new femoral stem designs (Baleani et al., 2000; Pettersen et al., 2009), to compare different stem geometries (Bieger et al., 2012; Bieger et al., 2013; Fottner et al., 2009; Nadorf et al., 2014; Østbyhaug et al., 2010), and to assess the effects of modular necks (Enoksen et al., 2014; Fottner et al., 2011) or shoulderless stems (Bieger et al., 2016).

Recently, another experimental method based on micro-CT imaging has been proposed to estimate the micromotion of cementless femoral components. The technique relies on radiopaque markers placed at the bone-implant interface and measures the three-dimensional markers displacement between a loaded and an unloaded case (Gortchacow et al., 2011). The technique reported up to 200 simultaneous measurement points located on a 20 mm long region of the metaphyseal part of the stem, with an accuracy of  $15\ \mu\text{m}$ . It was successfully used to compare straight and anatomical cementless femoral stem designs (Gortchacow et al., 2012).

Finite element modeling (FEM) has also been extensively used to estimate implant micromotion. One of the benefits of finite element models over experimental methods in pre-clinical testing is that they allow to test hypotheses about implant position (Bah et al., 2011; Reggiani et al., 2008) or bone-implant contact (Abdul-Kadir et al., 2008; Reimeringer et al., 2016), which are parameters that are especially complicated to control *in vitro*. Because finite element models provide complete maps of micromotion around cementless femoral stems, they are not restricted to pre-clinical testing of new implant designs (Bah et al., 2015; Gabarre et al., 2016; Viceconti et al., 2006), but can also be used for patient-specific pre-operative planning (Reggiani et al., 2007). However, for a clinical application in pre-operative planning, such patient-specific models need to be thoroughly validated against experimental measurements. A few patient-specific models of micromotion around cementless femoral stems were validated against experiments, usually through a handful of measurement points, either using LVDTs (Abdul-Kadir et al., 2008; Pancanti et al., 2003; Pettersen et al., 2009; Reggiani et al., 2008; Viceconti et al., 2006; Viceconti et al., 2000) or with other pointwise custom-made techniques (Ploeg et al., 2011; Reggiani et al., 2007; Tarala et al., 2010).



## Fluid flow at the bone-implant interface

Fluid flow was proposed to play a role on peri-implant healing and aseptic loosening already in the mid 1990s (Huiskes et al., 1997; Prendergast et al., 1996; Prendergast et al., 1997), and several studies since then focused on fluid flow estimation at the bone-implant interface. Because fluid flow at the bone-implant interface is particularly complicated to measure experimentally, most studies that concentrated on this aspect turned to finite element modelling. The tissues surrounding the implant are soft and deformable porous matrices that are saturated with interstitial fluid, and are generally represented using the poroelasticity theory (Cowin, 1999).

Prendergast et al. hypothesized that biophysical stimuli such as fluid velocity in the interfacial tissue could control the differentiation of the mesenchymal stem cells hosted in the tissue and hence, peri-implant healing (Prendergast et al., 1997). They investigated this hypothesis using a biphasic finite element model reproducing an animal experiment, where a cylindrical implant instrumented with a piston to generate micromotion was implanted in the condyles of dogs. The model showed that biophysical stimuli such as shear strain or interstitial fluid velocity were changing as healing progressed (Prendergast et al., 1996; Prendergast et al., 1997). In particular, they observed that bone formation occurred when fluid velocity decreased. From these observations, they proposed a mechano-regulatory algorithm that controls the tissue differentiation depending on a combination of shear strain and fluid velocity, where high values of fluid velocities would lead to fibrous tissue formation and low values to bone formation. Following this work, mechano-regulatory algorithms based on interstitial fluid velocity have been widely used to study the effects of different parameters on peri-implant healing and were corroborated through *in vivo* experiments (Ambard et al., 2006; Andreykiv et al., 2008; Geris et al., 2010; Guérin et al., 2009; Johansson et al., 2011; Khayyeri et al., 2009; Swider et al., 2011).

Most mechano-regulatory models are applied to simplified 2D or axisymmetric geometries that can easily be reproduced experimentally for model validation. Their results provide cues about the direct link between micromotion, fluid flow and peri-implant healing, and pave the way for more complex models of fluid flow at the interface, to investigate the mechanism behind fluid flow and cell differentiation. Among those more complex models that were used, some focused on fluid-enabled wear particles transport around cementless femoral stems, and used poroelastic modeling of a coronal cut of an anatomically realistic bone-implant interface (Alidousti et al., 2011; Alidousti et al., 2014). Another model concentrated on the role of micromotion-induced fluid flow in bone resorption around cemented im-

plants (Mann et al., 2014). This model was based on fluid-structure interaction modeling of retrieved transverse sections of cemented implants. The geometries were represented in detail and micromotion was measured experimentally on the transverse sections, leading to an accurate estimation of fluid velocities in the cement.

Finally, despite the difficulties in measuring peri-implant fluid flow experimentally, one study used high-resolution MRI to compute fluid velocities around an idealized bone-implant interface (Conroy et al., 2006). This technique holds promises for future validations of complex finite element models of fluid flow at the bone-implant interface.

### **Limitations of the current state of the art**

Multiple factors are involved in aseptic loosening of the femoral component in cementless hip arthroplasty, such as implant design, material, surface coatings, individual genetic variations, bone-implant micromotion, wear particles, biological compounds, and fluid flow at the interface. All these elements have been shown to play a role, either in fibrous tissue formation, or in peri-implant osteolysis. Some studies suggested that, regardless of the exact sequence of biological and mechanical events involved, aseptic loosening hinges on the early stages of peri-implant healing (Kärrholm et al., 1994; Mjöberg, 1994). However, the initial mechanical environment around the stem remains largely ill-defined.

Among those initial mechanical factors that play an important role in preventing aseptic loosening, primary stability and micromotion of the stem were shown to be critical for the long-term success of cementless total hip arthroplasty (Engh et al., 1992). Femoral stem micromotion is highly inhomogeneous and important local variations were already demonstrated through finite element models (Abdul-Kadir et al., 2008; Bah et al., 2015; Pancanti et al., 2003; Ploeg et al., 2011) and experimental measurements (Gortchacow et al., 2012; Kassi et al., 2005; Østbyhaug et al., 2010; Viceconti et al., 2000). Additionally, many design modifications of the femoral stems have been proposed, claiming to bring better primary stability to the stem (Khanuja et al., 2011). Many of these modifications, such as the addition of a collar or changes in the geometry, are likely to influence the distribution of bone-implant micromotion locally. FE models provide complete maps of micromotion around the stem, but few of these models are validated against experimental measurements. Furthermore, current techniques available to measure experimentally micromotion are limited to a handful of measurement points at the interface. Micro-CT-based imaging techniques allow full-field measurement of implant micromotion through digital volume correlation (DVC) (Sukjamsri et al., 2015). Nevertheless, DVC is limited to measurement around non-metallic implants, be-

cause of the metal artefacts generated by metal implants with micro-CT imaging. Recently, a technique combining radiopaque markers with micro-CT imaging was introduced to bypass artefacts emerging when imaging metallic implants (Gortchacow et al., 2012). It allows hundreds of simultaneous measurement points, but is limited to a small portion of the implant.

Much research also pointed out to the important role of fluid flow in aseptic loosening. Fluid flow influences healing probably through a combination of different mechanisms, such as direct mechanical stimulation of cells and transport of morphogens, wear particles or nutrients. A major current focus in biomechanics research is to conduct *in vitro* and *in silico* mechanobiology experiments to better understand how cells react to mechanical stimuli such as fluid-induced shear stress (Geris et al., 2003; Meulen et al., 2002; Thompson et al., 2010). However, the magnitude of these stimuli is poorly defined. A few studies tried to quantify fluid velocities induced by cementless implants micromotion (Alidousti et al., 2011; Conroy et al., 2006), but most of them were conducted with simplified geometries or homogeneous micromotion. Yet local micro-mechanical conditions and geometry are known to influence healing to a great extent (Andreykiv et al., 2008; Simmons et al., 2001b; Simmons et al., 2001a), and are highly susceptible to impact the fluid flow around the implant as well.

In regard to these limitations, there is an interesting potential of development in the field of cementless hip arthroplasty, through a better characterization of the initial local mechanical conditions around femoral stems.

## **Thesis Objectives**

This thesis addresses different aspects of the initial local mechanical environment around cementless femoral stems. In particular, micromotion and fluid-flow at the bone-implant interface, which may affect the long-term success of cementless implants, were estimated at the local level. The thesis was divided into three objectives, each of which was a subject of a chapter:

The first objective, detailed in Chapter 2, was to develop an experimental technique to allow full-field measurement of micromotion around a cementless femoral stem.

The second objective, described in Chapter 3, was to compare the primary stability of collared and collarless stems by measuring local interfacial micromotion using the technique developed in Chapter 2.

The third objective, developed in Chapter 4, was to quantify micromotion-induced fluid

flow around a cementless femoral stem, using an anatomically realistic poroelastic finite element model of the bone-implant interface, and local measurements of micromotion made in Chapter 3.

## References

- Abdul-Kadir, Mohammed Rafiq et al. (2008). "Finite element modelling of primary hip stem stability: The effect of interference fit". In: *Journal of Biomechanics* 41.33, pp. 587–594.
- Abu-Amer, Yousef, Isra Darwech, and John C Clohisy (2007). "Aseptic loosening of total joint replacements: mechanisms underlying osteolysis and potential therapies." In: *Arthritis Research and Therapy* 9 Suppl 1, S6.
- Alidousti, Hamidreza, Mark Taylor, and Neil W Bressloff (2011). "Do capsular pressure and implant motion interact to cause high pressure in the periprosthetic bone in total hip replacement?" In: *Journal of Biomechanical Engineering* 133.1212, p. 121001.
- (2014). "Periprosthetic wear particle migration and distribution modelling and the implication for osteolysis in cementless total hip replacement." In: *Journal of the Mechanical Behavior of Biomedical Materials* 32, pp. 225–244.
- Ambard, Dominique and Pascal Swider (2006). "A predictive mechano-biological model of the bone-implant healing". In: *European Journal of Mechanics - A/Solids* 25.66, pp. 927–937.
- Andreykiv, A, F van Keulen, and Patrick J Prendergast (2008). "Computational mechanobiology to study the effect of surface geometry on peri-implant tissue differentiation." In: *Journal of Biomechanical Engineering* 130.55, p. 051015.
- Arnsdorf, Emily J et al. (2009a). "Mechanically induced osteogenic differentiation - the role of RhoA, ROCKII and cytoskeletal dynamics". In: *Journal of Cell Science* 122.44, pp. 546–553.
- Arnsdorf, Emily J, Padmaja Tummala, and Christopher R Jacobs (2009b). "Non-Canonical Wnt Signaling and N-Cadherin Related  $\beta$ -Catenin Signaling Play a Role in Mechanically Induced Osteogenic Cell Fate". In: *PloS One* 4.44, e5388.
- Aspenberg, Per and P Herbertsson (1996). "Periprosthetic bone resorption. Particles versus movement." In: *The Journal of bone and joint surgery. British volume* 78.44, pp. 641–646.
- Aspenberg, Per and Harm M Van der Vis (1998). "Migration, particles, and fluid pressure. A discussion of causes of prosthetic loosening." In: *Clinical Orthopaedics and Related Research* 352352, pp. 75–80.
- Australian Orthopaedic Association National Joint Replacement Registry (2015). *Annual Report*.

- Bah, Mamadou T et al. (2011). "Efficient computational method for assessing the effects of implant positioning in cementless total hip replacements." In: *Journal of Biomechanics* 44.77, pp. 1417–1422.
- Bah, Mamadou T et al. (2015). "Inter-subject variability effects on the primary stability of a short cementless femoral stem". In: *Journal of Biomechanics* 48.66, pp. 1032–1042.
- Baleani, Massimiliano, Luca Cristofolini, and Aldo Toni (2000). "Initial stability of a new hybrid fixation hip stem: Experimental measurement of implant–bone micromotion under torsional load in comparison with cemented and cementless stems". In: *Journal of Biomedical Materials Research* 50.44, pp. 605–615.
- Beck, Ryan T, Kenneth D Illingworth, and Khaled J Saleh (2012). "Review of periprosthetic osteolysis in total joint arthroplasty: An emphasis on host factors and future directions". In: *Journal of orthopaedic research : official publication of the Orthopaedic Research Society* 30.44, pp. 541–546.
- Bieger, Ralf et al. (2012). "Primary stability and strain distribution of cementless hip stems as a function of implant design". In: *Clinical Biomechanics* 27.22, pp. 158–164.
- Bieger, Ralf et al. (2013). "Biomechanics of a short stem: In vitro primary stability and stress shielding of a conservative cementless hip stem." In: *Journal of orthopaedic research : official publication of the Orthopaedic Research Society* 31.88, pp. 1180–1186.
- Bieger, Ralf et al. (2016). "Primary stability of a shoulderless Zweymüller hip stem: a comparative in vitro micromotion study". In: *Journal of Orthopaedic Surgery and Research* 11.11, p. 500.
- Britton, J R, C G Lyons, and Patrick J Prendergast (2004). "Measurement of the Relative Motion Between an Implant and Bone under Cyclic Loading". In: *Strain* 40.44, pp. 193–202.
- Carlsson, Lars et al. (1986). "Osseointegration of titanium implants". In: *Acta Orthopaedica* 57.44, pp. 285–289.
- Conroy, Mark J et al. (2006). "High-resolution magnetic resonance flow imaging in a model of porous bone–implant interface". In: *Magnetic Resonance Imaging* 24.55, pp. 657–661.
- Cowin, Stephen C (1999). "Bone poroelasticity". In: *Journal of Biomechanics* 32.33, pp. 217–238.
- Davies, J E (2003). "Understanding peri-implant endosseous healing". In: *Journal of dental education* 67.88, pp. 932–949.
- Donahue, T L Haut et al. (2003). "Mechanosensitivity of bone cells to oscillating fluid flow induced shear stress may be modulated by chemotransport". In: *Journal of Biomechanics* 36.99, pp. 1363–1371.
- Engh, Charles A et al. (1992). "Quantification of Implant Micromotion, Strain Shielding, and Bone Resorption With Porous-Coated Anatomic Medullary Locking Femoral Prostheses". In: *Clinical Orthopaedics and Related Research* 285285, pp. 13–29.

- Enoksen, Cathrine H et al. (2014). "Initial stability of an uncemented femoral stem with modular necks. An experimental study in human cadaver femurs". In: *Clinical Biomechanics* 29.33, pp. 330–335.
- Ethgen, Olivier et al. (2004). "Health-Related Quality of Life in Total Hip and Total Knee Arthroplasty". In: *The Journal of Bone and Joint Surgery. American Volume* 86.55, pp. 963–974.
- Fahlgren, Anna et al. (2010). "Fluid pressure and flow as a cause of bone resorption." In: *Acta Orthopaedica* 81.44, pp. 508–516.
- Ferrier, G M et al. (2000). "The effect of cyclic pressure on human monocyte-derived macrophages in vitro." In: *The Journal of bone and joint surgery. British volume* 82.55, pp. 755–759.
- Feyen, H and A J Shimmin (2014). "Is the length of the femoral component important in primary total hip replacement?" In: *The Bone and Joint Journal* 96-B.44, pp. 442–448.
- Fottner, Andreas et al. (2009). "Biomechanical evaluation of two types of short-stemmed hip prostheses compared to the trust plate prosthesis by three-dimensional measurement of micromotions". In: *Clinical Biomechanics* 24.55, pp. 429–434.
- Fottner, Andreas et al. (2011). "Biomechanical evaluation of different offset versions of a cementless hip prosthesis by 3-dimensional measurement of micromotions". In: *Clinical Biomechanics* 26.88, pp. 830–835.
- Gabarre, Sergio et al. (2016). "Comparative Analysis of the Biomechanical Behaviour of Two Cementless Short Stems for Hip Replacement: Linea Anatomic and Minihip". In: *PloS One* 11.77, e0158411.
- Geris, Liesbet et al. (2003). "Assessment of Mechanobiological Models for the Numerical Simulation of Tissue Differentiation around Immediately Loaded Implants". In: *Computer Methods in Biomechanics and Biomedical Engineering* 6.55, pp. 277–288.
- Geris, Liesbet et al. (2010). "Mechanical loading affects angiogenesis and osteogenesis in an in vivo bone chamber: a modeling study." In: *Tissue Engineering Part A* 16.1111, pp. 3353–3361.
- Gortchacow, Michael et al. (2011). "A new technique to measure micromotion distribution around a cementless femoral stem". In: *Journal of Biomechanics* 44.33, pp. 557–560.
- Gortchacow, Michael et al. (2012). "Simultaneous and multisite measure of micromotion, subsidence and gap to evaluate femoral stem stability". In: *Journal of Biomechanics* 45.77, pp. 1232–1238.
- Gortchacow, Michael, Alexandre Terrier, and Dominique P Pioletti (2013). "A Flow Sensing Model for Mesenchymal Stromal Cells Using Morphogen Dynamics". In: *Biophysical journal* 104.1010, pp. 2132–2136.
- Götze, Christian et al. (2002). "Primary stability in cementless femoral stems: custom-made versus conventional femoral prosthesis". In: *Clinical Biomechanics* 17.44, pp. 267–273.

- Govey, Peter M, Alayna E Loiselle, and Henry J Donahue (2013). “Biophysical Regulation of Stem Cell Differentiation”. In: *Current Osteoporosis Reports* 11.22, pp. 83–91.
- Guérin, Gaëtan, Dominique Ambard, and Pascal Swider (2009). “Cells, growth factors and bioactive surface properties in a mechanobiological model of implant healing”. In: *Journal of Biomechanics* 42.1515, pp. 2555–2561.
- Haudenschild, Anne K et al. (2009). “Pressure and distortion regulate human mesenchymal stem cell gene expression.” In: *Annals of biomedical engineering* 37.33, pp. 492–502.
- Hemmingsen, Mette et al. (2013). “The Role of Paracrine and Autocrine Signaling in the Early Phase of Adipogenic Differentiation of Adipose-derived Stem Cells”. In: *PloS One* 8.55, e63638.
- Hendrix, R W et al. (1983). “Arthrography after total hip arthroplasty: a modified technique used in the diagnosis of pain.” In: *Radiology* 148.33, pp. 647–652.
- Hooper, G J et al. (2009). “Revision following cemented and uncemented primary total hip replacement: a seven-year analysis from the New Zealand Joint Registry.” In: *The Journal of bone and joint surgery. British volume* 91.44, pp. 451–458.
- Huiskes, Rik, W D Van Driel, and Patrick J Prendergast (1997). “A biomechanical regulatory model for periprosthetic fibrous-tissue differentiation”. In: *Journal of Materials Science* 8.1212, pp. 785–788.
- Issa, Kimona and Michael A Mont (2013). “Total hip replacement: Mortality and risks”. In: *The Lancet* 382.98989898, pp. 1074–1076.
- Jasty, Murali et al. (1997). “Enhanced stability of uncemented canine femoral components by bone ingrowth into the porous coatings”. In: *The Journal of Arthroplasty* 12.11, pp. 106–113.
- Johansson, Lars et al. (2011). “Fluid-induced osteolysis: modelling and experiments.” In: *Computer Methods in Biomechanics and Biomedical Engineering* 14.44, pp. 305–318.
- Kärrholm, J et al. (1994). “Does early micromotion of femoral stem prostheses matter? 4-7-year stereoradiographic follow-up of 84 cemented prostheses.” In: *The Journal of bone and joint surgery. British volume* 76.66, pp. 912–917.
- Kassi, Jean-Pierre et al. (2005). “Stair climbing is more critical than walking in pre-clinical assessment of primary stability in cementless THA in vitro”. In: *Journal of Biomechanics* 38.55, pp. 1143–1154.
- Khanuja, Harpal S et al. (2011). “Cementless femoral fixation in total hip arthroplasty.” In: *The Journal of Bone and Joint Surgery. American Volume* 93.55, pp. 500–509.
- Khayeri, Hanifeh et al. (2009). “Corroboration of mechanobiological simulations of tissue differentiation in an in vivo bone chamber using a lattice-modeling approach”. In: *Journal of orthopaedic research : official publication of the Orthopaedic Research Society* 27.1212, pp. 1659–1666.



- Kreke, Michelle R, William R Huckle, and Aaron S Goldstein (2005). "Fluid flow stimulates expression of osteopontin and bone sialoprotein by bone marrow stromal cells in a temporally dependent manner." In: *Bone* 36.66, pp. 1047–1055.
- Learmonth, Ian D, Claire Young, and Cecil Rorabeck (2007). "The operation of the century: total hip replacement". In: *The Lancet* 370.95979597, pp. 1508–1519.
- Mai, Kenny T et al. (2010). "Cementless Femoral Fixation in Total Hip Arthroplasty". In: *Am J Orthop*.
- Mann, Kenneth A and Mark A Miller (2014). "Fluid-structure interactions in micro-interlocked regions of the cement-bone interface". In: *Computer Methods in Biomechanics and Biomedical Engineering* 17.1616, pp. 1809–1820.
- Matthews, J B et al. (2000a). "Comparison of the response of primary human peripheral blood mononuclear phagocytes from different donors to challenge with model polyethylene particles of ..." In: *Biomaterials* 21.20, pp. 2033–2044.
- Matthews, J B et al. (2000b). "Evaluation of the response of primary human peripheral blood mononuclear phagocytes to challenge with in vitro generated clinically relevant UHMWPE particles of known size and dose." In: *Journal of Biomedical Materials Research* 52.22, pp. 296–307.
- Meulen, Marjolein C H van der and Rik Huiskes (2002). "Why mechanobiology?" In: *Journal of Biomechanics* 35.44, pp. 401–414.
- Mjöberg, Bengt (1994). "Theories of wear and loosening in hip prostheses: Wear-induced loosening vs loosening-induced wear-a review". In: *Acta Orthopaedica* 65.33, pp. 361–371.
- Nadorf, J et al. (2014). "Fixation of the shorter cementless GTS<sup>TM</sup> stem: biomechanical comparison between a conventional and an innovative implant design." In: *Archives of orthopaedic and trauma surgery* 134.55, pp. 719–726.
- Nam, Denis, Mathias P G Bostrom, and Anna Fahlgren (2013). "Emerging Ideas: Instability-induced Periprosthetic Osteolysis Is Not Dependent on the Fibrous Tissue Interface". In: *Clinical Orthopaedics and Related Research* 471.66, pp. 1758–1762.
- National Joint Registry for England, Wales, Northern Ireland and the Isle of Man (2015). "13th Annual Report". In:
- Noble, P C et al. (1988). "The Anatomic Basis of Femoral Component Design". In: *Clinical Orthopaedics and Related Research* 235235, pp. 148–165.
- Ollivere, B et al. (2012). "Current concepts in osteolysis". In: *The Journal of bone and joint surgery. British volume* 94 B.11, pp. 10–15.
- Ong, Kevin L et al. (2010). "Risk of Subsequent Revision after Primary and Revision Total Joint Arthroplasty". In: *Clinical Orthopaedics and Related Research* 468.1111, pp. 3070–3076.
- Østbyhaug, Per Olav et al. (2010). "Primary stability of custom and anatomical uncemented femoral stems". In: *Clinical Biomechanics* 25.44, pp. 318–324.



- Pabinger, C and A Geissler (2014). "Utilization rates of hip arthroplasty in OECD countries." In: *Osteoarthritis and cartilage* 22.66, pp. 734–741.
- Pancanti, Alberto, Marek Bernakiewicz, and Marco Viceconti (2003). "The primary stability of a cementless stem varies between subjects as much as between activities". In: *Journal of Biomechanics* 36.66, pp. 777–785.
- Pedersen, A B et al. (2014). "Association between fixation technique and revision risk in total hip arthroplasty patients younger than 55 years of age. Results from the Nordic Arthroplasty Register Association." In: *Osteoarthritis and cartilage / OARS, Osteoarthritis Research Society* 22.55, pp. 659–667.
- Pettersen, Sune H, Tina S Wik, and Bjørn Skallerud (2009). "Subject specific finite element analysis of implant stability for a cementless femoral stem". In: *Clinical Biomechanics* 24.66, pp. 480–487.
- Pilliar, R M, J M Lee, and C Maniopoulos (1986). "Observations on the Effect of Movement on Bone Ingrowth into Porous-Surfaced Implants". In: *Clinical Orthopaedics and Related Research* 208208, pp. 108–113.
- Ploeg, Bas van der et al. (2011). "Toward a more realistic prediction of peri-prosthetic micro-motions". In: *Journal of Orthopaedic Research* 30.77, pp. 1147–1154.
- Prendergast, Patrick J and Rik Huiskes (1996). "Finite element analysis of fibrous tissue morphogenesis - A study of the osteogenic index with a biphasic approach". In: *Mechanics of Composite Materials* 32.22, pp. 144–150.
- Prendergast, Patrick J, Rik Huiskes, and Kjeld Søballe (1997). "Biophysical stimuli on cells during tissue differentiation at implant interfaces". In: *Journal of Biomechanics* 30.66, pp. 539–548.
- Raghavendra, Sangeetha, Marjorie C Wood, and Thomas D Taylor (2005). "Early wound healing around endosseous implants: a review of the literature." In: *The International journal of oral and maxillofacial implants* 20.33, pp. 425–431.
- Reggiani, B et al. (2007). "Predicting the subject-specific primary stability of cementless implants during pre-operative planning: Preliminary validation of subject-specific finite-element models". In: *Journal of Biomechanics* 40.1111, pp. 2552–2558.
- Reggiani, Barbara et al. (2008). "Sensitivity of the Primary Stability of a Cementless Hip Stem to Its Position and Orientation". In: *Artificial Organs* 32.77, pp. 555–560.
- Reimeringer, M and N Nuño (2016). "The influence of contact ratio and its location on the primary stability of cementless total hip arthroplasty: A finite element analysis". In: *Journal of Biomechanics* 49.77, pp. 1064–1070.
- Robertsson, O et al. (1997). "Intracapsular pressure and loosening of hip prostheses. Preoperative measurements in 18 hips." In: *Acta Orthopaedica Scandinavica* 68.33, pp. 231–234.

- Sharp, Lindsay A, Yong W Lee, and Aaron S Goldstein (2009). "Effect of low-frequency pulsatile flow on expression of osteoblastic genes by bone marrow stromal cells". In: *Annals of biomedical engineering* 37.33, pp. 445–453.
- Simmons, Craig A, Shaker A Meguid, and Robert M Pilliar (2001a). "Differences in osseointegration rate due to implant surface geometry can be explained by local tissue strains". In: 19.22, pp. 187–194.
- Simmons, Craig A, S A Meguid, and R M Pilliar (2001b). "Mechanical regulation of localized and appositional bone formation around bone-interfacing implants." In: *Journal of Biomedical Materials Research* 55.11, pp. 63–71.
- Søballe, Kjeld et al. (1992). "Tissue ingrowth into titanium and hydroxyapatite-coated implants during stable and unstable mechanical conditions". In: *Journal of Orthopaedic Research* 10.22, pp. 285–299.
- Steward, Andrew J and Daniel J Kelly (2014). "Mechanical regulation of mesenchymal stem cell differentiation". In: *Journal of Anatomy* 227.66, pp. 717–731.
- Su, E P and R L Barrack (2013). "Cementless femoral fixation: not all stems are created equally". In: *The Bone and Joint Journal* 95-B.1111, pp. 53–56.
- Sukjamsri, Chamaiporn et al. (2015). "Digital volume correlation and micro-CT: An in-vitro technique for measuring full-field interface micromotion around polyethylene implants". In: *Journal of Biomechanics* 48.1212, pp. 3447–3454.
- Sundfeldt, Mikael et al. (2002). "Effect of submicron polyethylene particles on an osseointegrated implant: an experimental study with a rabbit patello-femoral prosthesis." In: *Acta Orthopaedica Scandinavica* 73.44, pp. 416–424.
- Sundfeldt, Mikael et al. (2006). "Aseptic loosening, not only a question of wear: A review of different theories". In: *Acta Orthopaedica* 77.22, pp. 177–197.
- Swider, Pascal et al. (2011). "Sensitivity analysis of periprosthetic healing to cell migration, growth factor and post-operative gap using a mechanobiological model". In: *Computer Methods in Biomechanics and Biomedical Engineering* 14.99, pp. 763–771.
- Tarala, M et al. (2010). "Experimental versus computational analysis of micromotions at the implant–bone interface". In: *Proceedings of the Institution of Mechanical Engineers, Part H: Journal of Engineering in Medicine* 225.11, pp. 8–15.
- Terheyden, Hendrik et al. (2011). "Osseointegration - communication of cells". In: *Clinical Oral Implants Research* 23.1010, pp. 1127–1135.
- Thompson, M S et al. (2010). "In vitro models for bone mechanobiology: applications in bone regeneration and tissue engineering". In: *Proceedings of the Institution of Mechanical Engineers, Part H: Journal of Engineering in Medicine* 224, pp. 1533–1541.
- Uccelli, Antonio, Lorenzo Moretta, and Vito Pistoia (2008). "Mesenchymal stem cells in health and disease". In: *Nature Reviews Immunology* 8.99, pp. 726–736.

- Vanhegan, I S et al. (2012). "A financial analysis of revision hip arthroplasty". In: *The Journal of bone and joint surgery. British volume* 94-B.55, pp. 619–623.
- Viceconti, Marco et al. (2000). "Large-sliding contact elements accurately predict levels of bone–implant micromotion relevant to osseointegration". In: *Journal of Biomechanics* 33.1212, pp. 1611–1618.
- Viceconti, Marco et al. (2006). "Primary stability of an anatomical cementless hip stem: A statistical analysis". In: *Journal of Biomechanics* 39.77, pp. 1169–1179.
- Vis, Harm M Van der et al. (1998a). "Fluid pressure causes bone resorption in a rabbit model of prosthetic loosening." In: *Clinical Orthopaedics and Related Research* 350350, pp. 201–208.
- Vis, Harm M Van der et al. (1998b). "Short periods of oscillating fluid pressure directed at a titanium-bone interface in rabbits lead to bone lysis". In: *Acta Orthopaedica Scandinavica* 69.11, pp. 5–10.
- Wagner, Diane R et al. (2008). "Hydrostatic pressure enhances chondrogenic differentiation of human bone marrow stromal cells in osteochondrogenic medium." In: *Annals of biomedical engineering* 36.55, pp. 813–820.
- Willert, Hans Georg, Manfred Semlitsch, and Leonard F Peltier (1996). "Tissue Reactions to Plastic and Metallic Wear Products of Joint Endoprostheses." In: *Clinical Orthopaedics and Related Research* 333, p. 4.
- Wolff, Julius (2010). "The classic: on the inner architecture of bones and its importance for bone growth. 1870." In: *Clinical orthopaedics and related research* 468.44, pp. 1056–1065.
- Wyatt, Michael et al. (2014). "Survival outcomes of cemented compared to uncemented stems in primary total hip replacement". In: *World Journal of Orthopedics* 5.55, p. 591.



# Chapter 2

## Full-field micromotion measurement around cementless femoral stems

*This chapter is based on:*

Full-field measurement of micromotion around a cementless femoral stem using micro-CT imaging and radiopaque markers.

V. Malfroy Camine, H. A. Rüdiger, D. P. Pioletti, A. Terrier, 2016

Journal of Biomechanics



## Abstract

A good primary stability of cementless femoral stems is essential for the long-term success of total hip arthroplasty. Experimental measurement of implant micromotion with linear variable differential transformers is commonly used to assess implant primary stability in pre-clinical testing. But these measurements are often limited to a few distinct points at the interface. New techniques based on micro-computed tomography (micro-CT) have recently been introduced, such as Digital Volume Correlation (DVC) or markers-based approaches. DVC is however limited to measurement around non-metallic implants due to metal-induced imaging artifacts, and markers-based techniques are confined to a small portion of the implant. In this paper, we present a technique based on micro-CT imaging and radiopaque markers to provide the first full-field micromotion measurement at the entire bone-implant interface of a cementless femoral stem implanted in a cadaveric femur.

Micromotion was measured during compression and torsion. Over 300 simultaneous measurement points were obtained. Micromotion amplitude ranged from 0 to 24  $\mu\text{m}$  in compression and from 0 to 49  $\mu\text{m}$  in torsion. Peak micromotion was distal in compression and proximal in torsion. The technique bias was 5.1  $\mu\text{m}$  and its repeatability standard deviation was 4  $\mu\text{m}$ . The method was thus highly reliable and compared well with results obtained with linear variable differential transformers (LVDTs) reported in the literature.

These results indicate that this micro-CT based technique is perfectly relevant to observe local variations in primary stability around metallic implants. Possible applications include pre-clinical testing of implants and validation of patient-specific models for pre-operative planning.

## Introduction

During the past two decades, the number of cementless hip arthroplasties has increased significantly from 13'650 procedures in 2003 to 27'031 in 2014 (Australian Orthopaedic Association National Joint Replacement Registry, 2015), and it is now the preferred type of fixation for patients under 70 years old.

However, the cumulative revision rate at 14 years reaches 8% and aseptic loosening remains among the most common causes for revision of cementless femoral components. For this reason, improving the long-term success of cementless femoral stems continues to be a major focus in the field of total hip arthroplasty.

A good primary stability of the implant is widely recognized as the most important factor for a successful cementless hip arthroplasty. Primary stability is characterized by the amount of relative bone-implant micromotion at the interface, right after implantation and before osseointegration takes place. Many researchers have reported that excessive implant micromotion leads to fibrous tissue formation and failed bone ingrowth (Engh et al., 1992; Pilliar et al., 1986; Søballe et al., 2009).

Much research in the recent years has focused on measuring bone-implant micromotion for the pre-clinical testing of implants. An optimal experimental micromotion measurement technique for the pre-clinical testing of femoral stems should be able to evaluate micromotion at every point of the bone-implant interface while having a bias below 10  $\mu\text{m}$  (Viceconti et al., 2000). Considering the maximum micromotion still allowing osseointegration is around 100  $\mu\text{m}$ , this bias value would represent a relative error of 10%. Current techniques available to measure implant micromotion rely mostly on linear variable differential transformers (LVDTs) (Enoksen et al., 2014; Fottner et al., 2009; Kassi et al., 2005; Monti et al., 1999; Østbyhaug et al., 2010; Pettersen et al., 2009). Despite their excellent accuracy, they allow only a handful of simultaneous measurement points. Finite element (FE) modeling is another popular method to estimate micromotion of cementless stems. It provides information on local micromotion and can be used for the pre-clinical testing of implants (Abdul-Kadir et al., 2008; Bah et al., 2015; Ploeg et al., 2011; Viceconti et al., 2006) as well as for patient-specific pre-operative planning (Pettersen et al., 2009; Reggiani et al., 2007). But experimental validation of FE models predictions remains challenging, restraining a more extensive use of these models in clinical practice (Taylor et al., 2015). More recently, micromotion measurement techniques based on micro-computed tomography (micro-CT) imaging were introduced, and demonstrated great potential. Notwithstanding the very high number of measurement points they can collect, they were limited to measurement around non-metallic implants

due to imaging artifacts (Sukjamsri et al., 2015) or confined to a small portion of the implant (Gortchacow et al., 2012; Gortchacow et al., 2011).

In the present study, we extend a micromotion measurement technique based on radiopaque markers and micro-CT imaging (Gortchacow et al., 2011) to measure three dimensional micromotion at the entire bone-implant interface of a cementless femoral stem implanted in a cadaveric femur. The method will allow to measure micromotion for axial compression and torsion. Our objective is to guarantee a bias inferior to 10  $\mu\text{m}$  and a good repeatability to enable rigorous pre-clinical testing of cementless implants primary stability.

## Methods

### *Cadaveric femur and femoral stem preparation*

A left human cadaveric femur, formalin-fixed, was prepared for implantation by a senior orthopedic surgeon. The surgeon performed femoral neck osteotomy and femoral broaching according to the recommendations of the implant's manufacturer. After broaching, around 1000 stainless steel spherical markers of diameter 600  $\mu\text{m}$  (MPS Micro Precision Systems AG, Biel, Switzerland) were manually press-fitted on the endosteal surface of the femoral canal and the cancellous bone of the metaphysis using a spatula. Appropriate care was taken to get a uniform distribution of bone markers in the canal (Fig. 2.1).

A collared, straight cementless femoral stem with a standard offset neck (Corail®Hip System, size 11, DePuy Synthes Joint Reconstruction, Warsaw, IN, USA) was selected for implantation. The stem is made of forged titanium alloy (TiAl6V4) and is fully coated with 155  $\mu\text{m}$  of hydroxyapatite. To facilitate the accommodation of the bone-implant construct inside the experimental setup, the stem femoral neck was cut 27 mm medial and parallel to the implant extraction threaded hole axis. 30 tantalum spherical markers of diameter 800  $\mu\text{m}$  (X-medics Scandinavia, Frederiksberg, Denmark) were glued (Loctite 401, Loctite Corporation, Dublin, Ireland) on the stem surface, within drilled holes of 1 mm depth and 850  $\mu\text{m}$  diameter (Fig. 2.1). The surgeon then proceeded to the femoral stem insertion in the broached femur.

### *Loading devices*

Two custom loading devices were developed to apply axial compression and torsion on the stem. The loading devices had to fit inside a micro-CT scanner and had to be sufficiently permeable to X-ray. Each device was composed of two parts: the loading system and the



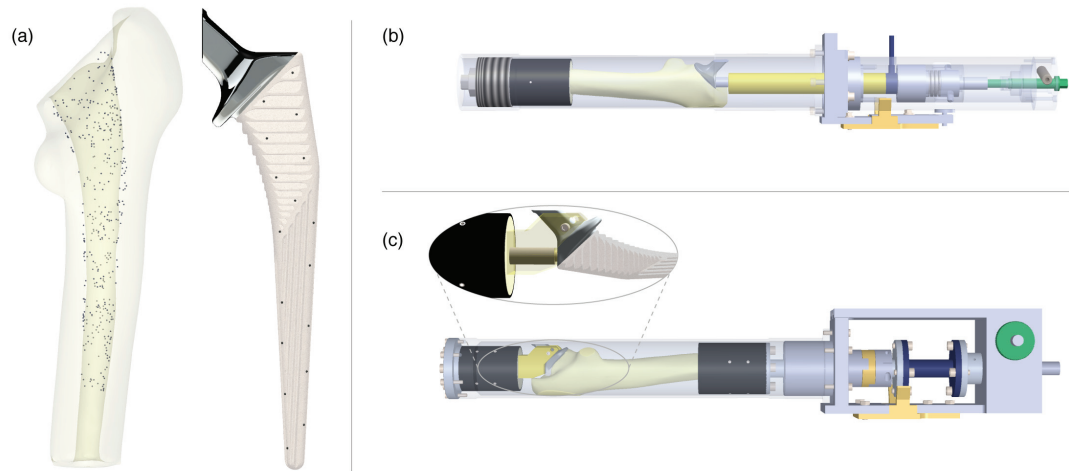


**Figure 2.1:** *Experimental setup. (a) Bone markers spread inside the femoral canal (left). Stem neck cut and implant markers stuck on implant surface (right). (b) Compression loading device. The distal femur is cemented (black). Compression is applied through a cylinder (yellow) driven by a screw jack (green) and is controlled by a load cell (blue) (c) Torsion loading device. The proximal stem is restrained by a clamping system (yellow). The proximal stem and the distal femur are cemented (black). Torsion is applied through a worm gear (green) and is controlled by a torque sensor (blue).*

sample holder, enclosed in a 2 mm thick tube made of 6060 aluminum alloy (Fig. 2.1).

The compression device was modified from an existing one (Gortchacow et al., 2012). The distal part of the femur was cut away at approximately 220 mm from the tip of the greater trochanter. A template was used to pot the distal femur and ensure its alignment (load axis along stem axis) inside the device, using the stem extraction threaded hole. The femur was distally potted with epoxy resin (Neukadur Multicast 20, Altropol Kunststoff GmbH, Stockelsdorf, Germany), 30 mm away from the distal end of the stem. Minimal reaming of the surface of the greater trochanter laterally (2-3 mm) was performed to enable proper fitting inside the device. The applied load was monitored by a load cell (LCM202-5KN, Omega Engineering, Inc., Stamford, CO, USA).

The torsion device applied an axial torsion on the bone-stem system. The proximal part of the stem was restrained by a clamping system. The stem extraction threaded hole was used to ensure stem alignment along the torsion axis. The stem neck was clamped by two steel cone point screws. The distal femur and the proximal clamping system were potted with epoxy resin inside a template, before insertion in the device. A torsion was applied to the distal femur through a rotary shaft driven by a worm gear. The torque was monitored by a reaction torque cell (TQM301-45N, Omega Engineering, Inc., Stamford, CO, USA).

### ***Micro-CT scanning protocol***

To measure micromotion, the bone-implant interface was first scanned during loading and then after loading with a micro-CT scanner (Skyscan 1076 *in vivo* micro-CT, Bruker micro-CT, Kontich, Belgium). These two scans are referred to hereafter as loaded scan and unloaded scan respectively. The acquisition parameters for the scans were the following: 1 mm aluminum filter, voltage 100 kV, current 100  $\mu$ A, exposure time 310 ms, rotation step 0.7°, 360° scanning, scanning width 68 mm, and frame averaging 2. The scanning length was 21 mm. To cover the whole implant length, 7 scans at different positions along the stem were combined by moving the motorized sample's stage accordingly. Scanning duration for one 21 mm scan was 24 min, resulting in 170 min of scanning to cover the whole stem. Scans were then reconstructed to a final isotropic voxel size of 35  $\mu$ m (NRecon v 1.6.10.4, Bruker micro-CT, Kontich, Belgium). A ring artifact correction of level 4 and a beam hardening correction of 20% were applied to improve the image quality.

### ***Image processing and micromotion computation***

The reconstructed images were processed in Amira (Amira v6.0.1, FEI, Hillsboro, OR, USA). Segmentation of bone and implant markers was completely automatized, using the difference in size and radiopacity of bone and implant markers (Fig. 2.2). The centroids of all markers were extracted and filtered by size to eliminate noise and clusters of contiguous markers.

Micromotion analysis was performed by a custom algorithm (Matlab r2016a, The Mathworks, Inc., Natick, MA, USA). The loaded and unloaded scans did not share the same coordinate system. The coordinate system of the unloaded scan was used as a reference. The implant was considered rigid so that the coordinate systems of both scans could be aligned using rigid body registration. The correspondence between implant markers in the loaded and unloaded scans was found using an iterative closest point (ICP) algorithm (Besl et al., 1992). The rigid transformation matrix between the loaded and unloaded scans was then computed, and applied to all markers from the loaded scan, so that in the end, all markers from the loaded and unloaded scans were in the same coordinate system.

Micromotion was defined as the three dimensional displacement between corresponding loaded and unloaded bone markers. The correspondence between bone markers was computed with the ICP algorithm. Mismatched markers were then eliminated using median absolute deviation to remove outliers (Leys et al., 2013). The micromotion vector was separated into components tangential and normal to the stem surface. Micromotion was then

interpolated using natural neighbor interpolation and displayed on the stem surface.

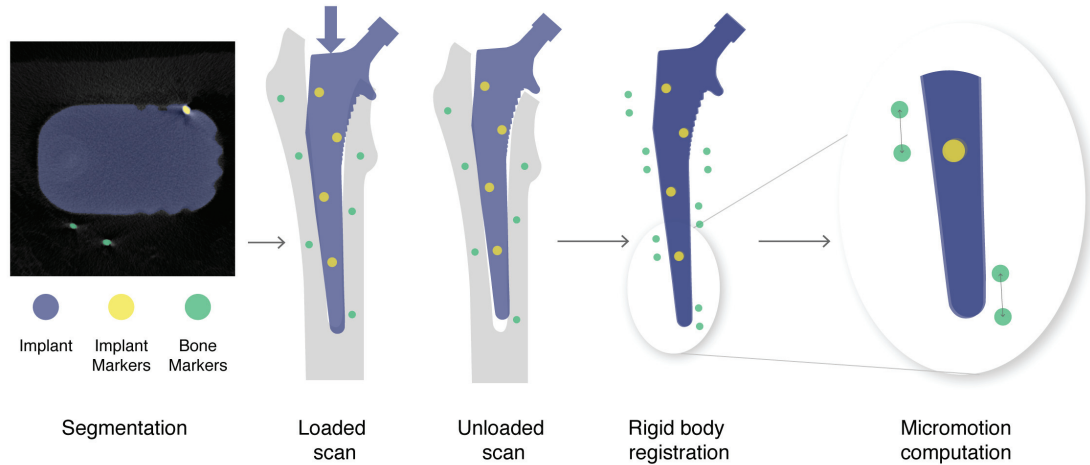


**Figure 2.2:** Image processing and micromotion computation. Bone and implant markers are segmented on micro-CT scans. Implant markers from the loaded scan are superimposed to implant markers from the unloaded scan. Micromotion is the displacement between corresponding bone markers from the registered loaded scan to the unloaded scan.

### ***Micromotion measurement in compression and torsion***

For compression testing, a load of 1800 N was applied on the stem. The load was chosen according to the average load during walking measured with instrumented hip implants (Bergmann et al., 2010b; Bergmann et al., 2010a). The bone was preconditioned with 50 compressive load cycles before compression testing. For torsion testing, a torque of 17 N m was applied on the stem. Moment and direction were chosen according to average moment acting on instrumented hip implants during stair climbing (Bergmann et al., 2010b; Bergmann et al., 2010a). The bone was preconditioned with 50 torsional load cycles before torsion testing. All tests were performed at room temperature.

### ***Bias and repeatability estimation***

Bias and repeatability were measured in both compression and torsion to evaluate the technique reliability. The bias (a measure of the difference between the average of measurements made on the same object and its true value) was estimated by measuring micromotion between three pairs of successive unloaded scans (Fig. 2.3). Each 3D component of micromotion followed a normal distribution, with mean 0. The bias was defined as the 95% confidence interval (95% CI) of micromotion measurement, corresponding to  $\pm 1.96 \cdot SD$ , where SD is the standard deviation of micromotion pooled over the three pairs of measurement.

To estimate repeatability, micromotion measurements in compression and torsion were repeated three times (Fig. 2.3), under repeatability conditions (same laboratory, same operator, same apparatus, and all tests performed on the same day). Corresponding markers were matched between the three pairs of measurements. The repeatability standard deviation ( $sr$ ) was calculated as the pooled standard deviation of repeated measurements. The 95% repeatability limit ( $r$ ) (the maximum difference between two results obtained under repeatability conditions that can be attributed to the test method precision) was defined as  $1.96 \cdot \sqrt{2} \cdot sr$  according to current ASTM recommendations (ASTM, 2013).

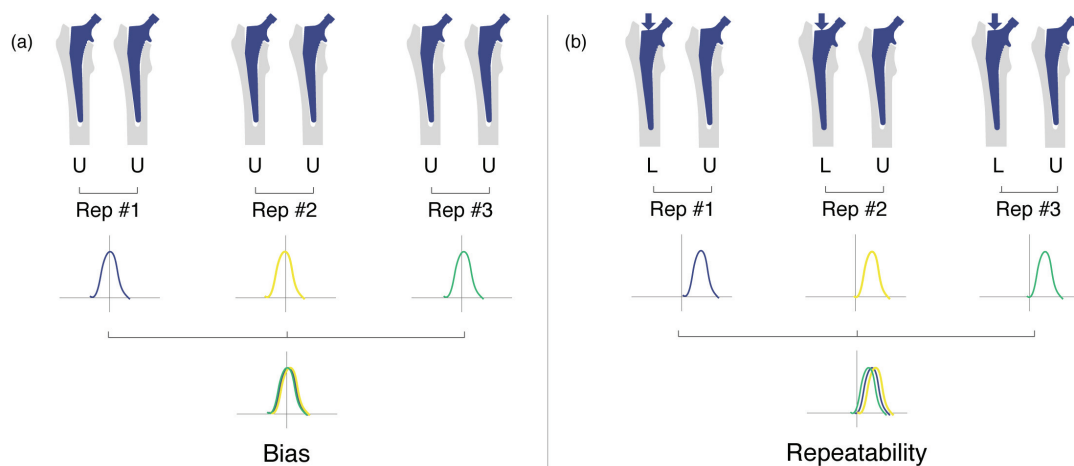


**Figure 2.3:** Bias and repeatability estimation protocols. Both protocols were applied successively for compression and torsion (a) Three pairs of unloaded scans (U) are performed. For each pair of scan (Rep), micromotion is measured. Bias is estimated on these three repeated measurements. (b) Three pairs of unloaded (U) and loaded (L) scans are performed. For each pair of scan (Rep), micromotion is measured. Repeatability is estimated on these three repeated measurements.

### Data analysis and statistics

For measurement analysis, the femoral stem was divided into three zones: the metaphyseal zone, the middle diaphyseal zone, and the distal diaphyseal zone, similar to the recommendations of Gruen et al. (1979). Normal and tangential micromotion in compression and torsion were compared in each zone with a Mann-Whitney U test. For each loading case, micromotion between zones were also compared using the same Mann-Whitney U test.

## Results

### *Bias and repeatability*

Micromotion was simultaneously measured at 313 points on the bone-implant interface for compression and 337 points for torsion. The bias of the method reached a maximum of 5.1  $\mu\text{m}$  (Table 2.1). The bias was consistent between directions as well as between loading cases. The repeatability standard deviation (sr) ranged from 3.1  $\mu\text{m}$  to 4.1  $\mu\text{m}$ . It was also comparable between directions and loading cases. The repeatability limit reached a maximum of 10.6  $\mu\text{m}$  for compression and 11.5  $\mu\text{m}$  for torsion.

	Bias		Repeatability	
	SD	95% CI	sr	r
<b>Compression</b>				
Lateral to medial	2.4	4.7	3.2	9.0
Anterior to posterior	2.6	5.1	3.8	10.6
Inferior to superior	1.9	3.7	3.1	8.7
<b>Torsion</b>				
Lateral to medial	2.4	4.7	3.9	10.9
Anterior to posterior	2.4	4.7	4.0	11.2
Inferior to superior	1.9	3.7	4.1	11.5

**Table 2.1:** Reliability assessment of Micro-CT based measurement of micromotion - Values expressed in micrometers. SD: bias standard deviation; 95% CI: bias 95% confidence interval; sr: repeatability standard deviation; r: repeatability 95% limit.

### *Micromotion in compression and torsion*

In compression, normal micromotion was below 6  $\mu\text{m}$  around 95% of the stem surface but reached 24  $\mu\text{m}$  at the tip of the stem (Fig. 2.4). Tangential micromotion was higher than normal micromotion and concentrated on the stem's middle and distal diaphyseal zones. In torsion, high micromotion was concentrated on the stem's metaphyseal and middle diaphyseal parts (Fig. 2.4).

Median micromotion was higher in torsion than in compression (Table 2.2). In compression, micromotion was low proximally and higher distally, whereas in torsion micromotion was

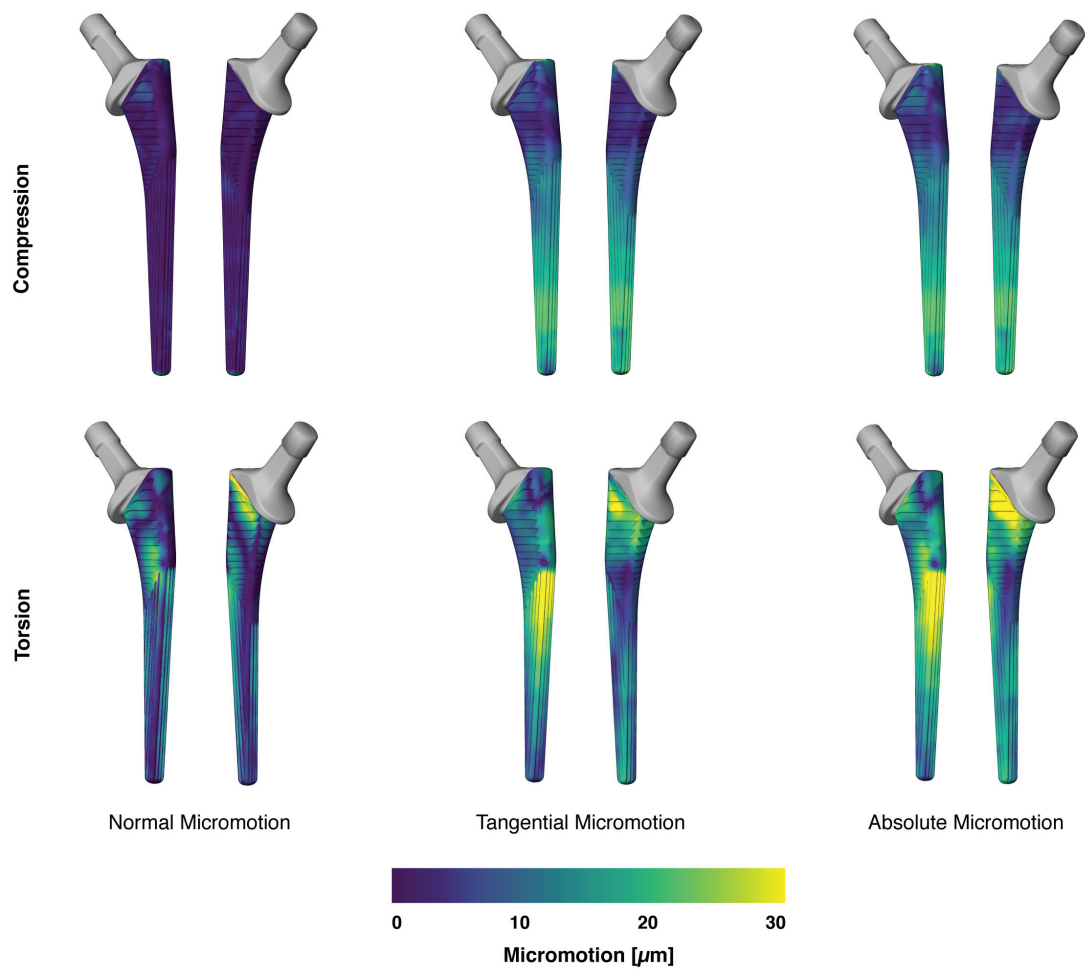


**Figure 2.4:** Normal, tangential, and absolute micromotion measured around a cementless femoral stem - Anterior/lateral and posterior/medial views of the stem displayed successively from left to right for each case. Top row shows results obtained in compression. The bottom row shows results obtained in torsion.

high proximally and lower distally. For both loading cases, the differences between micromotion distribution in each zone of the stem was significant. Absolute micromotion was significantly ( $p < 0.0001$ ) higher in torsion than in compression in the metaphyseal and middle diaphyseal zones, while it was significantly lower on the distal diaphysis (Fig. 2.5).

	<b>Min</b>	<b>Max</b>	<b>Median</b>
<b>Compression</b>			
Lateral to medial	-7.8	10.8	1.9
Anterior to posterior	-12.0	13.7	0.4
Inferior to superior	-24.0	5.0	12.3
Absolute	0.8	24.0	13.3
<b>Torsion</b>			
Lateral to medial	-32.5	44.1	-1.5
Anterior to posterior	-42.2	33.8	-7.5
Inferior to superior	-7.8	15.2	0.8
Absolute	2.4	48.7	20.9

**Table 2.2:** Minimum, maximum, and median micromotion ( $\mu\text{m}$ ) along the different anatomical axis for compression and torsion.

## Discussion

Micro-CT based techniques such as Digital Volume Correlation (DVC) have been recently used to measure displacement and strain fields in the bone (Roberts et al., 2014). However, extension of micro-CT DVC to measurements at the bone-implant interface faces complications due to artifacts generated by thick metal implants: in consequence of the high atomic number of the metallic implant, the bone would be obscured, streak artifacts would be generated and beam hardening would impact the gray levels at the bone-implant interface (Boas et al., 2012). Our aim was to develop a new technique to measure micromotion all around the femur-stem interface, with a bias lower than  $10 \mu\text{m}$  and a good repeatability to allow thorough pre-clinical testing of implants. We proposed a methodology based on radiopaque markers and micro-CT imaging, and measured micromotion around a cementless stem in a cadaveric femur under compressive and torsional loadings. Instead of imaging directly the interface, the radiopaque markers representing the bone and implant surfaces were used.

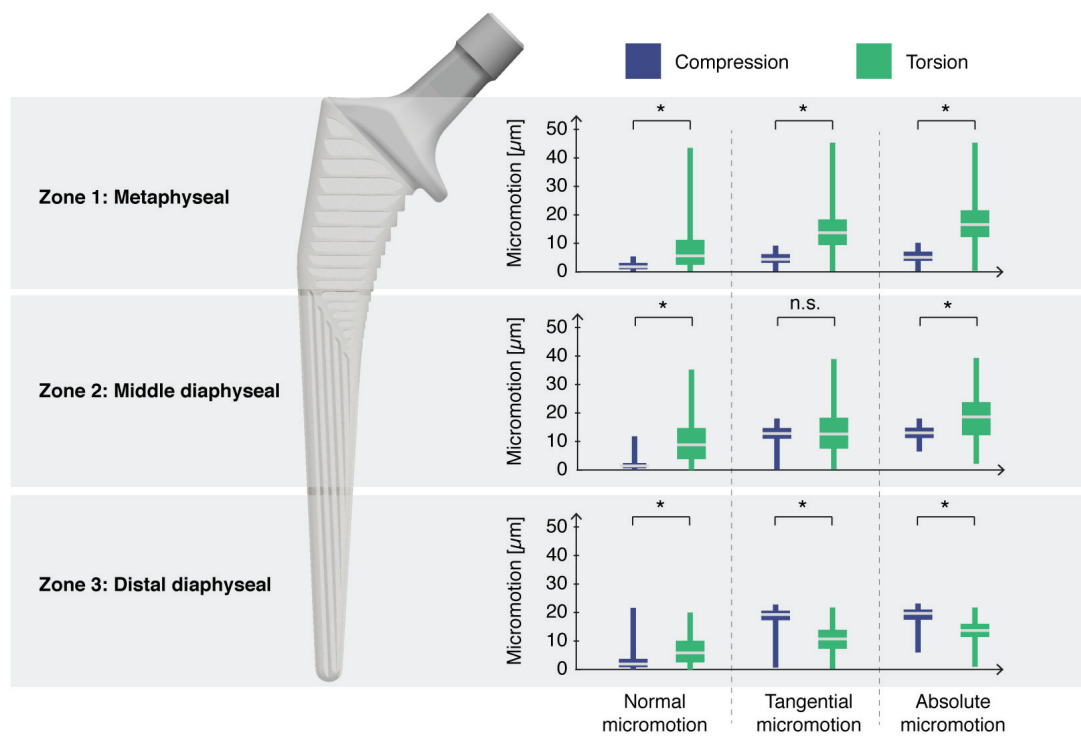


**Figure 2.5:** Distribution of normal, tangential, and absolute micromotion in compression and torsion by zone of the femoral stem. Box plots show median value (white line), 1<sup>st</sup> and 3<sup>rd</sup> quartiles (bottom and top of the box), and minimum and maximum values (whiskers). Stars (\*) indicate significant difference between pairs of distributions (p-value < 0.0001) using Mann-Whitney U test.



In combination with appropriate scanning parameters, this approach represents the first reported experimental technique leading to a full-field map of interface micromotion around the entire stem.

We tested and compared micromotion values in compression and torsion. We obtained over 300 measurement points spread at the bone-stem interface, and were able to observe local variations of micromotion depending on the loading case. The maximum bias was  $5.1 \mu\text{m}$  and the repeatability limit was  $11.5 \mu\text{m}$ , which demonstrates that the technique is highly reliable. The direction of micromotion was distinctly inferior for compression, which is consistent with the axial compressive loading applied. In torsion, normal and tangential micromotion were both comparable in amplitude, in good agreement with an axial torsion of the stem. The stem used in this study is designed to achieve metaphyseal fixation, and consistently, bone-implant gap was particularly low in this zone (Fig. A.1). The metaphyseal region corresponded indeed to a region of low micromotion in compression, but we observed high micromotion in torsion. Generally speaking, there didn't seem to be a direct visual correspondence between local bone-implant gap and micromotion.

The validity of the rigid body assumption for the implant has been rigorously verified by calculating the root mean square error (RMSE) of the rigid body registration. The RMSE was approximately  $3 \mu\text{m}$ , negligible compared to the expected values of interfacial micromotion. Scanning duration was 170 min which is a rather long scanning time. It remained however acceptable, because load relaxation was limited to 1% load loss in compression and 4% in torsion during this time. The fixation of the bone markers was challenging. The markers diameter was chosen to let them penetrate the bone trabeculae, but in the distal medullary canal, cancellous bone is rare. In this region, the markers were simply deposited on the endosteal surface of the bone. Bone markers contiguous to the stem and not well fixed to the bone were a major concern because they could move along with the implant and lead to the underestimation of micromotion. To avoid this issue, the automatic segmentation script removed all bone markers that were in contact with the femoral stem from the measurement. Despite all our efforts, some markers in the metaphyseal area did not enter bone trabeculae and were in direct contact with both the bone and the implant. This situation modifies the original interface and can have an impact on the measurement. However, our results were compatible with measurements obtained with LVDTs. This encourages us to think that this modification of the interface does not change dramatically the magnitude of micromotion. With our method, the distal femur was cemented at approximately half the length of the femur (i.e. at the level of the isthmus) for both loading cases, which is not representative of the actual constraints on the bone and modifies the stress and strain distributions in the femur.

However, we were limited by the size of our micro-CT scanner and moving the constraint further away was impossible. For the same reason, the compressive loading was applied on the stem extraction threaded hole of the stem shoulder instead of the implant neck and axial compression and torsion were tested separately, which does not represent a physiological loading of the stem. However, this simplified loading case is easily reproducible in a FE element model and would be perfectly suited for the purpose of FE model validation. Finally, this study was limited to one formalin-fixed femur, for which the mechanical properties are degraded compared to a fresh bone (Currey et al., 1995; Öhman et al., 2008; Stefan et al., 2010). Nevertheless, this allowed us to demonstrate the feasibility of the technique, while avoiding tissue degradation which would have emerged with a fresh frozen bone during the multiple tests conducted in this study.

In general, our results were in good agreement with results reported in the literature. We measured absolute micromotion values that ranged from 0 to 40  $\mu\text{m}$ . Pettersen et al. (2009) measured micromotion in the same range using LVDTs around straight cementless stems in fresh-frozen femurs. Similarly, Abdul-Kadir et al. (2008) measured micromotion of up to 20  $\mu\text{m}$  with LVDTs for an axial compression on the stem shoulder, which is identical to our results. We found higher micromotion in torsion (stair climbing) than in compression (walking). This result compares well with results from Enoksen et al. (2014) and Kassi et al. (2005) obtained with LVDTs or with measurements from postmortem retrieval sections by Mann et al. (2012). The patterns of micromotion revealed that for axial compression, micromotion was low proximally and high distally. Pancanti et al. (2003) observed a similar pattern with a FE model. Moreover, this finding is consistent with the femoral stem design, thought to achieve stabilization in the metaphyseal area (Vidalain, 2010). In torsion, we found high micromotion proximally and lower micromotion distally. Kassi et al. (2005) and Pancanti et al. (2003) also measured higher micromotion proximally but they had a second region of high micromotion at the tip of the stem. Differences in loading and constraints can be possible explanations for this variation.

The reliability of the method was evaluated through bias and repeatability. Maximum bias was 5.1  $\mu\text{m}$ . Although this value is high compared to the accuracy that can be obtained with LVDTs, it remains sufficient to be used for the validation of FE models or for comparing different stems designs. The repeatability standard deviation reached a maximum of 4.1  $\mu\text{m}$ . This value encompasses random errors due to the precision of loading, to the transmission of load to the femoral stem, and to the viscoelastic behavior of bone. It can be compared to similar measures of repeatability performed for LVDTs setups: Monti et al. (1999) obtained a maximum value of 5  $\mu\text{m}$  for intra-specimen standard deviation, Viceconti et al. (2000)

measured a maximum intra-specimen variability of 9  $\mu\text{m}$ , while Kassi et al. (2005) and Østbyhaug et al. (2010) got values of 3  $\mu\text{m}$  and 1.65  $\mu\text{m}$  respectively for repeatability standard deviation. The repeatability of micro-CT based micromotion measurement is thus similar to the repeatability of LVDT-based micromotion measurement.

The technique we proposed here relies on radiopaque markers with different radiopacity and size attached to the bone and the implant to overcome the difficulty of imaging directly the bone-implant interface. The bias and repeatability of the technique were comparable to those of LVDT-based measurements, making it a technique as reliable as the current gold standard. This resulted in a unique full-field map of micromotion around a cementless femoral stem, that may be used to compare the local effects of different implant designs or to corroborate FE results. Notably, the validation of patient-specific models that predict the level of bone-implant micromotion may be a promising application of the proposed technique. Indeed, a validated model could be used for pre-operative planning to compare the performance of different stem designs, of different surgical techniques, or of different stem positions for a given patient. This may improve our understanding of primary implant stability and may lead to enhanced long-term success of cementless total hip arthroplasty.

## Acknowledgements

This work was supported by the Swiss National Science Foundation (#141152) and the SwissLife Jubiläumstiftung. The authors would like to thank DePuy Synthes (DePuy Synthes Joint Reconstruction, Warsaw, IN, USA) for donating the femoral stem and providing CAD files, the Lausanne University Hospital (CHUV) for providing the cadaveric femur, and Alejandro Dominguez and the Centre Universitaire Romand de Médecine Légale (CURML) for the CT-scans of the femur.

## References

- ASTM (2013). “E177 - 14 - Standard Practice for Use of the Terms Precision and Bias in ASTM Test Methods”. In:
- Abdul-Kadir, Mohammed Rafiq et al. (2008). “Finite element modelling of primary hip stem stability: The effect of interference fit”. In: *Journal of Biomechanics* 41.33, pp. 587–594.
- Australian Orthopaedic Association National Joint Replacement Registry (2015). *Annual Report*.
- Bah, Mamadou T et al. (2015). “Inter-subject variability effects on the primary stability of a short cementless femoral stem”. In: *Journal of Biomechanics* 48.66, pp. 1032–1042.

- Bergmann, G et al. (2010a). “Erratum: Realistic loads for testing hip implants (Bio-Medical Materials and Engineering (2010) 20 (65-75))”. In: *Bio-Medical Materials and Engineering* 20.66, p. 381.
- (2010b). “Realistic loads for testing hip implants”. In: *Bio-Medical Materials and Engineering* 20.22, pp. 65–75.
- Besl, P J and H D McKay (1992). “A method for registration of 3-D shapes”. In: *IEEE Transactions on Pattern Analysis and Machine Intelligence* 14.22, pp. 239–256.
- Boas, F Edward and Dominik Fleischmann (2012). “CT artifacts: Causes and reduction techniques”. In: *Imaging in Medicine* 4.22, pp. 229–240.
- Currey, John D et al. (1995). “Effect of formaldehyde fixation on some mechanical properties of bovine bone”. In: *Biomaterials* 16.1616, pp. 1267–1271.
- Engh, Charles A et al. (1992). “Quantification of Implant Micromotion, Strain Shielding, and Bone Resorption With Porous-Coated Anatomic Medullary Locking Femoral Prostheses”. In: *Clinical Orthopaedics and Related Research* 285285, pp. 13–29.
- Enoksen, Cathrine H et al. (2014). “Initial stability of an uncemented femoral stem with modular necks. An experimental study in human cadaver femurs”. In: *Clinical Biomechanics* 29.33, pp. 330–335.
- Fottner, Andreas et al. (2009). “Biomechanical evaluation of two types of short-stemmed hip prostheses compared to the trust plate prosthesis by three-dimensional measurement of micromotions”. In: *Clinical Biomechanics* 24.55, pp. 429–434.
- Gortchacow, Michael et al. (2011). “A new technique to measure micromotion distribution around a cementless femoral stem”. In: *Journal of Biomechanics* 44.33, pp. 557–560.
- Gortchacow, Michael et al. (2012). “Simultaneous and multisite measure of micromotion, subsidence and gap to evaluate femoral stem stability”. In: *Journal of Biomechanics* 45.77, pp. 1232–1238.
- Gruen, Thomas A, Gregory M McNeice, and Harlan C Amstutz (1979). “‘Modes of Failure’ of Cemented Stem-type Femoral Components”. In: *Clinical Orthopaedics and Related Research* 141141, pp. 17–27.
- Kassi, Jean-Pierre et al. (2005). “Stair climbing is more critical than walking in pre-clinical assessment of primary stability in cementless THA in vitro”. In: *Journal of Biomechanics* 38.55, pp. 1143–1154.
- Leys, Christophe et al. (2013). “Detecting outliers: Do not use standard deviation around the mean, use absolute deviation around the median”. In: *Journal of Experimental Social Psychology* 49.44, pp. 764–766.
- Mann, Kenneth A et al. (2012). “Interface Micromotion of Uncemented Femoral Components from Postmortem Retrieved Total Hip Replacements”. In: *The Journal of Arthroplasty* 27.22, pp. 238–245.

- Monti, Luisa, Luca Cristofolini, and Marco Viceconti (1999). "Methods for Quantitative Analysis of the Primary Stability in Uncemented Hip Prostheses". In: *Artificial Organs* 23.99, pp. 851–859.
- Öhman, Caroline et al. (2008). "The effects of embalming using a 4compressive mechanical properties of human cortical bone". In: *Clinical Biomechanics* 23.1010, pp. 1294–1298.
- Østbyhaug, Per Olav et al. (2010). "Primary stability of custom and anatomical uncemented femoral stems". In: *Clinical Biomechanics* 25.44, pp. 318–324.
- Pancanti, Alberto, Marek Bernakiewicz, and Marco Viceconti (2003). "The primary stability of a cementless stem varies between subjects as much as between activities". In: *Journal of Biomechanics* 36.66, pp. 777–785.
- Pettersen, Sune H, Tina S Wik, and Bjørn Skallerud (2009). "Subject specific finite element analysis of implant stability for a cementless femoral stem". In: *Clinical Biomechanics* 24.66, pp. 480–487.
- Pilliar, R M, J M Lee, and C Maniopoulos (1986). "Observations on the Effect of Movement on Bone Ingrowth into Porous-Surfaced Implants". In: *Clinical Orthopaedics and Related Research* 208208, pp. 108–113.
- Ploeg, Bas van der et al. (2011). "Toward a more realistic prediction of peri-prosthetic micro-motions". In: *Journal of Orthopaedic Research* 30.77, pp. 1147–1154.
- Reggiani, B et al. (2007). "Predicting the subject-specific primary stability of cementless implants during pre-operative planning: Preliminary validation of subject-specific finite-element models". In: *Journal of Biomechanics* 40.1111, pp. 2552–2558.
- Roberts, Bryant C, Egon Perilli, and Karen J Reynolds (2014). "Application of the digital volume correlation technique for the measurement of displacement and strain fields in bone: A literature review". In: *Journal of Biomechanics* 47.55, pp. 923–934.
- Søballe, Kjeld et al. (2009). "Hydroxyapatite coating modifies implant membrane formation". In: *Acta Orthopaedica Scandinavica* 63.22, pp. 128–140.
- Stefan, Unger, Blauth Michael, and Schmoelz Werner (2010). "Effects of three different preservation methods on the mechanical properties of human and bovine cortical bone". In: *Bone* 47.66, pp. 1048–1053.
- Sukjamsri, Chamaiporn et al. (2015). "Digital volume correlation and micro-CT: An in-vitro technique for measuring full-field interface micromotion around polyethylene implants". In: *Journal of Biomechanics* 48.1212, pp. 3447–3454.
- Taylor, Mark and Patrick J Prendergast (2015). "Four decades of finite element analysis of orthopaedic devices: Where are we now and what are the opportunities?" In: *Journal of Biomechanics* 48.55, pp. 767–778.

- Viceconti, Marco et al. (2000). “Large-sliding contact elements accurately predict levels of bone–implant micromotion relevant to osseointegration”. In: *Journal of Biomechanics* 33.1212, pp. 1611–1618.
- Viceconti, Marco et al. (2006). “Primary stability of an anatomical cementless hip stem: A statistical analysis”. In: *Journal of Biomechanics* 39.77, pp. 1169–1179.
- Vidalain, Jean Pierre (2010). “Twenty-year results of the cementless Corail stem”. In: *International Orthopaedics* 35.22, pp. 189–194.

# Chapter 3

## The effects of a collar on the primary stability of cementless femoral stems

*This chapter is based on:*

Effect of a collar on subsidence and local micromotion of cementless femoral stems.

V. Malfroy Camine, H. A. Rüdiger, D. P. Pioletti, A. Terrier, 2016

Submitted for review and publication



## Abstract

The addition of a collar to the design of femoral stems in total hip arthroplasty (THA) is thought to improve primary axial and rotational stability. However, there is still substantial controversy as to whether collared designs are preferable to collarless designs in cementless THA. A perfect contact between the collar and the calcar requires additional surgical steps and may be difficult to achieve. The collar may also prevent the complete settling of the stem. Reported revision rates indicate no significant difference in the long-term survival of collarless and collared versions of the same stem, and biomechanical evidences that a collar does improve primary stability are scarce. The aim of this cadaveric study is to quantitatively compare the difference in primary stability between collarless and collared versions of the same femoral stem. Specifically, we asked: (1) Does a collar prevent stem subsidence? (2) Is there a difference in local micromotion around collarless and collared designs during compressive or torsional loadings?

Collarless and collared versions of the same cementless femoral stem were implanted in two groups of six fresh-frozen cadaveric femurs. Each implanted femur was then subsequently tested for axial compressive and torsional loadings. A micro-CT based technique was applied to quantify implant subsidence and compute the map of local micromotion around the femoral stems. Micromotion of collarless and collared stems was compared in each Gruen zone using a Mann-Whitney-U test.

Subsidence was  $41.0 \mu\text{m} \pm 29.9 \mu\text{m}$  for collarless stems and  $37.0 \mu\text{m} \pm 44.6 \mu\text{m}$  for collared ones, and there was no significant difference between the two groups. For compressive loading, micromotion was  $19.5 \mu\text{m} \pm 5 \mu\text{m}$  in collarless stems and  $43.3 \mu\text{m} \pm 33.1 \mu\text{m}$  in collared ones. For torsional loading, micromotion was  $96.9 \mu\text{m} \pm 59.8 \mu\text{m}$  with collarless stems and  $118.7 \mu\text{m} \pm 45.0 \mu\text{m}$  with collared ones. We found no significant difference in local micromotion between collarless and collared design, except in Gruen zone 1 for compression ( $p = 0.001$ ), where mean micromotion was  $7.0 \mu\text{m} \pm 0.6 \mu\text{m}$  in the collarless group and  $22.6 \mu\text{m} \pm 25.5 \mu\text{m}$  in the collared group. A good primary stability was achieved in most cases for both stem designs with a mean micromotion of  $37.4 \mu\text{m}$  in compression and  $119.9 \mu\text{m}$  in torsion, which is below the threshold for osseointegration ( $<150 \mu\text{m}$ ).

The results of this study indicate a similar primary stability between collarless and collared stems, and no influence of the collar on subsidence or micromotion at the local level. Further studies are required to investigate whether collars may be advantageous in the presence of higher loads, undersized stems, or for decreased bone densities.



## Introduction

Since the introduction of cementless total hip arthroplasty (THA) in the late 1950s, many design modifications have been proposed to improve the primary stability and long-term survival of femoral stems. Collared designs are thought to enhance primary stability and hence osseointegration by improving resistance to axial, rotational, and varus forces at the proximal bone implant interface. This might be of particular importance in view of the current trend to allow for early weight bearing after total hip arthroplasty. However, the use of collared designs is controversial, as some surgeons raised concerns in regards to their downsides. For an optimal load transmission, a perfect contact between the collar and the calcar is a mandatory prerequisite. But this necessitates additional surgical steps and increases the duration of surgery. In addition, the presence of a collar may prevent the full settling of the stem in the medullary canal. Finally, a collar may complicate extraction when removal of an integrated stem becomes necessary.

Clinical studies have reported no difference in the revision rate of collarless and collared versions of the same stem (Hutt et al., 2014). In contrast, Demey et al. (2011) reported that a collar increased the force required to initiate implant subsidence and intraoperative periprosthetic fractures. The choice between collarless or collared design appears to be mainly based on the surgeon's preference.

Primary stability is characterized by interfacial bone-implant micromotion before osseointegration occurs. A good primary implant stability is associated with low micromotion, and is critical for the long-term success of THA. Nevertheless, quantitative data on the differences in primary stability between collarless and collared stems are scarce, and the available studies are based on finite-element models, which were not validated experimentally (Ebramzadeh et al., 2004; Mandell et al., 2004).

Therefore, the purpose of this study was to determine whether there is a difference in primary stability between collarless and collared versions of the same femoral stem. Specifically, we asked the following questions: (1) Does a collar prevent stem subsidence? (2) Is there a difference in local micromotion around collarless and collared designs during compressive and (3) torsional loadings? To answer these questions, we used a novel *in vitro* technique providing the complete map of local micromotion on the intramedullary surface of femoral stems (Gortchacow et al., 2012; Gortchacow et al., 2011; Malfroy Camine et al., 2016).

## Materials and methods

Collarless and collared versions of the same cementless femoral stem were implanted in two groups of six fresh-frozen cadaveric femurs. Each implanted femur was then subsequently tested for axial compressive and torsional loading. A micro-CT based technique was applied to quantify implant subsidence and local micromotion around the femoral stems.

### *Human cadaver femurs*

Twelve fresh-frozen human cadaveric femurs (National Disease Research Interchange, Philadelphia, PA, USA) were wrapped in saline-soaked gauze, placed in airtight plastic bags and stored at -70 °C immediately after dissection. The selection criteria excluded femurs of individuals with a history of radiation or malignant disease, or previous femoral fractures. There were three female and nine male donors, ranging in age from 32 to 93 years old (mean 71 years old). Mean donor weight was 83 kg (range 56 - 143 kg) and mean donor body mass index (BMI) was 29 kg/m<sup>2</sup> (range 18.3-47.8 kg/m<sup>2</sup>) (Table B.1).

Before broaching of the medullary canal, the specimens were thawed overnight at room temperature in saline solution and remaining soft tissues were removed. Femoral neck cut and compaction broaching were performed by a senior orthopedic surgeon following the recommendations of the manufacturer and using the original instrumentation. Briefly, the proximal metaphyseal bone was compacted using the bone tamp. The broaches were then impacted in increasing sizes with multiple hammer blows manually until axial stability was achieved. Then, rotational stability was tested by turning the broach handle manually clock and counter-clock wise. The stem was considered clinically stable when no macroscopic movement at the bone-implant interface could be observed. Around 1000 stainless steel spherical markers (diameter 600 μm, MPS Micro Precision Systems AG, Biel, Switzerland) were then manually press-fitted uniformly in the metaphyseal cancellous bone and on the endosteal surface of the femoral canal using a spatula.

### *Implant system*

Six collarless and six collared versions of the same cementless femoral stem (Corail®Hip System, DePuy Synthes Joint Reconstruction, Warsaw, IN, USA) were selected for implantation (Fig. 3.1). The stem is made of forged titanium alloy (TiAl6V4), with standard offset neck, and is fully coated with 155 μm of hydroxyapatite. Thirty-seven tantalum spherical markers of diameter 800 μm (X-medics Scandinavia, Frederiksberg, Denmark) were glued (Loctite 401, Loctite 55 Corporation, Dublin, Ireland) uniformly on the stem surface, within drilled holes

of 1 mm depth and 850  $\mu\text{m}$  diameter. Due to the limited size of the micro-CT scanner, the femoral necks of the stems were cut 27 mm medial and parallel to the implant extraction threaded hole axis. Femoral stems were then implanted, and the femurs were wrapped in saline-soaked gauze, placed in airtight plastic bags and stored again at  $-70\text{ }^{\circ}\text{C}$ .

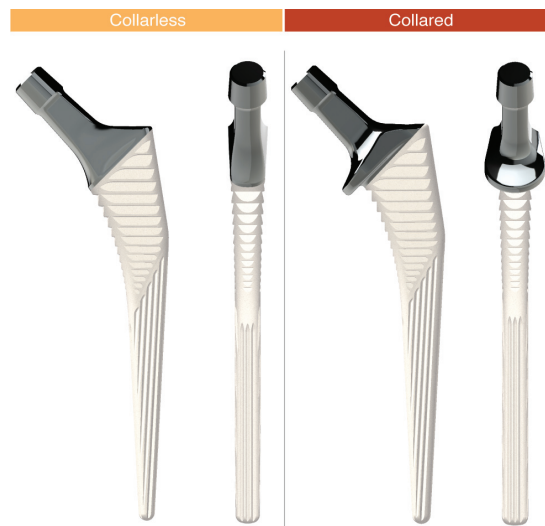


**Figure 3.1:** Collarless (left) and collared (right) versions of the straight cementless femoral stem.

### ***Implant loading***

Before testing, the femurs were thawed at room temperature, and kept humid with saline-soaked gauze during all subsequent preparation and testing steps. All femurs were successively tested for axial compression and axial torsion using two separate loading devices, designed to fit inside a micro-CT scanner (Fig. 3.2). The test setup and devices have been previously described in details (Malfroy Camine et al., 2016).

For compression testing, distal part of each femur was potted in epoxy resin 30 mm away from the distal end of the stem. Minimal reaming of the lateral surface of the greater trochanter (2-3 mm) was performed to enable proper fitting inside the device. For each femur, a load corresponding to 230% of donor's body weight (BW) was applied on the shoulder of the stem, aligned with the stem extraction threaded hole axis. The load was chosen according to the average load during walking measured with instrumented hip implants (Bergmann et al., 2010b; Bergmann et al., 2010a). Before testing, the bone was pre-conditioned with 10 successive compressive loads, to enable full settling of the stem in the bone cavity.

For torsion testing, the femurs were again potted distally with epoxy resin and a clamping system was used to restrain the proximal stem. For each femur, a moment corresponding to

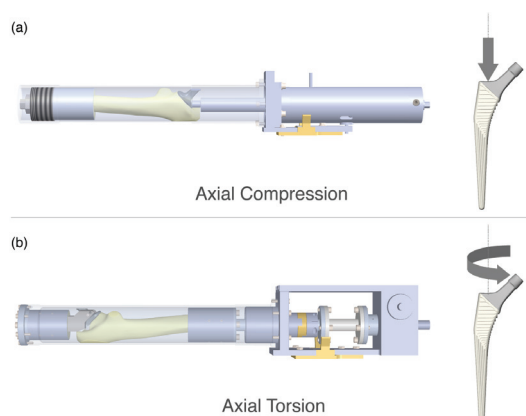


**Figure 3.2:** Loading devices designed to fit inside the micro-CT scanner. (a) Axial compression loading device. The distal femur is cemented and compression is applied through a cylinder driven by a screw jack. (b) Axial torsion loading device. The proximal stem is restrained by a clamping system. The proximal stem and the distal femur are cemented. Torsion is applied through a worm gear.

2.3% BW  $\times$ m was applied around the stem extraction threaded hole axis (internal rotation of the stem). The load was chosen according to the average moment during stair climbing measured with instrumented hip implants (Bergmann et al., 2010b; Bergmann et al., 2010a). Before testing, the bone was pre-conditioned with 10 successive torsional loads.

#### ***Subsidence and micromotion measurement***

Subsidence was defined as the irreversible vertical migration of the implant after loading, while local micromotion was defined as the reversible elastic motion of the stem during loading. Implant subsidence and micromotion were measured for both compressive and torsional loadings using a previously described micro-CT technique (Malfroy Camine et al., 2016), that enables *in vitro* measurements around femoral stems with a measurement bias of 5.5  $\mu$ m.

To measure implant subsidence and local micromotion in compression, three successive micro-CT scans of the whole bone-implant interface were performed: the first scan was performed without load and represented the initial state before pre-conditioning of the bone, the second scan was performed while compressive load was applied, and the third scan was performed after the compressive load had been removed. Bone and implant markers were then automatically segmented on the reconstructed images, and the three scans were rigidly registered based on implant markers positions to align all scans in the same coordinate system. Subsidence was calculated as the mean vertical displacement of corresponding bone markers between the initial unloaded scan and the final unloaded scan. Local micromotion

was obtained from the 3D displacement vector between corresponding bone markers in the loaded scan and the final unloaded scan (Fig. 3.3). Similarly, to measure local implant micromotion in torsion, two successive micro-CT scans of the whole bone-implant interface were performed: the first scan was obtained while torsional load was applied, and the second one after the torsional load had been removed. Local micromotion was computed from the 3D displacement vector between corresponding bone markers in the loaded scan and the unloaded scan.

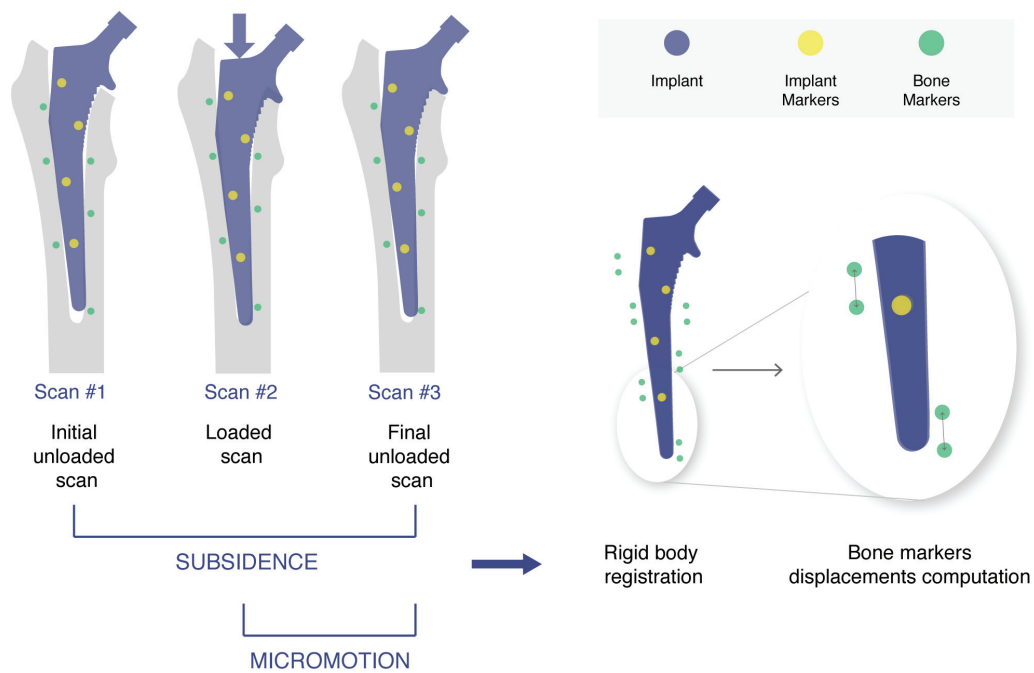


**Figure 3.3:** Subsidence and micromotion computation. Three successive scans are performed, an initial unloaded scan, a loaded scan, and a final unloaded scan. The scans are aligned in the same coordinate system using rigid registration of implant markers. Subsidence is the displacement of corresponding bone markers from the registered initial unloaded scan to the final unloaded scan. Micromotion is the displacement of corresponding bone markers from the registered loaded scan to the final unloaded scan.

### Data analysis

Two femurs in the collarless group did not complete the testing. One femur was excluded due to a periprosthetic fracture during compressive loading. Another femur had to be excluded because measurement data were unusable after a failure of the imaging system.

All data analysis was carried out in MATLAB (Matlab r2016a, The Mathworks, Inc., Natick, MA, USA). The micromotion vector was calculated at each point and its absolute value (i.e.

magnitude) was determined. The micromotion vector was further divided into its tangential and normal components, relative to the stem surface. Natural-neighbor interpolation between all measurement points was used to create maps of micromotion on each stem's surface.

The femoral stems were divided into 12 zones corresponding to Gruen zones 1 to 3, 5 to 10, and 12 to 14 (Gruen et al., 1979). To investigate the relationship between median micromotion or median subsidence, and donor's age, weight, BMI, and implant size, the Spearman's rank correlation coefficient was evaluated and its significance was assessed using a permutation test. A Mann-Whitney U-test was chosen to compare collarless and collared stems subsidence, because this test does not make assumptions about homogeneity of variances or normal distributions of the data. The same Mann-Whitney U-test was used to compare median micromotion between collarless and collared stems in each Gruen zone. The significance level for all statistical tests performed was set to 0.05.

## Results

Mean stem subsidence was  $41.0 \mu\text{m} \pm 29.9 \mu\text{m}$  in the collarless group and  $37.0 \mu\text{m} \pm 44.6 \mu\text{m}$  in the collared group. The difference between these groups was not statistically significant ( $p=0.352$ ) (Fig. 3.4).

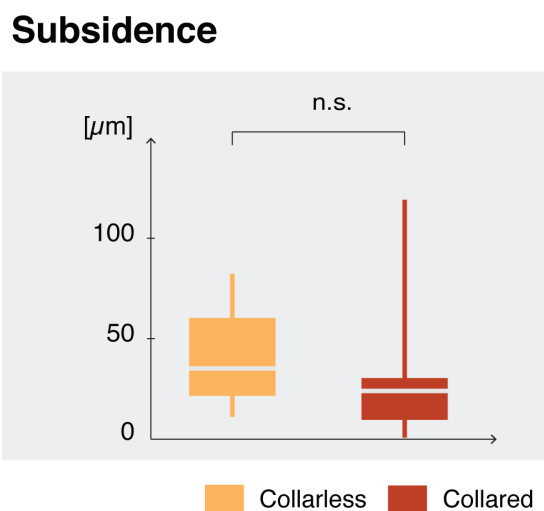


**Figure 3.4:** Subsidence of collarless ( $n=4$ ) and collared ( $n=6$ ) stems. Box plots show median value (light grey line), 1<sup>st</sup> and 3<sup>rd</sup> quartiles (bottom and top of the box), and minimum and maximum values (whiskers). *n.s.* indicates non-significant difference between pairs of distributions ( $p$ -value  $< 0.05$ ) using Mann-Whitney U test.

We obtained between 213 and 432 simultaneous measurement points uniformly distributed around each implant, resulting in full-field maps of micromotion around the stems for compressive and torsional loads (Fig. 3.5). In compression, mean absolute micromotion was  $19.5 \mu\text{m} \pm 5 \mu\text{m}$  in the collarless group and  $43.3 \mu\text{m} \pm 33.1 \mu\text{m}$  in the collared group. The only significant local difference between the collarless and the collared group occurred for absolute micromotion in Gruen zone 1 ( $p = 0.01$ ), with a mean absolute micromotion of  $7.0 \mu\text{m} \pm 0.6 \mu\text{m}$  for the collarless group and  $22.6 \mu\text{m} \pm 25.5 \mu\text{m}$  for the collared group (Fig. 3.6). In all other Gruen zones, there was no significant difference between the collarless and collared groups, for absolute micromotion, and components of micromotion normal and tangential to the stem's surface. For both stem designs, micromotion was lower around the proximal part of the stem (Gruen zones 1,7, 8 and 14) and higher distally.

In torsion, absolute micromotion was higher than in compression, with a mean of  $96.9 \mu\text{m} \pm 59.8 \mu\text{m}$  in the collarless group and  $118.7 \mu\text{m} \pm 45.0 \mu\text{m}$  in the collared group. There was no significant difference between collarless and collared stems in all Gruen zones in regards to absolute micromotion, or normal or tangential components (Fig. 3.7).

There was no significant correlation between patient's age, weight, BMI or implant size, and stem subsidence or micromotion ( $p > 0.05$ ). For all stems, mean micromotion was  $37.4 \mu\text{m}$  in compression and  $119.9 \mu\text{m}$  in torsion, which is below the reported maximum threshold allowing osseointegration ( $< 150 \mu\text{m}$ ) (Engh et al., 1992; Pilliar et al., 1986). One of the femur in the collared group presented with much higher stem micromotion in torsion than the rest of the femurs. For this femur, mean micromotion in torsion was  $252.9 \mu\text{m}$  and micromotion reached a maximum of  $625.9 \mu\text{m}$  locally, in Gruen zone 1.

## Discussion

Collared stems in cementless THA have gained increasing popularity based on the hypothesis that they enhance implant primary stability. However, there is only limited evidence to support this hypothesis. Clinical studies did not show any significant benefit of collared stems in terms of implant survival (Jameson et al., 2013; Meding et al., 1997). Biomechanical studies were limited to finite element modeling (Ebramzadeh et al., 2004; Mandell et al., 2004), which are insufficiently backed by experimental data. Our objective was to determine if there is a significant difference in primary stability between collarless and collared stems, by measuring subsidence and local micromotion around collarless and collared stems in cadaveric femurs, using a previously described micro-CT based *in vitro* technique. We found no significant differences in subsidence or local micromotion between collarless and col-

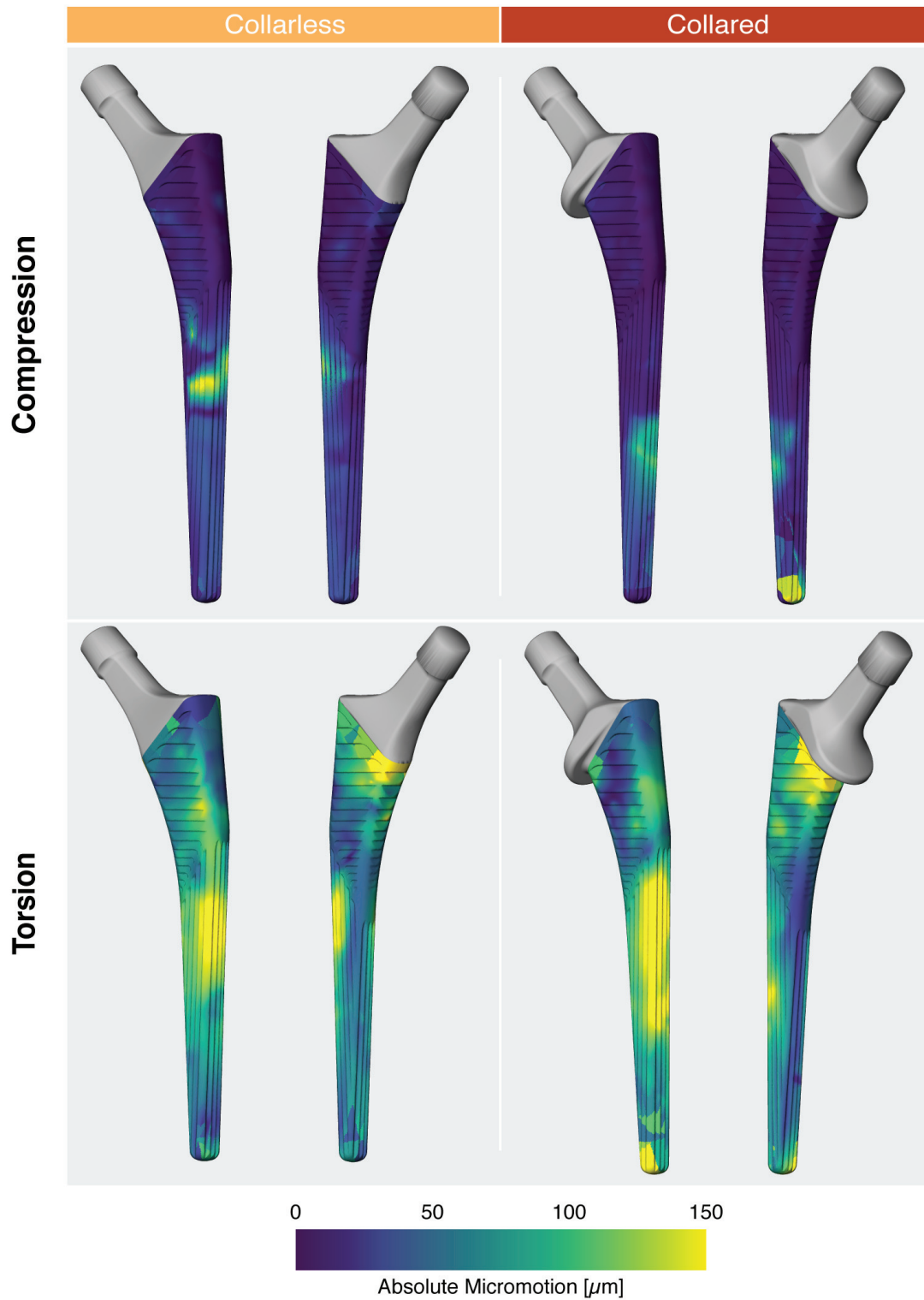


**Figure 3.5:** Sample distribution of absolute micromotion around one collarless stem and one collared stem - Anterior/lateral and posterior/medial views of the stem displayed successively from left to right for each case. Top row shows results obtained in compression. The bottom row shows results obtained in torsion.



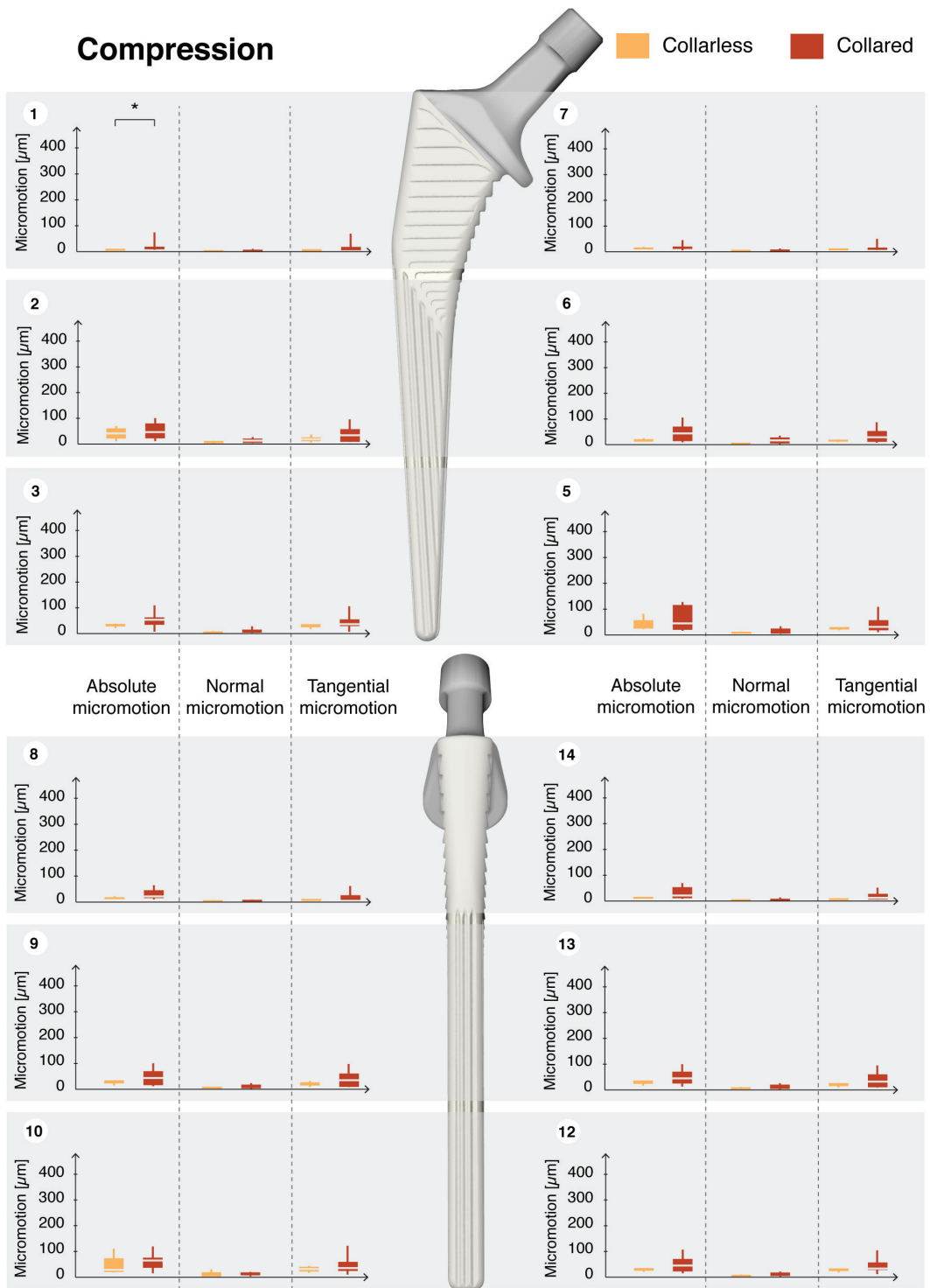


**Figure 3.6:** Distribution of absolute, normal, and tangential micromotion in compression by Gruen zone around collarless (n=4) and collared (n=6) stems. Box plots show median value (light grey line), 1<sup>st</sup> and 3<sup>rd</sup> quartiles (bottom and top of the box), and minimum and maximum values (whiskers). Star (\*) indicates significant difference between pairs of distributions (p-value<0.05) using Mann-Whitney U test.

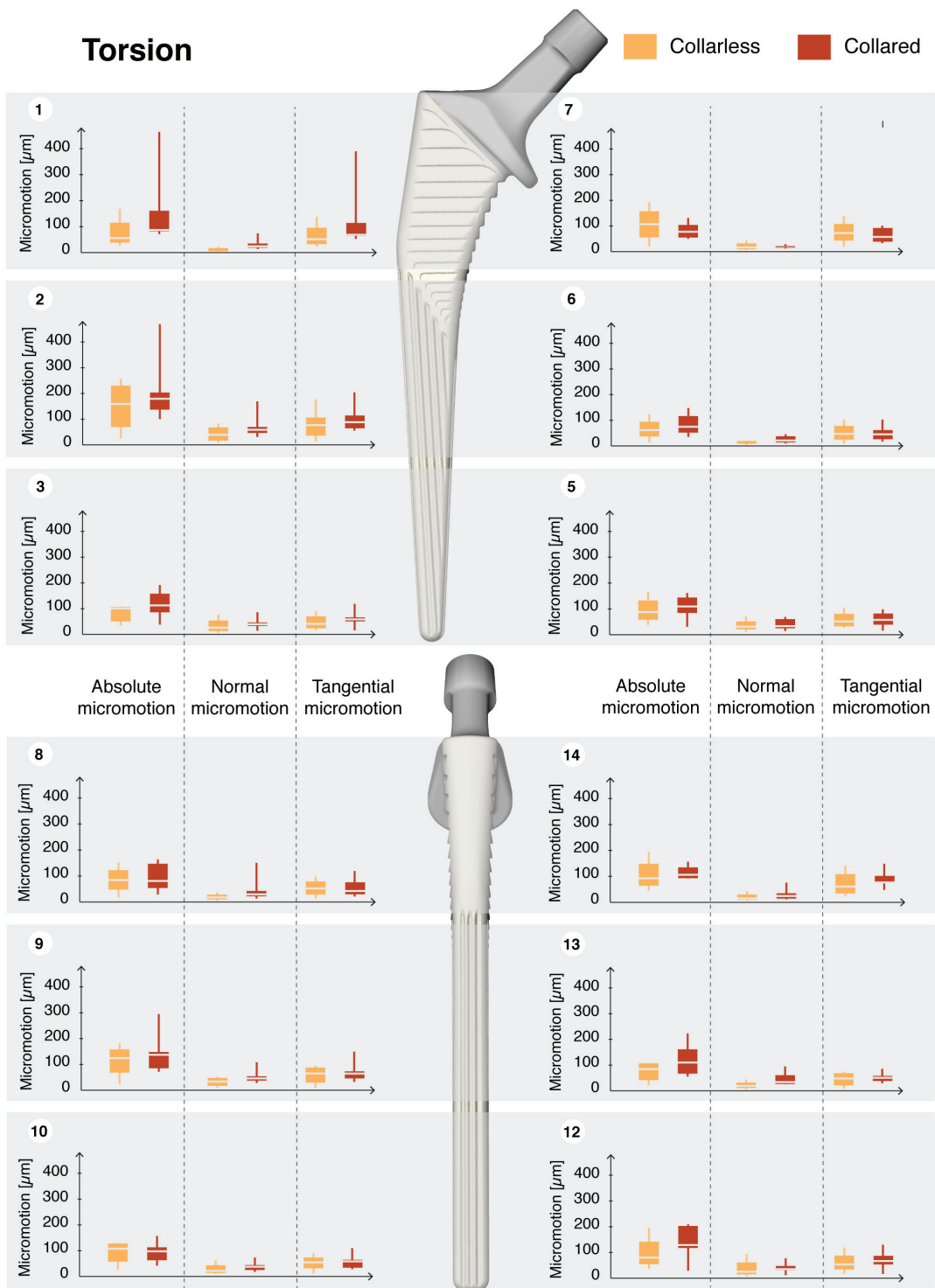


**Figure 3.7:** Distribution of absolute, normal, and tangential micromotion in torsion by Gruen zone around collarless (n=4) and collared (n=6) stems. Box plots show median value (light grey line), 1<sup>st</sup> and 3<sup>rd</sup> quartiles (bottom and top of the box), and minimum and maximum values (whiskers).

lared designs, except for a small variation in micromotion in Gruen zone 1 in compression. Both stem designs had good primary stability, with mean micromotion below the 150  $\mu\text{m}$  osseointegration limit.

There are a number of weaknesses in this study. First, the sample size in this technically demanding study is small and anatomy and bone quality vary between the two study groups. Moreover, the implantation of the stems into dissected cadaveric femurs is facilitated by the absence of soft tissue and a strong press-fit was achieved in all cases. It is possible that in a clinical setting, where the positioning and press-fit may not be optimal, the results could be very different. In addition, the loading protocol used in this study separated axial compressive load and axial torsional load, in order to enable stem's loading inside a micro-CT scanner. The axial compressive load was applied at the axis stem's body and not on the femoral head due to technical reasons. Rotational forces in the frontal plane might be insufficiently represented by this setup. Consequently, the results may have been partially affected by the fact that these loadings are not physiological. The loads applied in this work correspond to those encountered during activities of daily living under full weight bearing. Higher loads (e.g. during stumbling or in obese patients) may lead to different results. Finally, owing to the complexity of the experimental protocol, multiple thawing and freezing cycles of the femurs were necessary. In order to preserve the mechanical properties of bone, all freezing and thawing steps were performed within saline solution and the bones were kept humid at all times in between. Previous research showed that multiple freezing and thawing of fresh frozen bone did not affect the specimen's mechanical properties when the above precautions were strictly applied (Kang et al., 1997; Linde et al., 1993).

The absence of significant difference in subsidence between collarless and collared stems is consistent with the work of Meding et al. (1997), who found no difference in subsidence in a prospective randomized study that compared identical cementless stems with and without collar up to 5 years postoperatively. Demey et al. (2011) found in a cadaveric study that collared designs required a significantly higher force to initiate subsidence of the stem and to cause a periprosthetic fracture than collarless stems. However, the force necessary to initiate subsidence of the stem was superior to 3000 N for both groups, which is a much higher load than the ones experienced during activities of daily living. Such high loads might only be encountered in heavy patients or during high impact activities or falls (Bergmann et al., 2016).

Our measurements of micromotion during compression and torsion are in general agreement with previous reports (Bieger et al., 2012; Fottner et al., 2011). Our observation that micromotion is higher in torsion than in compression, regardless of the presence of a collar,

was also reported by several authors (Enoksen et al., 2014; Kassi et al., 2005; Østbyhaug et al., 2010). The technique we used to measure local micromotion, based on micro-CT imaging, offers a novel understanding of the biomechanics behind cementless stems primary stability. The absence of significant difference in local micromotion between collarless and collared in most Gruen zones is in line with clinical studies indicating similar revision rates for both types of implants (Jameson et al., 2013; Meding et al., 1997). This result suggests that there is no significant difference in primary stability between collarless and collared implants. We observed significantly higher absolute micromotion for collared stems in Gruen zone 1 for compressive but not for torsional loading. However, this difference was small (15  $\mu\text{m}$ ), and in view of the results in all other Gruen zones for both types of loading, it seems unlikely that collars are associated with a relevant decrease in primary stability.

Of note, we observed a periprosthetic fracture in one of the specimen implanted with a collarless implant during compressive loading. Despite that some authors reported that collarless stems are at a higher risk of periprosthetic fractures than collared stems (Demey et al., 2011), we don't think that the fracture in this specimen can be conclusively attributed to the collarless design. Indeed, we adapted the load to the donor's body weight, and this resulted for this overweight donor in an extreme load of over 3200N, which we believe explains the fracture. In conclusion, we did not observe differences in primary stability (subsidence and micromotion) between collarless and collared stems, within the limitations of *in vitro* measurements partly replicating activities of daily living. This finding could be beneficial to help surgeons decide between a collarless or a collared implant, as no consensus on this question has been reached yet. Further studies remain necessary to investigate whether collars may be advantageous in the presence of higher loads, undersized stems, or for decreased or increased bone densities or anatomical variants (e.g. varus or valgus necks).

### **Acknowledgements**

This work has been supported by Swiss National Science Foundation (#141152) and the SwissLife Jubiläumstiftung. The authors thank DePuy Synthes (DePuy Synthes Joint Reconstruction, Warsaw, IN, USA) for donating the implants, instruments and CAD files, and Alejandro Dominguez and the Centre Universitaire Romand de Médecine Légale (CURML) for the CT-scans of the femurs.

## References

- Bergmann, G et al. (2010a). “Erratum: Realistic loads for testing hip implants (Bio-Medical Materials and Engineering (2010) 20 (65-75))”. In: *Bio-Medical Materials and Engineering* 20.66, p. 381.
- (2010b). “Realistic loads for testing hip implants”. In: *Bio-Medical Materials and Engineering* 20.22, pp. 65–75.
- Bergmann, Georg et al. (2016). “Standardized loads acting in hip implants”. In: *PloS One* 11.55, e0155612.
- Bieger, Ralf et al. (2012). “Primary stability and strain distribution of cementless hip stems as a function of implant design”. In: *Clinical Biomechanics* 27.22, pp. 158–164.
- Demey, Guillaume et al. (2011). “Does a Collar Improve the Immediate Stability of Uncemented Femoral Hip Stems in Total Hip Arthroplasty? A Bilateral Comparative Cadaver Study”. In: *The Journal of Arthroplasty* 26.88, pp. 1549–1555.
- Ebramzadeh, E et al. (2004). “Initial stability of cemented femoral stems as a function of surface finish, collar, and stem size”. In: *The Journal of Bone and Joint Surgery. American Volume* 86A.11, pp. 106–115.
- Engh, Charles A et al. (1992). “Quantification of Implant Micromotion, Strain Shielding, and Bone Resorption With Porous-Coated Anatomic Medullary Locking Femoral Prostheses”. In: *Clinical Orthopaedics and Related Research* 285285, pp. 13–29.
- Enoksen, Cathrine H et al. (2014). “Initial stability of an uncemented femoral stem with modular necks. An experimental study in human cadaver femurs”. In: *Clinical Biomechanics* 29.33, pp. 330–335.
- Fottner, Andreas et al. (2011). “Biomechanical evaluation of different offset versions of a cementless hip prosthesis by 3-dimensional measurement of micromotions”. In: *Clinical Biomechanics* 26.88, pp. 830–835.
- Gortchacow, Michael et al. (2011). “A new technique to measure micromotion distribution around a cementless femoral stem”. In: *Journal of Biomechanics* 44.33, pp. 557–560.
- Gortchacow, Michael et al. (2012). “Simultaneous and multisite measure of micromotion, subsidence and gap to evaluate femoral stem stability”. In: *Journal of Biomechanics* 45.77, pp. 1232–1238.
- Gruen, Thomas A, Gregory M McNeice, and Harlan C Amstutz (1979). “‘Modes of Failure’ of Cemented Stem-type Femoral Components”. In: *Clinical Orthopaedics and Related Research* 141141, pp. 17–27.
- Hutt, Jonathan et al. (2014). “The effect of a collar and surface finish on cemented femoral stems: A prospective randomised trial of four stem designs”. In: *International Orthopaedics* 38.66, pp. 1131–1137.

- Jameson, S S et al. (2013). “Independent predictors of failure up to 7.5 years after 35 386 single-brand cementless total hip replacements”. In: *The Bone and Joint Journal* 95-B.66, pp. 747–757.
- Kang, Q, YHH An, and R J Friedman (1997). “Effects of multiple freezing-thawing cycles on ultimate indentation load and stiffness of bovine cancellous bone”. In: *American Journal of Veterinary Research* 58.1010, pp. 1171–1173.
- Kassi, Jean-Pierre et al. (2005). “Stair climbing is more critical than walking in pre-clinical assessment of primary stability in cementless THA in vitro”. In: *Journal of Biomechanics* 38.55, pp. 1143–1154.
- Linde, Frank and Hans Christian Florian Sørensen (1993). “The effect of different storage methods on the mechanical properties of trabecular bone”. In: *Journal of Biomechanics* 26.1010, pp. 1249–1252.
- Malfroy Camine, Valérie et al. (2016). “Full-field measurement of micromotion around a cementless femoral stem using micro-CT imaging and radiopaque markers”. In: *Journal of Biomechanics*.
- Mandell, Jay A et al. (2004). “A conical-collared intramedullary stem can improve stress transfer and limit micromotion”. In: *Clinical Biomechanics* 19.77, pp. 695–703.
- Meding, John B et al. (1997). “Comparison of collared and collarless femoral components in primary uncemented total hip arthroplasty”. In: *The Journal of Arthroplasty* 12.33, pp. 273–280.
- Østbyhaug, Per Olav et al. (2010). “Primary stability of custom and anatomical uncemented femoral stems”. In: *Clinical Biomechanics* 25.44, pp. 318–324.
- Pilliar, R M, J M Lee, and C Maniopoulos (1986). “Observations on the Effect of Movement on Bone Ingrowth into Porous-Surfaced Implants”. In: *Clinical Orthopaedics and Related Research* 208208, pp. 108–113.

# Chapter 4

## Micromotion-induced fluid flow around a cementless femoral stem

*This chapter is based on:*

Micromotion-induced peri-prosthetic fluid flow around  
a cementless femoral stem.

V. Malfroy Camine, A. Terrier, D. P. Pioletti, 2016

To be submitted for review and publication



## **Abstract**

Micromotion-induced interstitial fluid flow at the bone-implant interface has been proposed to play an important role in aseptic loosening of cementless implants. High fluid velocities are thought to promote aseptic loosening through activation of osteoclasts, shear stress-induced control of mesenchymal stem cells differentiation, or transport of molecules. In this study, our objective was to quantify micromotion-induced fluid flow around a cementless femoral stem using a finite element model based on experimental local micromotion measurements in compression and torsion.

The relative influence of micromotion, bone-implant gap and material properties on peak fluid velocity was investigated using a full-factorial design and an idealized 2D model of the bone-implant interface. Models of transverse sections around a femoral stems were generated based on computed tomography images and micromotion measurement of the same femur. Additionally, a 3D model including a simplified stem's geometry was built and the shear stress experienced by cells hosted in the peri-implant tissues was estimated.

The analysis of the full-factorial design showed that local micromotion had the most influence on peak fluid velocity at the interface. Remarkable variations in fluid velocity were observed in the macrostructures at the surface of the implant in the 2D transverse sections of a the stem. Finally, the 3D model predicted peak fluid velocities extending up to 2.2 mm/s in the granulation tissue and to 3.9 mm/s in the trabecular bone. Peak shear stresses on the cells hosted in these tissues ranged from 0.1 Pa to 12.5 Pa. These results offer insight into mechanical stimuli encountered at the bone-implant interface. They could be beneficial to interpret the results of mechanobiology studies on the effects of fluid flow on bone or mesenchymal stem cells.



## Introduction

During the past two decades, the number of cementless hip replacements has increased significantly (Wyatt et al., 2014). With the rising number of young patients undergoing hip replacement, improving the long-term success of cementless femoral stems has become a crucial issue in the field of total hip replacement.

Aseptic loosening is the main cause for revision of cementless hip stems, accounting for 54% of all causes for revision (Wyatt et al., 2014). It is characterized by the formation of a fibrous tissue at the bone-implant interface and areas of osteolysis around the implant. Aseptic loosening is a complex process, usually due to a combination of mechanical and biological factors, but is largely related to the initial phases of peri-implant healing (Kärrholm et al., 1994; Mjöberg, 1994). Shortly after implantation, a soft and porous tissue saturated with interstitial fluid fills the gap between the bone and the implant. This granulation tissue hosts mesenchymal stem cells (MSCs) that have the ability to differentiate into osteoblasts, leading to bone formation. The fate of MSCs is directly linked to mechanical and biochemical stimuli in their environment.

Among the factors that are known to play a role in implant loosening, primary stability of the implant is critical. Primary stability corresponds to the initial mechanical fixation of the implant, and is characterized by relative bone-implant micromotion at the interface. Excessive bone-implant micromotion indicates a poor implant primary stability and has been shown to promote the formation of interfacial fibrous tissue, leading to aseptic loosening (Engel et al., 1992; Søballe et al., 1992).

Fluid flow has also been shown to play an important role in promoting aseptic loosening. High fluid velocities (Fahlgren et al., 2010) and pressures (Vis et al., 1998) have been reported to cause osteolysis, independently from the presence of wear particles. Fluid shear stress is also known to play a role in controlling MSCs osteoblastic differentiation (Arnsdorf et al., 2009b; Arnsdorf et al., 2009a; Kreke et al., 2005; Sharp et al., 2009; Yourek et al., 2010).

It has been suggested that micromotion and fluid flow at the bone-implant interface could be intimately related (Prendergast et al., 1997). Implant micromotion deforms the surrounding bone and granulation tissue, hereby pumping interstitial fluid and generating fluid flow. Micromotion-induced fluid flow would thus have the potential to affect the outcome of peri-implant healing, through stimulation of the MSCs hosted in the bone and the granulation tissue, activation of the osteoclasts, or transport of morphogens, nutrients, oxygen or wear particles.

For this reason, there has been a growing interest to quantify micromotion-induced fluid flow around implants, in order to help study its effects on peri-implant healing and osseointegration. Various studies in the recent years tried to characterize micromotion-induced fluid flow (Alidousti et al., 2011; Conroy et al., 2006; Mann et al., 2014). Most of these studies considered simplified bone and implant geometries, uni-directional homogeneous micromotion, or were limited to 2D fluid velocities. However, the heterogeneous local micromechanical environment is known to play an important role in peri-implant healing (Simmons et al., 2001b; Simmons et al., 2001a).

The aim of this study is to characterize and quantify micromotion-induced fluid flow at the bone-implant interface of a cementless femoral stem, using finite element (FE) modeling with accurate geometries and boundary conditions. The research project is divided into three specific objectives (i) to determine conditions that cause high fluid velocities at the bone-implant interface using design of experiments and an idealized 2D model of the bone-implant interface, (ii) to quantify micromotion-induced fluid velocities in representative transverse sections of a cementless femoral stem, and (iii) to quantify micromotion-induced 3D fluid velocities around the whole bone-implant interface of a cementless femoral stem, and the resulting shear stress on cells hosted in peri-implant tissues.

## Methods

### *Idealized parametric model of the bone-implant interface*

An idealized 2D poroelastic model of the bone-implant interface was created and combined with a full factorial design of experiments (DOE) approach, to explore the effects of gap size, implant micromotion, material properties of the granulation tissue and interstitial fluid on peak fluid velocity in the trabecular bone and granulation tissue. The final design included two levels and seven factors, resulting in 128 ( $2^7$ ) conditions (Table 4.1).

The choice of gap size and micromotion levels was made so as to span the variety of results measured experimentally in Chapter 2 & 3. To study the effects of variations in material properties of the granulation tissue, the levels of each material property were chosen to span a range of proposed values in the literature. Indeed, different values for Young's modulus, porosity and permeability have been proposed - depending on where and when the tissue was collected - and the commonly used value for Poisson's ratio (0.167) is based on a value measured in cartilage (Isaksson et al., 2009; Jurvelin et al., 1997). Finally, the value of the fluid viscosity in the gap is also not experimentally characterized, and water and bone marrow

were chosen to span the possible viscosity values.

Factors	Low level	High level	References
Gap size	0.5 mm	5 mm	Chapter 2 & 3
Micromotion	5 $\mu\text{m}$	250 $\mu\text{m}$	Chapter 2 & 3
Young's modulus of granulation tissue	0.5 MPa	1.5 MPa	[1]*, [2,3]**
Poisson's ratio of granulation tissue	0.1	0.3	[4]***, [5]***
Porosity of granulation tissue	0.7	0.9	[6]†
Permeability of granulation tissue	$1 \times 10^{-14} \text{ m}^2$	$5 \times 10^{-14} \text{ m}^2$	[6]†, [7]*
Interstitial fluid's viscosity	0.001 Pa.s	0.1 Pa.s	[8]††

[1] (Leong et al., 2008)

[4] (Jurvelin et al., 1997)

[7] (Fahlgren et al., 2012)

[2] (Kraaij et al., 2014)

[5] (Kiviranta et al., 2006)

[8] (Gurkan et al., 2008)

[3] (Moerman et al., 2016)

[6] (Diamond, 1999)

\* Measured in granulation tissue

\*\* Measured in the bone-implant interface tissue of loosened implants

\*\*\* Measured in cartilage

† Measured in blood clots

†† Measured in bone marrow

**Table 4.1:** Sensitivity study: full-factorial design factors and levels.

*Model's geometry* The model was composed of three concentric rings: the most central one represented the granulation tissue, which was surrounded by a ring of trabecular bone and a ring of cortical bone (Fig. ). The most central boundary represented a 1 cm diameter implant. The implant was considered completely rigid and impermeable compared to the surrounding tissues. The cortical and trabecular thicknesses were 5 mm. The gap between the implant and trabecular bone was considered as fully filled with granulation tissue.

*Material properties* Granulation tissue, trabecular and cortical bone were modeled as poroelastic and saturated with interstitial fluid (Table 4.2). The poroelastic properties of trabecular and cortical bone were obtained from the literature. The poroelastic properties of granulation tissue are ill-defined. Some studies have focused on characterizing the poroelastic properties of the fibrous tissue that forms ultimately at the bone-implant interface of loosened implants, and we assumed that granulation tissue had similar properties. The Biot-Willis effective stress coefficient, which relates the volume of fluid expelled or sucked into

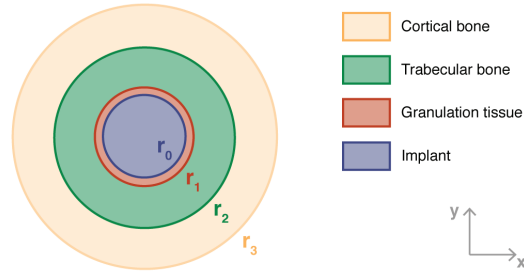


**Figure 4.1:** Geometry of the idealized model -  $r_i$  designates boundaries of the model.

a porous material element with the volumetric change of the same element, was unknown for trabecular bone and granulation tissue. Because of inhibition of pore compression, a stiff porous matrix has a Biot-Willis coefficient close to its porosity, and a soft porous matrix has a Biot-Willis coefficient close to 1 (Podichetty et al., 2014). Therefore, we assumed Biot-Willis coefficients of 0.8 for trabecular bone and 1 for granulation tissue. The properties of the interstitial fluid were those of water.

Material	Density	Young's modulus	Poisson's ratio	Porosity	Permeability	Biot-Willis coefficient	Viscosity
Cortical Bone	1875 kg/m <sup>3</sup> [1]	15.75 GPa [2]	0.325 [2]	0.05 [2]	1.5 × 10 <sup>-20</sup> m <sup>2</sup> [3]	0.14 [4]	
Trabecular Bone	1875 kg/m <sup>3</sup> [1]	1 GPa [5]	0.25 [6]	0.8 [5]	4.7 × 10 <sup>-10</sup> m <sup>2</sup> [5]	0.8	
Granulation Tissue	1100 kg/m <sup>3</sup> [7]	0.99 MPa [8]	0.167 [9]	0.8 [10]	3 × 10 <sup>-14</sup> m <sup>2</sup> [11]	0.95	
Interstitial Fluid	1000 kg/m <sup>3</sup>						1e-3 Pa.s

- [1] (Ashman et al., 1984) [4] (Cowin, 1999) [7] (Nahirnyak et al., 2006) [10] (Diamond, 1999)  
 [2] (Smit et al., 2002) [5] (Kohles et al., 2002) [8] (Leong et al., 2008) [11] (Fahlgren et al., 2012)  
 [3] (Johnson et al., 1982) [6] ((Sebaa et al., 2006) [9] (Isaksson et al., 2009)

**Table 4.2:** Poroelastic material properties used in the model.

*Boundary and initial conditions* The external boundary of the cortical bone was fully constrained. Micromotion of the implant was imposed by a sinusoidal displacement in the x-direction, at a frequency of 1 Hz. We introduced a phase shift of  $-\frac{\pi}{2}$  to enable a gradual initial ramping of micromotion and help convergence (Equation C.8). The implant boundary was impermeable to fluid and the external boundary of cortical bone was open boundary to fluid flow (Equation C.9). For the initial conditions, the system was considered to be at rest, with a fluid pore pressure at 1 atm in all tissues (Equation C.10).

*Finite element analysis* The model was meshed with solid triangular elements (Table C.1) and implemented in COMSOL (COMSOL Multiphysics®v. 5.2a., www.comsol.com, COMSOL AB, Stockholm, Sweden) using the poroelasticity interface. The time-dependent partial differential equations were solved with a fully-coupled approach using the Newton-Raphson iteration method and a direct MUMPS solver. Time steps sizes were determined automatically using backward differentiation formula.

The full factorial design was generated and analyzed in Minitab (Minitab 17 Statistical Software, www.minitab.com, Minitab, Inc., State College, PA, USA) using ANOVA. Only main effects and 2-way interactions were considered.

### ***Fluid flow in representative transverse section of a cementless femoral stem***

Representative transverse sections of the bone-implant interface of a left human fresh frozen cadaveric femur implanted with a cementless collared stem were built, based on the geometry obtained from CT data. Two CT-scans were performed after broaching of the bone cavity and after implantation respectively. The geometry of the bone-implant interface was reconstructed from the post-broaching CT-scan. Cortical and trabecular bone were segmented manually in the Amira software (Amira v6.0.1, FEI, Hillsboro, OR, USA) and the surfaces were reconstructed in Geomagic (Geomagic Studio 2014, 3D Systems, Rock Hill, SC, USA). The bone surfaces were aligned to the post-implantation CT-scan and the implant surface, obtained from the CAD file, was subtracted in Solidworks (Solidworks 2015, Solidworks Corp., Dassault Systemes, Waltham, MA, USA).

The material properties (Table 4.2), initial and boundary conditions were similar to those of the idealized model. The amplitude and direction of micromotion were defined according to the interpolation function of 3D bone-implant micromotion around the stem, measured locally using a micro-CT based technique (Fig. C.1). Transverse sections taken at 24 mm, 72 mm, and 120 mm from the tip of the stem were extracted in Solidworks. The models were meshed with triangular elements (Table C.1). The model was solved in COMSOL, similar to what was described for the idealized model. Three transverse cuts along the femoral stem were analyzed (Fig. 4.2), each for two loading cases: compression and torsion. Outcome measures of the models included average and peak fluid velocity in each tissue.

### ***3D fluid flow around a simplified cementless femoral stem***

A 3D FE model of the same femur where micromotion was measured experimentally was built, based on the geometry obtained from CT data. The bone surfaces were reconstructed

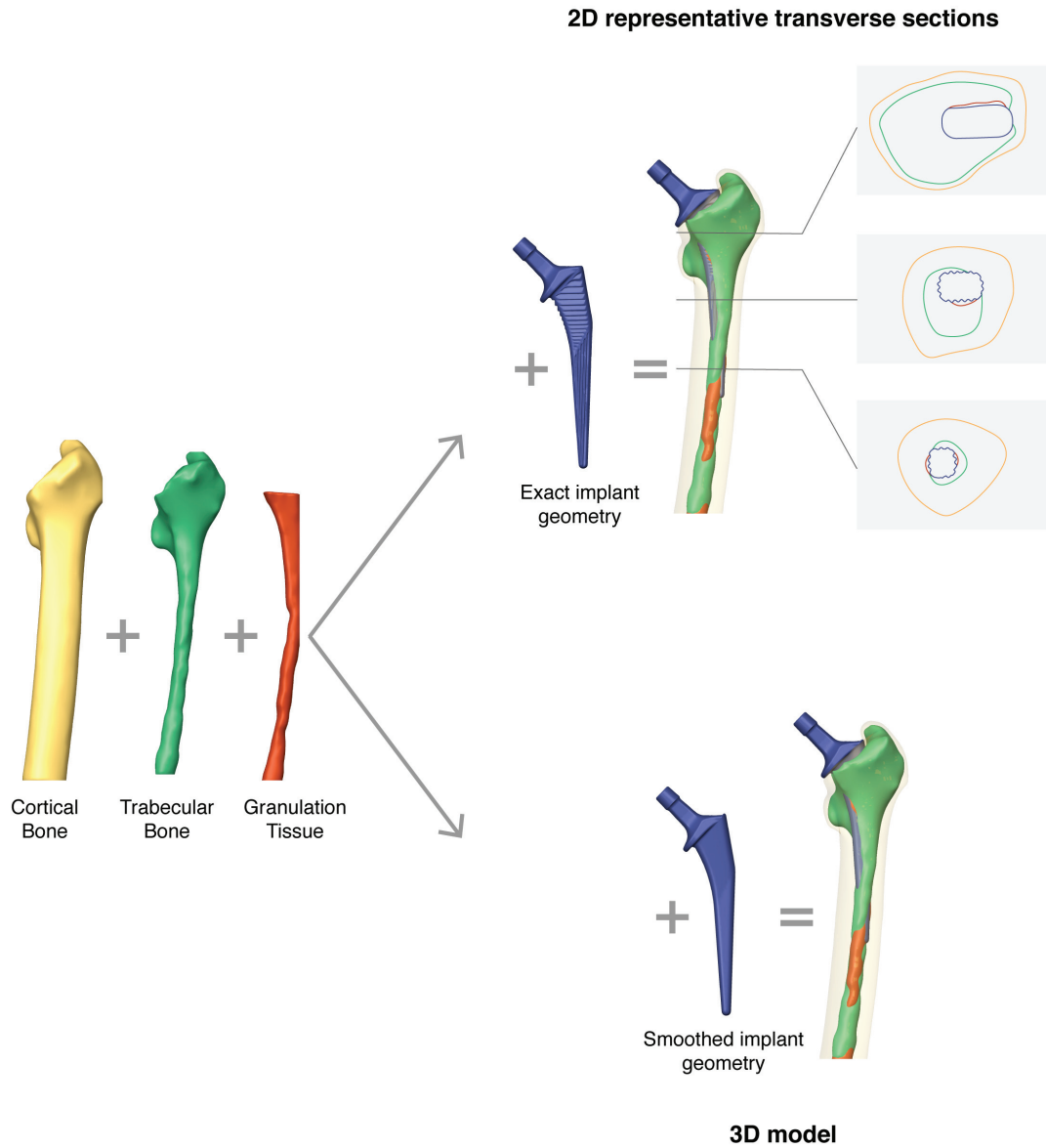


**Figure 4.2:** Assembly of geometry for the 2D representative transverse sections and the simplified 3D model - The representative transverse sections are built from the cortical bone (yellow), trabecular bone (green), granulation tissue (red) and accurate implant surfaces (blue). The 3D model is built by combining the cortical bone, trabecular bone, granulation tissue and simplified implant surfaces.

in a similar way as described above and aligned to the post-implantation CT-scan. A simplified version of the implant surface, without macrostructures, was subtracted in Solidworks (Fig. 4.2).

The material properties, initial and boundary conditions were identical to the transverse sections models described previously. The model was meshed with tetrahedral elements (Table C.1) and solved in COMSOL, similar to what was described above. Outcome measures of the model included average and peak fluid velocity in each tissue, and the peak shear stress on cells located in trabecular bone and granulation tissue. The peak shear stress on cells was estimated assuming spherical cells embedded in a porous matrix (Wang et al., 2000):

$$\tau = \frac{3}{\pi} \frac{\mu \mathbf{v}}{\sqrt{\kappa}} \quad (4.1)$$

where  $\tau$  is the peak shear stress on cells,  $\mu$  is the interstitial fluid viscosity,  $\mathbf{v}$  is the peak fluid's velocity in the tissue and  $\kappa$  is the permeability.

## Results

### *Idealized parametric model of the bone-implant interface*

Peak fluid velocity in the tissues of the bone-implant interface reached two maxima over one micromotion cycle due to inflow and outflow, at approximately 25% and 75% of the load cycle. The maximal fluid velocity was encountered in the trabecular bone. Peak fluid velocity ranged from 5  $\mu\text{m/s}$  to 1277  $\mu\text{m/s}$ , depending on the levels of parameters included in the full factorial design.

The analysis of the full factorial design of experiments showed that gap size, micromotion, tissue's permeability and interstitial fluid viscosity had a significant ( $p < 0.05$ ) effect on peak fluid velocity at the bone-implant interface (Table 4.3). Micromotion was the parameter that influenced the most the peak fluid velocity, with higher micromotion resulting in higher fluid velocity. The mean fluid velocity for all low micromotion conditions was 18  $\mu\text{m/s}$ , versus 1062  $\mu\text{m/s}$  for all high micromotion conditions. Low gap size resulted in significantly higher fluid velocity and low fluid viscosity induced lower peak fluid velocity, but they both contributed to less than 3 % of the total sum of squares. Additionally, several 2-way interactions were also significant, including the interaction between gap size and micromotion that contributed to 2.6% of the total sum of squares.

Source	DOF	%TSS	p-value
<b>Linear</b>	7	89.50%	<0.001
Gap size	1	2.60%	<0.001
Micromotion	1	84.20%	<0.001
Granulation tissue's permeability	1	0.10%	0.003
Interstitial fluid's viscosity	1	2.60%	<0.001
<b>2-Way Interactions</b>	21	7.90%	<0.001
Gap size x Micromotion	1	2.60%	<0.001
Gap size x Interstitial fluid's viscosity	1	0.90%	<0.001
Micromotion x Granulation tissue's permeability	1	0.90%	0.004
Micromotion x Interstitial fluid's viscosity	1	2.60%	<0.001
Granulation tissue's permeability x Interstitial fluid's viscosity	1	0.90%	0.017
<b>Residuals</b>	99	2.60%	

**Table 4.3:** ANOVA for the full factorial design. Degrees of freedom (DOF) and percentages of the total sum of squares (%TSS) are listed. Only significant effects are displayed.



***Fluid flow in representative transverse sections of a cementless femoral stem***

The average fluid velocity in the granulation tissue was maximal for the metaphyseal transverse section in torsion with  $57 \mu\text{m/s}$  (Fig. 4.3). In the trabecular bone, the maximum average fluid velocity occurred in the middle diaphyseal transverse section for the torsion case, with  $145 \mu\text{m/s}$ .

In the three representative transverse sections, the peak fluid velocity in the granulation tissue ranged from  $3 \mu\text{m/s}$  to  $230 \mu\text{m/s}$  for compression, and from  $25 \mu\text{m/s}$  to  $446 \mu\text{m/s}$  in torsion. In the trabecular bone, the maximum fluid velocity extended from  $47 \mu\text{m/s}$  to  $2403 \mu\text{m/s}$ . The interstitial fluid velocities in cortical bone were much lower than in other tissues, the maximum was reached in the metaphyseal transverse section, in torsion, with  $3 \mu\text{m/s}$ . On the middle and diaphyseal transverse sections, regions of higher fluid velocity were observed at the corners of the quadrangular section of the implant. On the other hand, we observed notably lower fluid velocities inside the recesses of the vertical grooves, while local peaks of fluid velocities could be observed around the crests of the grooves.

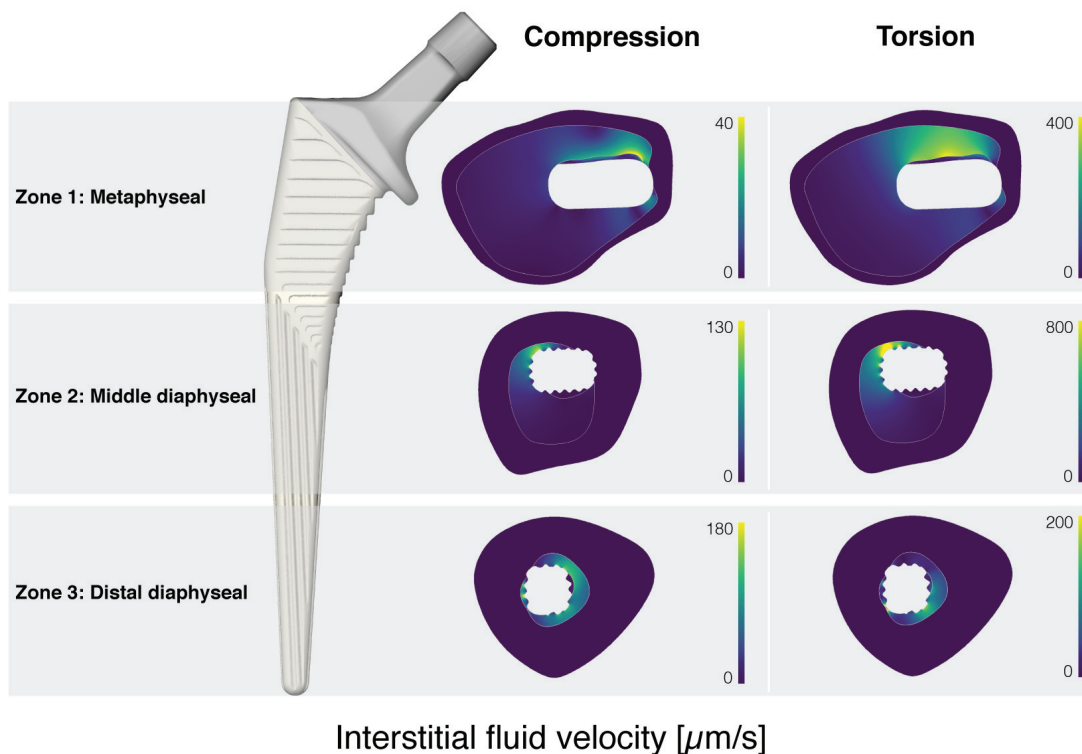


**Figure 4.3:** Distribution of micromotion-induced interstitial fluid absolute velocities at representative transverse sections of the bone-implant interface in compression and torsion at  $t=0.25 \text{ s}$ .

### ***3D fluid flow around a simplified cementless femoral stem***

The average fluid velocity in the granulation tissue was  $9\ \mu\text{m/s}$  in compression and  $15\ \mu\text{m/s}$  in torsion. In the trabecular bone, the average fluid velocity was much higher, with  $21\ \mu\text{m/s}$  in compression and  $128\ \mu\text{m/s}$  in torsion.

The peak fluid velocity in the granulation tissue was maximal close to the distal end of the stem for both loading cases, reaching  $412\ \mu\text{m/s}$  in compression and  $2273\ \mu\text{m/s}$  in torsion (Fig. 4.4). In the trabecular bone, peak fluid velocities occurred distally in compression with  $1804\ \mu\text{m/s}$  and on the middle and distal diaphysis in torsion with a maximum at  $3913\ \mu\text{m/s}$ . The interstitial fluid velocities in cortical bone were much lower than in other tissues, and the highest fluid velocities recorded (up to  $5.5\ \mu\text{m/s}$ ) were at the distal end of the stem for both loading cases. The most important component of the 3D fluid velocity was in the longitudinal direction.

Peak shear stress in granulation tissue was  $2.3\ \text{Pa}$  and  $12.5\ \text{Pa}$  for compression and torsion respectively. In trabecular bone, shear stress on cells reached  $0.1\ \text{Pa}$  and  $0.2\ \text{Pa}$  for compression and torsion.

## **Discussion**

Micromotion-induced fluid flow at the bone-implant interface is believed to play an important role in the initial phases of peri-implant healing, through stimulation of cells hosted in the surrounding tissues. However, quantification of micromotion-induced fluid velocities around accurate geometries and based on the local mechanical environment of the prosthesis was missing. In this study, our objective was to use FE modeling to characterize and quantify micromotion-induced fluid velocity at the bone-implant interface of a cementless femoral stem using accurate geometries and experimentally measured local micromotion. Using design of experiments and an idealized 2D model of the bone-implant interface, we observed that micromotion was the most influential parameter on peak fluid velocity at the interface. The geometry of the interface, represented by the gap size, as well as the interactions between gap size and micromotion, played also a significant role, underlining the need for accurate geometries and local micromotion measurements when estimating micromotion-induced fluid flow. We observed interesting flow patterns in the macrostructures at the surface of the implant in representative transverse sections of a cementless femoral stem, with lower fluid velocities inside the vertical grooves, and local peak velocities around the crests of the grooves and at the corners of the quadrangular section of the

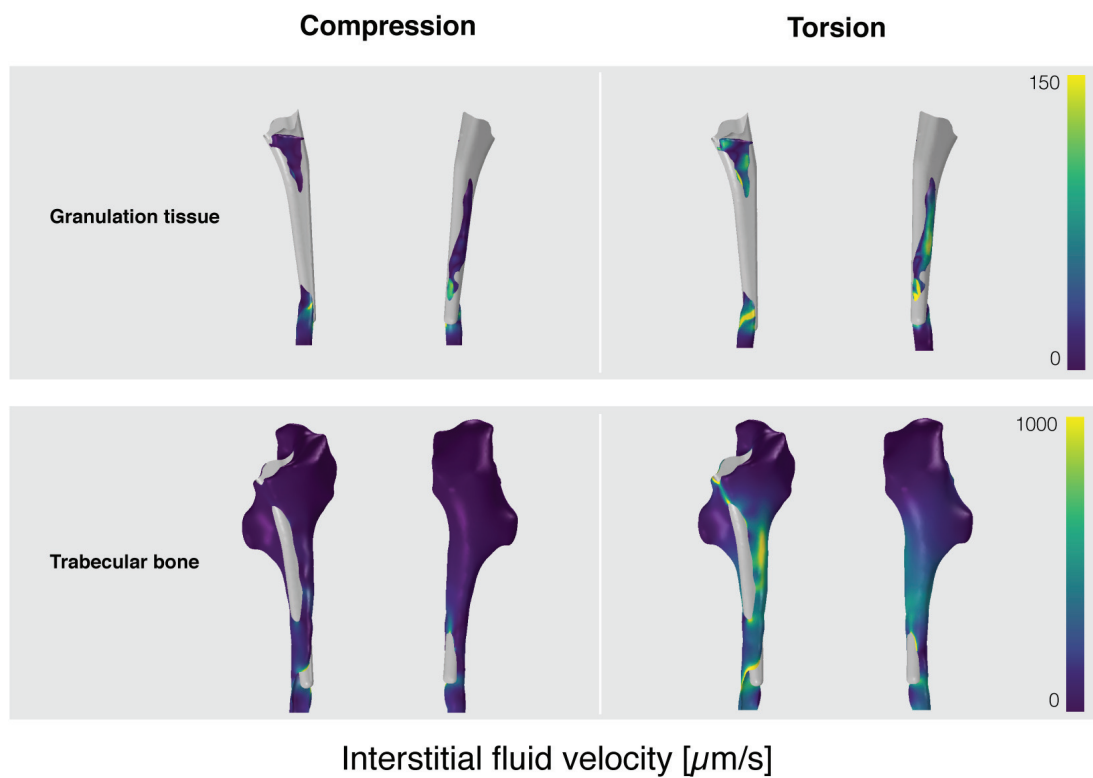


**Figure 4.4:** Distribution of micromotion-induced interstitial fluid velocities in the granulation tissue and trabecular bone around a simplified cementless femoral stem (gray) in compression and torsion at  $t=0.25$  s.

implant. Finally, using a 3D model of the bone-implant interface, we obtained a range of fluid velocities extending up to  $2200 \mu\text{m/s}$  in the granulation tissue and to  $3900 \mu\text{m/s}$  in the trabecular bone for a torsional loading case.

The main strength of the model developed as part of this work is that it captures the wide range of gap and micromotion conditions around the stem, thanks to full-field measurements. The exact sequence of events that links micromotion-induced fluid flow to aseptic loosening remains unknown. Nevertheless, the model presented in this study could be appropriate to test some of the hypotheses around the mechanisms behind aseptic loosening.

Previous researches already reported the important effect of surface geometries (Simmons et al., 2001b; Simmons et al., 2001a) and micromotion (Engh et al., 1992; Søballe et al., 1992) on peri-implant healing. Our findings are consistent with these studies, as we found that gap size and micromotion influenced peak fluid velocities to a greater extent than material properties. The 2D models of representative transverse sections of a cementless femoral stem showed that macrostructures on the implant surface could influence the local fluid velocities, with lower velocities inside the recesses of the vertical grooves, and locally higher velocities around the crests of the grooves. It is interesting to compare this result with histological analyses and push-out tests of the bone-implant interface of retrieved grooved implants, where local differences in bone healing were also observed between the crests and recesses of the grooves (Thomas et al., 1987). Indeed, bone formation appeared earlier at the crests of the grooves, and the bone formed at the crests resisted better to push out tests than the bone formed in the recesses of the grooves. Other studies that analyzed retrieved sections of the same implant as the one used in our study reported more bone formation at the corners of the quadrangular section of the stem (Hardy et al., 1999b; Hardy et al., 1999a).

For both types of macrostructures, it seems that locally higher fluid velocities correlate with bone formation, which is in contradiction with studies that propose that higher fluid velocities induce osteolysis (Fahlgren et al., 2010). However, they observed osteolysis for fluid velocities of  $20000 \mu\text{m/s}$ , while our range of values was in the order of hundreds of  $\mu\text{m/s}$ . Furthermore, flow chamber experiments showed that fluid shear stress in the order of 0.4 to 2.2 Pa could induce the osteogenic differentiation of MSCs, which relates well with the range of shear stresses in granulation tissue that we estimated. Other models that estimated micromotion-induced fluid flow at the bone-implant interface reported fluid velocities similar to what we estimated. The micromotion-induced peak fluid velocity at the bone-cement interface of retrieved transverse sections of cemented femoral stems varied from  $270 \mu\text{m/s}$  to  $15700 \mu\text{m/s}$  (Mann et al., 2014). In another model of capsular pressure and micromotion-induced fluid flow around a cementless femoral stem, fluid velocities extending up to 3000

$\mu\text{m/s}$  were observed (Alidousti et al., 2011). Finally, in a magnetic resonance imaging study, micromotion-induced fluid velocity in the gap around a canine bone implant model reached  $14000 \mu\text{m/s}$  (Conroy et al., 2006).

The present study has several limitations, and the most important one is that results for only one specimen are reported. Future works will require several samples to confirm the results obtained with this model and account for patient's variability. The geometries were reconstructed from a CT-scan with a resolution of 0.5 mm, meaning that gaps smaller than the resolution were not modeled. The material properties of granulation tissue are not well characterized, and the measured poroelastic properties for trabecular and cortical bone span a wide range of values. Additionally, the material properties of the interface are likely to be anisotropic and evolve as healing progresses. To evaluate the sensitivity of peak fluid velocities to the material properties of granulation tissue, we used design of experiments techniques. We found that despite some properties like the permeability of the tissue or the viscosity of the fluid influenced significantly the results, their role was minimal compared to the effects of gap size or micromotion. We also assumed that the mechanical behavior of the granulation tissue was linear elastic. However, small gaps and high micromotion could easily result in large strains, for which the linear elastic representation would no longer be valid. The hyperelastic properties of the interfacial fibrous tissue around loosened cementless stem were recently characterized. Further studies should evaluate the repercussions of the hyperelastic modeling of interfacial tissue on micromotion-induced fluid flow predictions.

The vertical grooves on the implant surface were modeled in the 2D models, and these macrostructures influenced remarkably the distribution of fluid velocities at the interface. However, the 2D transverse sections displayed significantly lower fluid velocities than the corresponding sections in the 3D model, showing that axial components of micromotion and fluid velocity are essential for an accurate estimation of micromotion-induced fluid velocities. The implant macrostructures were not included in the 3D model to reduce mesh size and computation time. Fluid-flow at the interface results from both implant micromotion and bone deformation following implant loading, however, our measurement of implant micromotion reports the relative displacement between the implant and bone and does not integrate bone strains. It is thus possible that our range of fluid velocities is slightly underestimated. Finally, Darcy's law is only valid for low Reynolds number  $Re \lesssim 10$  (Hassanizadeh et al., 1987). Using a characteristic pore length of  $1 \mu\text{m}$  for granulation tissue and 1 mm for trabecular bone, we estimated Reynolds numbers of 0.001 and 1 for each tissue respectively. Therefore, in this study, Darcy's flow was a reasonable assumption. However, higher fluid velocities arising with higher implant micromotion could lead to non-Darcy's flows.

This study provided a first estimation of local micromotion-induced fluid flow around a cementless femoral stem in the initial stages of peri-implant healing. Though the mechanisms that link fluid flow at the initial bone-implant interface and peri-implant healing remain insufficiently understood, much research in the recent years focused on the influence of fluid flow on bone and mesenchymal stem cells. The range of fluid velocities and shear stresses estimated in this study is of great interest to relate mechanical stimuli encountered at the bone-implant interface with results from mechanobiology experiments. Furthermore, micromotion-induced fluid flow has been proposed to disturb the transport of morphogens in the peri-implant tissues, hereby affecting the osteogenic differentiation of mesenchymal stem cells (Gortchacow et al., 2013). In the future, a model of morphogens transport in the granulation tissue could be combined with the model developed in this study, to test this hypothesis.

## References

- Alidousti, Hamidreza, Mark Taylor, and Neil W Bressloff (2011). “Do capsular pressure and implant motion interact to cause high pressure in the periprosthetic bone in total hip replacement?” In: *Journal of Biomechanical Engineering* 133.1212, p. 121001.
- Arnsdorf, Emily J et al. (2009a). “Mechanically induced osteogenic differentiation - the role of RhoA, ROCKII and cytoskeletal dynamics”. In: *Journal of Cell Science* 122.44, pp. 546–553.
- Arnsdorf, Emily J, Padmaja Tummala, and Christopher R Jacobs (2009b). “Non-Canonical Wnt Signaling and N-Cadherin Related  $\beta$ -Catenin Signaling Play a Role in Mechanically Induced Osteogenic Cell Fate”. In: *PloS One* 4.44, e5388.
- Ashman, R B et al. (1984). “A continuous wave technique for the measurement of the elastic properties of cortical bone.” In: *Journal of Biomechanics* 17.55, pp. 349–361.
- Conroy, Mark J et al. (2006). “High-resolution magnetic resonance flow imaging in a model of porous bone–implant interface”. In: *Magnetic Resonance Imaging* 24.55, pp. 657–661.
- Cowin, Stephen C (1999). “Bone poroelasticity”. In: *Journal of Biomechanics* 32.33, pp. 217–238.
- Diamond, S L (1999). “Engineering design of optimal strategies for blood clot dissolution”. In: *Annual Review of Biomedical Engineering* 1.11, pp. 427–462.
- Engh, Charles A et al. (1992). “Quantification of Implant Micromotion, Strain Shielding, and Bone Resorption With Porous-Coated Anatomic Medullary Locking Femoral Prostheses”. In: *Clinical Orthopaedics and Related Research* 285285, pp. 13–29.
- Fahlgren, Anna et al. (2010). “Fluid pressure and flow as a cause of bone resorption.” In: *Acta Orthopaedica* 81.44, pp. 508–516.

- Fahlgren, Anna, Lars Johansson, and Ulf Edlund (2012). "Direct ex vivo measurement of the fluid permeability of loose scar tissue". In: *Acta of Bioengineering and Biomechanics*.
- Gortchacow, Michael, Alexandre Terrier, and Dominique P Pioletti (2013). "A Flow Sensing Model for Mesenchymal Stromal Cells Using Morphogen Dynamics". In: *Biophysical journal* 104.1010, pp. 2132–2136.
- Gurkan, Umut Atakan and Ozan Akkus (2008). "The Mechanical Environment of Bone Marrow: A Review". In: *Annals of biomedical engineering* 36.1212, pp. 1978–1991.
- Hardy, D C R, P Frayssinet, and P E Delince (1999a). "Osteointegration of hydroxyapatite-coated stems of femoral prostheses". In: *European Journal of Orthopaedic Surgery and Traumatology* 9.22, pp. 75–81.
- Hardy, D C et al. (1999b). "Histopathology of a well-functioning hydroxyapatite-coated femoral prosthesis after 52 months." In: *Acta orthopaedica Belgica* 65.11, pp. 72–82.
- Hassanizadeh, S Majid and William G Gray (1987). "High velocity flow in porous media". In: *Transport in Porous Media* 2.66, pp. 521–531.
- Isaksson, Hanna, Corrinus C van Donkelaar, and Keita Ito (2009). "Sensitivity of tissue differentiation and bone healing predictions to tissue properties". In: *Journal of Biomechanics* 42.55, pp. 555–564.
- Johnson, M W et al. (1982). "Fluid flow in bone in vitro". In: *Journal of Biomechanics* 15.1111, pp. 881–885.
- Jurvelin, J S, M D Buschmann, and E B Hunziker (1997). "Optical and mechanical determination of poisson's ratio of adult bovine humeral articular cartilage". In: *Journal of Biomechanics* 30.33, pp. 235–241.
- Kärholm, J et al. (1994). "Does early micromotion of femoral stem prostheses matter? 4-7-year stereoradiographic follow-up of 84 cemented prostheses." In: *The Journal of bone and joint surgery. British volume* 76.66, pp. 912–917.
- Kiviranta, Panu et al. (2006). "Collagen network primarily controls Poisson's ratio of bovine articular cartilage in compression". In: *Journal of orthopaedic research : official publication of the Orthopaedic Research Society* 24.44, pp. 690–699.
- Kohles, Sean S and Julie B Roberts (2002). "Linear Poroelastic Cancellous Bone Anisotropy: Trabecular Solid Elastic and Fluid Transport Properties". In: *Journal of Biomechanical Engineering* 124.55, p. 521.
- Kraaij, Gert et al. (2014). "Mechanical properties of human bone-implant interface tissue in aseptically loose hip implants". In: *Journal of the Mechanical Behavior of Biomedical Materials* 38, pp. 59–68.
- Kreke, Michelle R, William R Huckle, and Aaron S Goldstein (2005). "Fluid flow stimulates expression of osteopontin and bone sialoprotein by bone marrow stromal cells in a temporally dependent manner." In: *Bone* 36.66, pp. 1047–1055.



- Leong, P L and E F Morgan (2008). "Measurement of fracture callus material properties via nanoindentation". In: *Acta Biomaterialia* 4.55, pp. 1569–1575.
- Mann, Kenneth A and Mark A Miller (2014). "Fluid-structure interactions in micro-interlocked regions of the cement-bone interface". In: *Computer Methods in Biomechanics and Biomedical Engineering* 17.1616, pp. 1809–1820.
- Mjöberg, Bengt (1994). "Theories of wear and loosening in hip prostheses: Wear-induced loosening vs loosening-induced wear-a review". In: *Acta Orthopaedica* 65.33, pp. 361–371.
- Moerman, Astrid et al. (2016). "Structural and mechanical characterisation of the peri-prosthetic tissue surrounding loosened hip prostheses. An explorative study." In: *Journal of the Mechanical Behavior of Biomedical Materials* 62, pp. 456–467.
- Nahirnyak, Volodymyr M, Suk Wang Yoon, and Christy K Holland (2006). "Acousto-mechanical and thermal properties of clotted blood". In: *Journal of the Acoustical Society of America* 119.66, pp. 3766–3772.
- Podichetty, Jagdeep T and Sundararajan V Madihally (2014). "Modeling of porous scaffold deformation induced by medium perfusion". In: *Journal of Biomedical Materials Research Part B-Applied Biomaterials* 102.44, pp. 737–748.
- Prendergast, Patrick J, Rik Huiskes, and Kjeld Søballe (1997). "Biophysical stimuli on cells during tissue differentiation at implant interfaces". In: *Journal of Biomechanics* 30.66, pp. 539–548.
- Sebaa, N et al. (2006). "Ultrasonic characterization of human cancellous bone using the Biot theory: Inverse problem". In: *The Journal of the Acoustical Society of America* 120.44, pp. 1816–1824.
- Sharp, Lindsay A, Yong W Lee, and Aaron S Goldstein (2009). "Effect of low-frequency pulsatile flow on expression of osteoblastic genes by bone marrow stromal cells". In: *Annals of biomedical engineering* 37.33, pp. 445–453.
- Simmons, Craig A, Shaker A Meguid, and Robert M Pilliar (2001a). "Differences in osseointegration rate due to implant surface geometry can be explained by local tissue strains". In: 19.22, pp. 187–194.
- Simmons, Craig A, S A Meguid, and R M Pilliar (2001b). "Mechanical regulation of localized and appositional bone formation around bone-interfacing implants." In: *Journal of Biomedical Materials Research* 55.11, pp. 63–71.
- Smit, Theo H, Jacques M Huyghe, and Stephen C Cowin (2002). "Estimation of the poroelastic parameters of cortical bone." In: *Journal of Biomechanics* 35.66, pp. 829–835.
- Søballe, Kjeld et al. (1992). "Tissue ingrowth into titanium and hydroxyapatite-coated implants during stable and unstable mechanical conditions". In: *Journal of Orthopaedic Research* 10.22, pp. 285–299.



- Thomas, Kevin A et al. (1987). "The effect of surface macrotecture and hydroxylapatite coating on the mechanical strengths and histologic profiles of titanium implant materials". In: 21.1212, pp. 1395–1414.
- Vis, Harm M Van der et al. (1998). "Short periods of oscillating fluid pressure directed at a titanium-bone interface in rabbits lead to bone lysis". In: *Acta Orthopaedica Scandinavica* 69.11, pp. 5–10.
- Wang, S and J M Tarbell (2000). "Effect of Fluid Flow on Smooth Muscle Cells in a 3-Dimensional Collagen Gel Model". In: *Arteriosclerosis, Thrombosis, and Vascular Biology* 20.1010, pp. 2220–2225.
- Wyatt, Michael et al. (2014). "Survival outcomes of cemented compared to uncemented stems in primary total hip replacement". In: *World Journal of Orthopedics* 5.55, p. 591.
- Yourek, Gregory et al. (2010). "Shear stress induces osteogenic differentiation of human mesenchymal stem cells". In: *Regenerative Medicine* 5.55, pp. 713–724.



# Chapter 5

Conclusions  
and perspectives



## Summary of findings

Aseptic loosening of the femoral component emerged as a major issue in the field of cementless hip arthroplasty, limiting the long-term survival of the implants (Wyatt et al., 2014). Multiple mechanisms are involved in this process, including implant micromotion and fluid flow at the bone-implant interface (Sundfeldt et al., 2006). Several studies suggested that aseptic loosening stems from the initial mechanical environment during the early stages of peri-implant healing (Kärrholm et al., 1994; Mjöberg, 1994). This thesis focused on three different aspects of the initial local mechanical environment around cementless femoral stems: (i) the development of a technique to measure full-field micromotion around cementless femoral components; (ii) the comparison of collared and collarless femoral stems primary stability; (iii) the estimation of micromotion-induced fluid flow around a cementless femoral component. The findings for each of these aspects are detailed below.

In Chapter 2, the development of a micro-CT based technique to measure local implant micromotion around metallic cementless stems was detailed. The technique relied on radiopaque markers to bypass the difficulties arising when imaging the interface of metallic implants. It proved to be highly reliable, with a bias of  $5\ \mu\text{m}$  and a measurement repeatability similar to that of LVDTs, which are the current gold standard for micromotion measurement. Moreover, thanks to over 300 simultaneous measurement points, the technique provided the full-field map of micromotion around a cementless femoral stem.

Then, in Chapter 3, the developed micro-CT technique was used to compare the primary stability of the collared and collarless versions of the same cementless femoral stem. Subsidence and local micromotion were measured in two groups of cadaveric femurs implanted with either version of the stem. We found no significant difference in both subsidence and local micromotion between collared and collarless stems. Conjointly, these results suggest that there is no difference in primary stability between the two versions of the stem for activities of daily living.

Finally, in Chapter 4, a poroelastic finite element model of the bone-implant interface of a cementless stem during the proliferative phase of healing was developed. The model was built from accurate geometries obtained from CT scans of a femur that was part of the study in Chapter 3. Micromotion-induced fluid flow was quantified based on local measurements of micromotion determined in the same study. We obtained the local distribution of fluid velocities in the granulation tissue and bone that surround the implant, from which we inferred the range of shear stresses experienced by the cells hosted in each tissue.

## General discussion and future perspectives

### *Measuring micromotion around orthopedic implants*

Many studies have shown that excessive implant micromotion alone could lead to osteolysis or fibrous tissue formation (Engh et al., 1992; Jasty et al., 1997b; Pilliar et al., 1986; Søballe et al., 1992), while subsequent suppression of micromotion allowed osseointegration to take place (Aspenberg et al., 1996). In respect to these results, it is generally accepted that although the mechanisms that lead to aseptic loosening remain obscure, achieving a good primary stability of the implant could be sufficient to guarantee the long-term survival of cementless orthopaedic implants.

Animal experiments showed that implant micromotion below a threshold of 40  $\mu\text{m}$  led to complete osseointegration, while micromotion over a limit of 150  $\mu\text{m}$  caused aseptic loosening (Jasty et al., 1997a; Pilliar et al., 1986; Søballe et al., 1992). These results were corroborated by a study conducted with retrieved femoral stems that established similar thresholds for humans (Engh et al., 1992; Jasty et al., 1997b). It follows that to discriminate between stable and unstable implants, a micromotion measurement technique should have a bias below 10  $\mu\text{m}$  (Viceconti et al., 2000). The technique introduced in Chapter 2 satisfies this criterion with a bias of 5.5  $\mu\text{m}$ . However, LVDTs, which are the current reference technique for micromotion measurement, have a much better accuracy, below 1  $\mu\text{m}$ . The bias of the micro-CT based technique described in this thesis depends on several parameters. The first one is the accuracy of the rigid body registration of implant markers, which can be easily evaluated through the root mean square error of the registration. The number of implant markers we used (30 markers in Chapter 2, 37 markers in Chapter 3), was chosen to allow a minimum of 4 implant markers by scan for an accurate registration. But it is plausible that a higher number of implant markers could help to further reduce the technique's bias. Another parameter that influences this bias is the metal artifacts generated by the markers. Metal artifacts arise from different phenomena, such as beam hardening or Poisson's noise (Boas et al., 2012), and are more pronounced with high atomic numbers materials such as stainless steel or tantalum. These artifacts affect randomly the gray values of the markers and make the automatic segmentation of the markers less accurate. One possible solution to limit metal artifacts is to scan using a higher voltage. In this thesis, we used the maximum voltage possible with our micro-CT scanner, but higher voltages are possible with industrial micro-CT scanners. Finally, scanning at a better resolution could help to further enhance the technique's accuracy. However, the tradeoff would be a much longer scanning time. A combination of higher voltage, more implant markers and better resolution is likely to bring this micro-CT based

technique to the same level of accuracy as LVDT-based measurements.

The strong point of the technique introduced in this thesis, is that it is the first one allowing full-field experimental measurement of micromotion around metallic femoral stems. The technique could theoretically be applied to other orthopedic implants made of titanium alloys such as humeral stems, or knee prostheses. However, the applicability to other metallic implants with higher atomic number (Cr-Co or stainless steel implants) remains limited, due to the stronger metal artifacts generated by these materials. The method is also not restrained to cementless implants, and could be used advantageously to measure cement strains or micromotion around cemented stems, by mixing stainless steel markers with the cement. Measuring cement strains would however require external reference markers, and a higher scanning resolution to capture the smaller displacements fields in the cement.

Finally, the weak point of this technique is the modification of the bone-implant interface caused by the introduction of bone markers. Indeed, legitimate concerns arise as to whether these markers affect the original bone-implant frictional contact. However, the markers were necessary to materialize the endosteal bone surface that is obscured on the scans due to the presence of the metallic implant. Digital volume correlation (DVC) is another micro-CT based technique that provides full-field measurements of strains and displacements in porous materials such as bone (Roberts et al., 2014). DVC does not require the presence of markers, but is strongly affected by metal artefacts. Nevertheless, the emergence of nano-computed tomography (nano-CT) could remove this limitation. Nano-CT scanners incorporate new X-ray tubes, that generate X-ray radiations at a much higher voltage than traditional micro-CT (Kampschulte et al., 2016). Moreover, several nano-CT scanners can accommodate very large samples, which could address another limitation of the technique proposed in this thesis. Indeed, a loading setup that closely recreates the physiological loading of the implant could be more easily fitted in such a scanner. Given the recent democratization of nano-CT technologies, using markerless DVC to measure micromotion around metallic orthopaedic implants seems to be a reasonable outlook for the near future.

### ***Pre-clinical and clinical applications of full-field measurements of micromotion***

The most straightforward application of full-field micromotion measurements is the pre-clinical testing of orthopedic implants. This is all the more important given that between 24% and 30% of hip arthroplasty components available on the market have no evidence supporting their use (Krakovits, 1996; Kynaston-Pearson et al., 2013). Different aspects of pre-clinical testing can be addressed through primary stability assessment: the comparison of implant designs, of surgical techniques, or the suitability of certain types of implants for a

given pathology or patient's category (osteoporosis, hip dysplasia, obesity, young and active patients etc. . .). Full-field measurements allow to observe local differences in micromotion that could have gone otherwise unnoticed with pointwise measurement techniques. This is yet more relevant as even minor changes in design, susceptible to result in only local micromotion differences, have been shown to influence dramatically the long-term survival of implants (Hauptfleisch et al., 2006; Roy et al., 2002).

In Chapter 3, we applied full-field micromotion measurement to compare the primary stability between a collared and a collarless version of the same stem. The study revealed no significant differences in subsidence, or global and local micromotion between the two groups, and average micromotion was below the 150  $\mu\text{m}$  limit for all implants tested. The femoral stem (Corail®Hip System, DePuy Synthes Joint Reconstruction, Warsaw, IN, USA) used in Chapter 3 has excellent long-term survival, and outperforms several other highly successful femoral stems (Keurentjes et al., 2014). For a better understanding of conditions leading to subsequent implant failure and revision, it would be of great interest to compare this highly-performing implant with acknowledged failed designs through full-field micromotion measurement, and to establish benchmarks for future comparisons.

Another perspective opened by full-field measurements of micromotion is the possibility to correlate local micromotion with other parameters measured locally, in an attempt to better understand the conditions that ensure a good primary stability. It seems obvious that a lack of bone-implant contact is highly unfavorable to primary stability. In addition to the bone-implant contact ratio, the location of contact areas influences significantly the implant fixation (Reimeringer et al., 2016). Bone-implant gap is relatively easy to compute from micro-CT or clinical CT scans, and maps of bone-implant gap could be correlated with maps of micromotion. Additionally, even though bone-implant contact is a crucial factor, the bone quality at the contact points is also central. Information about local bone density can also be inferred from CT scans, and could be related to other informations on the local mechanical environment around the stem, such as gap or micromotion.

An interesting result obtained in Chapter 3 was the high variability between donors. This result suggests that, when studying the effects of small design modifications, standardized composite femurs might be more appropriate than cadaveric bones as a first step in pre-clinical testing. It also confirms that the primary stability of implants is probably highly patient-specific.

However, accounting for patient's variability during experimental pre-clinical testing of implants requires an excessive amount of cadaveric femurs. Patient-specific finite element

modeling is therefore an important tool in pre-clinical testing for its ability to simulate different patient's anatomies or loading conditions (Taylor et al., 2013; Zadpoor et al., 2015). Furthermore, patient-specific finite element models are not only useful in pre-clinical testing, but could also be highly profitable in clinical practice as a decision tool for pre-operative planning. Surgeons could use such a tool to test different stem designs or surgical approaches according to the patient's own anatomy, and to select the combination of implant design and surgical technique that could lead to the best possible implant primary stability and maximize the long-term success of the arthroplasty. Nonetheless, the introduction of patient-specific finite element models for pre-operative planning in clinical practice faces the challenge of validation (Taylor et al., 2015). In this context, full-field micromotion measurements are of major interest, as they would allow a comprehensive validation of patient-specific finite element models.

#### ***Fluid-flow at the bone-implant interface***

Finally, another application of full-field micromotion measurements was to serve as boundary conditions in models that investigate potential mechanisms behind aseptic loosening. Micromotion-induced fluid flow around cementless implants has been proposed to play a role in peri-implant osteolysis, through high fluid velocities and pressures (Aspenberg et al., 1998; Fahlgren et al., 2010). Moreover, several *in vitro* mechanobiology experiments demonstrated the role of fluid flow in the osteogenic differentiation of mesenchymal stem cells (Arnsdorf et al., 2009; Yourek et al., 2010). The idea that biophysical stimuli such as micromotion-induced fluid flow can control the outcome of peri-implant healing is already two decades old (Prendergast et al., 1996; Prendergast et al., 1997). But the exact chain of mechanical and biological events that lead to aseptic loosening of implants remain today enigmatic, partly because the biophysical stimuli at the initial bone-implant interface are ill-defined. The model developed in Chapter 4 provides the distribution of micromotion-induced fluid flow in the granulation tissue and bone around a femoral stem. The model is based on accurate geometries of the bone-implant interface and full-field micromotion obtained experimentally, leading to a realistic estimation of the range of fluid velocities and shear stresses in the implant-surrounding tissues.

An interesting application of this model arises in the context of *in vitro* mechanobiology experiments. The role of fluid flow on the osteogenic differentiation of mesenchymal stem cells is usually studied using parallel plate flow chambers (MacQueen et al., 2013). The cells are plated in monolayers at the bottom of the flow chamber and exposed to fluid shear stress. Different amounts of shear stresses have already been shown to induce different cell responses (Glossop et al., 2009; Stolberg et al., 2009). The range of fluid velocities and shear



stresses obtained with the model detailed in Chapter 4 could be helpful to relate the *in vivo* stimuli to which cells are exposed to different cell responses.

Another application of the model developed in Chapter 4 is to study transport phenomena at the bone-implant interface. Transport of oxygen, nutrients, solutes or wear particles is susceptible to influence the outcome of peri-implant healing. Furthermore, gradients of morphogens generated by fluid flow have been proposed as a flow-sensing mechanisms for mesenchymal stem cells, controlling their osteogenic differentiation (Gortchacow et al., 2013). The micromotion-induced fluid flow model could be coupled to the model of morphogen transport to test the hypothesis that different levels of micromotion can generate morphogen gradients and differential cell responses.

Finally, the model detailed in Chapter 4 could be combined with mechano-regulatory models that simulate the course of peri-implant healing. Several mechano-regulatory algorithms are based on interstitial fluid velocity and have been corroborated with animal experiments (Ambard et al., 2006; Andreykiv et al., 2008; Geris et al., 2010; Johansson et al., 2011). It would certainly be interesting to observe the effects of complex geometries and boundary conditions on the predictions of these algorithms.

## Concluding remarks

This thesis focused on the characterization of the initial local mechanical environment around cementless femoral components in total hip arthroplasty. With the aging population and the continual increase of arthroplasties in young patients, improving the long-term success of cementless implants is becoming a major challenge for the orthopedic community. The development of a technique to measure full-field micromotion around cementless femoral stems lays the foundation for improved pre-clinical testing of implants and validated tools for patient-specific preoperative planning. The simulation of micromotion-induced fluid flow paves the way towards further understanding of the mechanisms behind aseptic loosening. In sum, these findings can lead to an improvement of implant survival, reducing the need for implant revisions and their associated social and financial burden.

## References

Ambard, Dominique and Pascal Swider (2006). "A predictive mechano-biological model of the bone-implant healing". In: *European Journal of Mechanics - A/Solids* 25.66, pp. 927–937.

- Andreykiv, A, F van Keulen, and Patrick J Prendergast (2008). "Computational mechanobiology to study the effect of surface geometry on peri-implant tissue differentiation." In: *Journal of Biomechanical Engineering* 130.55, p. 051015.
- Arnsdorf, Emily J et al. (2009). "Mechanically induced osteogenic differentiation - the role of RhoA, ROCKII and cytoskeletal dynamics". In: *Journal of Cell Science* 122.44, pp. 546–553.
- Aspenberg, Per and P Herbertsson (1996). "Periprosthetic bone resorption. Particles versus movement." In: *The Journal of bone and joint surgery. British volume* 78.44, pp. 641–646.
- Aspenberg, Per and Harm M Van der Vis (1998). "Migration, particles, and fluid pressure. A discussion of causes of prosthetic loosening." In: *Clinical Orthopaedics and Related Research* 352352, pp. 75–80.
- Boas, F Edward and Dominik Fleischmann (2012). "CT artifacts: Causes and reduction techniques". In: *Imaging in Medicine* 4.22, pp. 229–240.
- Engl, Charles A et al. (1992). "Quantification of Implant Micromotion, Strain Shielding, and Bone Resorption With Porous-Coated Anatomic Medullary Locking Femoral Prostheses". In: *Clinical Orthopaedics and Related Research* 285285, pp. 13–29.
- Fahlgren, Anna et al. (2010). "Fluid pressure and flow as a cause of bone resorption." In: *Acta Orthopaedica* 81.44, pp. 508–516.
- Geris, Liesbet et al. (2010). "Mechanical loading affects angiogenesis and osteogenesis in an in vivo bone chamber: a modeling study." In: *Tissue Engineering Part A* 16.1111, pp. 3353–3361.
- Glossop, John R and Sarah H Cartmell (2009). "Effect of fluid flow-induced shear stress on human mesenchymal stem cells: Differential gene expression of IL1B and MAP3K8 in MAPK signaling". In: *Gene Expression Patterns* 9.55, pp. 381–388.
- Gortchacow, Michael, Alexandre Terrier, and Dominique P Pioletti (2013). "A Flow Sensing Model for Mesenchymal Stromal Cells Using Morphogen Dynamics". In: *Biophysical journal* 104.1010, pp. 2132–2136.
- Hauptfleisch, J et al. (2006). "The premature failure of the Charnley Elite-Plus stem - A confirmation of RSA predictions". In: *The Journal of bone and joint surgery. British volume* 88B.22, pp. 179–183.
- Jasty, M et al. (1997a). "In Vivo Skeletal Responses to Porous-Surfaced Implants Subjected to Small Induced Motions". In: *The Journal of Bone and Joint Surgery. American Volume* 79.55, pp. 707–714.
- Jasty, Murali et al. (1997b). "Enhanced stability of uncemented canine femoral components by bone ingrowth into the porous coatings". In: *The Journal of Arthroplasty* 12.11, pp. 106–113.
- Johansson, Lars et al. (2011). "Fluid-induced osteolysis: modelling and experiments." In: *Computer Methods in Biomechanics and Biomedical Engineering* 14.44, pp. 305–318.

- Kampschulte, M et al. (2016). "Nano-Computed Tomography: Technique and Applications". In: *RöFo - Fortschritte auf dem Gebiet der Röntgenstrahlen und der bildgebenden Verfahren* 188.22, pp. 146–154.
- Kärrholm, J et al. (1994). "Does early micromotion of femoral stem prostheses matter? 4-7-year stereoradiographic follow-up of 84 cemented prostheses." In: *The Journal of bone and joint surgery. British volume* 76.66, pp. 912–917.
- Keurentjes, J Christiaan et al. (2014). "Which Implant Should We Use for Primary Total Hip Replacement?" In: *Journal of Bone and Joint Surgery-American Volume* 96A, pp. 79–97.
- Krakovits, G (1996). "Which primary total hip replacement?" In: *The Journal of bone and joint surgery. British volume* 78B.33, p. 510.
- Kynaston-Pearson, F et al. (2013). "Primary hip replacement prostheses and their evidence base: systematic review of literature". In: *BMJ* 347, f6956.
- MacQueen, L, Y Sun, and Craig A Simmons (2013). "Mesenchymal stem cell mechanobiology and emerging experimental platforms". In: *Journal of The Royal Society Interface* 10.8484, p. 20130179.
- Mjöberg, Bengt (1994). "Theories of wear and loosening in hip prostheses: Wear-induced loosening vs loosening-induced wear-a review". In: *Acta Orthopaedica* 65.33, pp. 361–371.
- Pilliar, R M, J M Lee, and C Maniopoulos (1986). "Observations on the Effect of Movement on Bone Ingrowth into Porous-Surfaced Implants". In: *Clinical Orthopaedics and Related Research* 208208, pp. 108–113.
- Prendergast, Patrick J and Rik Huiskes (1996). "Finite element analysis of fibrous tissue morphogenesis - A study of the osteogenic index with a biphasic approach". In: *Mechanics of Composite Materials* 32.22, pp. 144–150.
- Prendergast, Patrick J, Rik Huiskes, and Kjeld Søballe (1997). "Biophysical stimuli on cells during tissue differentiation at implant interfaces". In: *Journal of Biomechanics* 30.66, pp. 539–548.
- Reimeringer, M and N Nuño (2016). "The influence of contact ratio and its location on the primary stability of cementless total hip arthroplasty: A finite element analysis". In: *Journal of Biomechanics* 49.77, pp. 1064–1070.
- Roberts, Bryant C, Egon Perilli, and Karen J Reynolds (2014). "Application of the digital volume correlation technique for the measurement of displacement and strain fields in bone: A literature review". In: *Journal of Biomechanics* 47.55, pp. 923–934.
- Roy, N et al. (2002). "3M Capital hip arthroplasty - 3-8-year follow-up of 208 primary hip replacements". In: *Acta Orthopaedica Scandinavica* 73.44, pp. 400–402.
- Søballe, Kjeld et al. (1992). "Tissue ingrowth into titanium and hydroxyapatite-coated implants during stable and unstable mechanical conditions". In: *Journal of Orthopaedic Research* 10.22, pp. 285–299.

- Stolberg, Sarah and Kara E McCloskey (2009). "Can shear stress direct stem cell fate?" In: *Biotechnology Progress* 25.11, pp. 10–19.
- Sundfeldt, Mikael et al. (2006). "Aseptic loosening, not only a question of wear: A review of different theories". In: *Acta Orthopaedica* 77.22, pp. 177–197.
- Taylor, Mark, Rebecca Bryan, and Francis Galloway (2013). "Accounting for patient variability in finite element analysis of the intact and implanted hip and knee: a review." In: *International Journal for Numerical Methods in Biomedical Engineering* 29.22, pp. 273–292.
- Taylor, Mark and Patrick J Prendergast (2015). "Four decades of finite element analysis of orthopaedic devices: Where are we now and what are the opportunities?" In: *Journal of Biomechanics* 48.55, pp. 767–778.
- Viceconti, Marco et al. (2000). "Large-sliding contact elements accurately predict levels of bone–implant micromotion relevant to osseointegration". In: *Journal of Biomechanics* 33.1212, pp. 1611–1618.
- Wyatt, Michael et al. (2014). "Survival outcomes of cemented compared to uncemented stems in primary total hip replacement". In: *World Journal of Orthopedics* 5.55, p. 591.
- Yourek, Gregory et al. (2010). "Shear stress induces osteogenic differentiation of human mesenchymal stem cells". In: *Regenerative Medicine* 5.55, pp. 713–724.
- Zadpoor, Amir A and Harrie Weinans (2015). "Patient-specific bone modeling and analysis: The role of integration and automation in clinical adoption". In: *Journal of Biomechanics* 48.55, pp. 750–760.

# Appendix A

Supplementary material  
to Chapter 2



## Bone-implant gap

Pre-operative, post-broaching and post-operative CT scans were performed. Bone and implant were segmented in Amira on the post-broaching and post-operative CT-scans respectively. The post-broaching scan was then rigidly registered to the post-operative scan. The post-broaching bone surface and post-operative implant surface were reconstructed from the segmented images, and the gap was computed as the distance between these two surfaces using the surface distance module of Amira.

Bone-implant gap ranged from 0 to 7.7 mm (Fig. A.1). Mean gap was 0.9 mm. The gap was below 1.5 mm on 80% of the stem. There was complete bone-implant contact (0 mm gap) on the most part of the metaphyseal portion of the stem and on the lateral distal diaphysis. There was a locally higher gap on the antero-medial part of the distal diaphysis and on the posterior middle diaphysis.



**Figure A.1:** Gap measured around the cementless femoral stem - Anterior/lateral and posterior/medial views of the stem displayed successively from left to right.

# Appendix **B**

Supplementary material  
to Chapter 3



**Donor information**

<b>Donor #</b>	<b>Gender</b>	<b>Age (y.o.)</b>	<b>Side</b>	<b>Height (m)</b>	<b>Weight (kg)</b>	<b>BMI</b>	<b>Implant</b>
1	Female	74	Right	1.52	74	32.0	Collared
2	Female	72	Left	1.57	74	30.0	Collared
3	Male	82	Left	1.68	91	32.2	Collared
4	Male	90	Left	1.70	89	30.8	Collared
5	Male	93	Right	1.75	56	18.3	Collared
6	Male	72	Left	1.83	68	20.3	Collared
7	Male	32	Right	1.73	77	25.7	Collarless
8	Male	67	Left	1.73	108	36.1	Collarless
9	Male	69	Right	1.68	65	23.0	Collarless
10	Male	54	Left	1.63	70	26.4	Collarless

**Table B.1:** *Donor information.*



# Appendix C

Supplementary material  
to Chapter 4



## Governing equations

Biot's poroelasticity theory was used to describe the mechanical behavior of the tissues at the bone-implant interface. It relates the linear elasticity equations for the solid matrix, the mass conservation equation for the viscous fluid, and Darcy's law for fluid flow through a porous matrix.

*Momentum conservation equation of the solid phase:* The inertia terms in Navier's equation for a solid in equilibrium are neglected because we assume a low post-operative loading frequency. The equation becomes:

$$\nabla \boldsymbol{\sigma} = 0 \quad (\text{C.1})$$

where  $\boldsymbol{\sigma}$  is the total stress tensor.

*Mass conservation equation of the fluid phase:* The mass conservation law links the increment in fluid content  $\zeta$  to the fluid velocity  $\mathbf{v}$ :

$$\frac{\partial \zeta}{\partial t} + \nabla \mathbf{v} = 0 \quad (\text{C.2})$$

*Darcy's law for fluid flow through a porous medium:* Darcy's law links the fluid velocity  $\mathbf{v}$  and the fluid pore pressure gradient:

$$\mathbf{v} = -\frac{\kappa}{\mu} \nabla p_f \quad (\text{C.3})$$

where  $\kappa$  is the permeability,  $\mu$  is the fluid's viscosity and  $p_f$  is the fluid pore pressure.

*Biot's constitutive equations:* The first constitutive relation links linearly the stress, strain, and pore pressure:

$$\boldsymbol{\sigma} = \mathbb{C} \boldsymbol{\varepsilon} - \alpha_B p_f \quad (\text{C.4})$$

where  $\mathbb{C}$  is the elasticity matrix of the drained porous matrix,  $\boldsymbol{\varepsilon}$  is the strain tensor, and  $\alpha_B$  is the Biot-Willis coefficient.

The Biot-Willis coefficient can be defined in terms of the drained and solid bulk moduli of the solid matrix as:

$$\alpha_B = 1 - \frac{K_d}{K_s} \quad (\text{C.5})$$

where  $K_d$  is the drained bulk modulus and  $K_s$  is the solid bulk modulus.

The second constitutive relation links the pore pressure  $p_f$  with the increment in fluid content  $\zeta$ , and the volumetric strain  $\epsilon_{\text{vol}}$ :

$$p_f = \frac{1}{S}(\zeta - \alpha_B \epsilon_{\text{vol}}) \quad (\text{C.6})$$

where  $S$  is the storage coefficient:

$$S = \frac{\phi}{K_f} + \frac{\alpha_B - \phi}{K_s} \quad (\text{C.7})$$

and  $\phi$  is the solid matrix porosity and  $K_f$  is the fluid bulk modulus.

The boundary conditions for the solid part were:

$$\begin{cases} \mathbf{u} = 0 & , \forall \mathbf{r} = \mathbf{r}_3 \\ \mathbf{u} = \mathbf{A} \sin(2\pi f t - \frac{\pi}{2}) & , \forall \mathbf{r} = \mathbf{r}_0 \end{cases} \quad (\text{C.8})$$

where  $\mathbf{u}$  is the displacement field,  $\mathbf{r}_3$  is the external boundary of cortical bone,  $\mathbf{A}$  is the amplitude of micromotion in the x-direction,  $f$  is the loading frequency and  $\mathbf{r}_0$  is the implant boundary.

The boundary conditions for the porous medium flow part were:

$$\begin{cases} \mathbf{n} \cdot \nabla p_f = 0 & , \forall \mathbf{r} = \mathbf{r}_0 \\ p_f = 1 \text{ atm} & , \forall \mathbf{r} = \mathbf{r}_3 \end{cases} \quad (\text{C.9})$$

where  $\mathbf{n}$  is a unit vector normal to the boundary and  $p_f$  is the fluid pore pressure

The initial conditions were:

$$\begin{cases} p_{f0} = 1 \text{ atm} \\ \mathbf{u}_0 = 0 \end{cases} \quad (\text{C.10})$$

## Mesh characteristics

A mesh sensitivity study was conducted with the 2D idealized model with a 0.5 mm gap, with numbers of degrees of freedom (DOF) ranging from 4'121 to 101'612. Peak von Mises stress and fluid velocity were used as outcome metrics. The extremely fine mesh with 101'612 DOF was used as the 'exact' answer to which other results were compared.

The results showed peak Darcy's velocity and von Mises stress relative errors of 3.5% and 0.3% respectively with 61'285 DOF. Further refinement to 74'870 DOF lead to errors of 0.2% and 0.3%, showing that ~70'000 DOF should be sufficient to apprehend accurately peak fluid velocities at the interface.

	Idealized parametric model (0.5 mm gap)	Idealized parametric model (5 mm gap)	Representative transverse section - proximal	Representative transverse section - middle diaphyseal	Representative transverse section - distal diaphyseal	3D model
<b>Number of cortical bone elements</b>	9'814	13'212	4'204	18'188	17'515	117'382
<b>Number of trabecular bone elements</b>	5'864	9'478	11'756	11'574	10'100	197'998
<b>Number of granulation tissue elements</b>	702	9'678	387	1'789	3'000	112'192
<b>Total number of elements</b>	16'380	32'368	16'347	31'551	30'615	427'572
<b>DOF</b>	74'870	147'071	74'729	144'002	139'645	1'880'519

**Table C.1:** Number of mesh elements and degrees of freedom (DOF) for each model.

## Experimental measurement of micromotion

The implanted femur was part of a larger study that was described in Chapter 3. Briefly, radiopaque markers were spread on the endosteal surface of the bone and at the surface of the femoral stem. Unloaded and loaded micro-computed tomography (micro-CT) scans of the bone-implant interface were performed to compute the relative displacement of bone and implant markers. This measurement resulted in hundreds of measurement points of 3D micromotion around the femoral stem. Micromotion values between measurement points were interpolated using natural neighbor interpolation and linearly extrapolated on the implant surface for visualization (Figure S1). Implant micromotion was measured separately for an axial compression case and an axial torsion case, simulating walking and stair climbing loading cases respectively.

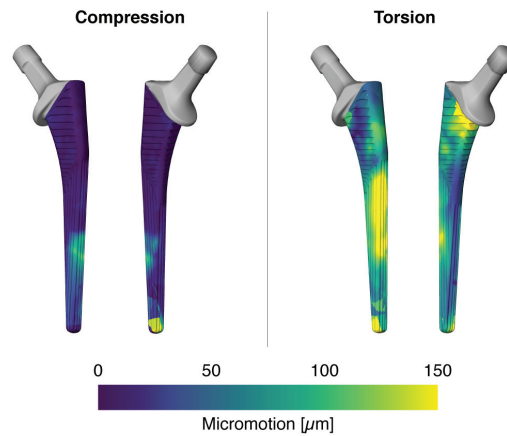


**Figure C.1:** Distribution of implant micromotion measured experimentally in compression and torsion and used as boundary conditions for the representative transverse sections models and for the simplified 3D model.



# Bibliography



- ASTM (2013). "E177 - 14 - Standard Practice for Use of the Terms Precision and Bias in ASTM Test Methods". In:
- Abdul-Kadir, Mohammed Rafiq et al. (2008). "Finite element modelling of primary hip stem stability: The effect of interference fit". In: *Journal of Biomechanics* 41.33, pp. 587–594.
- Abu-Amer, Yousef, Isra Darwech, and John C Clohisy (2007). "Aseptic loosening of total joint replacements: mechanisms underlying osteolysis and potential therapies." In: *Arthritis Research and Therapy* 9 Suppl 1, S6.
- Alidousti, Hamidreza, Mark Taylor, and Neil W Bressloff (2011). "Do capsular pressure and implant motion interact to cause high pressure in the periprosthetic bone in total hip replacement?" In: *Journal of Biomechanical Engineering* 133.1212, p. 121001.
- (2014). "Periprosthetic wear particle migration and distribution modelling and the implication for osteolysis in cementless total hip replacement." In: *Journal of the Mechanical Behavior of Biomedical Materials* 32, pp. 225–244.
- Ambard, Dominique and Pascal Swider (2006). "A predictive mechano-biological model of the bone-implant healing". In: *European Journal of Mechanics - A/Solids* 25.66, pp. 927–937.
- Andreykiv, A, F van Keulen, and Patrick J Prendergast (2008). "Computational mechanobiology to study the effect of surface geometry on peri-implant tissue differentiation." In: *Journal of Biomechanical Engineering* 130.55, p. 051015.
- Arnsdorf, Emily J et al. (2009a). "Mechanically induced osteogenic differentiation - the role of RhoA, ROCKII and cytoskeletal dynamics". In: *Journal of Cell Science* 122.44, pp. 546–553.
- Arnsdorf, Emily J, Padmaja Tummala, and Christopher R Jacobs (2009b). "Non-Canonical Wnt Signaling and N-Cadherin Related  $\beta$ -Catenin Signaling Play a Role in Mechanically Induced Osteogenic Cell Fate". In: *PloS One* 4.44, e5388.
- Ashman, R B et al. (1984). "A continuous wave technique for the measurement of the elastic properties of cortical bone." In: *Journal of Biomechanics* 17.55, pp. 349–361.
- Aspenberg, Per and P Herbertsson (1996). "Periprosthetic bone resorption. Particles versus movement." In: *The Journal of bone and joint surgery. British volume* 78.44, pp. 641–646.
- Aspenberg, Per and Harm M Van der Vis (1998). "Migration, particles, and fluid pressure. A discussion of causes of prosthetic loosening." In: *Clinical Orthopaedics and Related Research* 352352, pp. 75–80.
- Australian Orthopaedic Association National Joint Replacement Registry (2015). *Annual Report*.
- Bah, Mamadou T et al. (2011). "Efficient computational method for assessing the effects of implant positioning in cementless total hip replacements." In: *Journal of Biomechanics* 44.77, pp. 1417–1422.
- Bah, Mamadou T et al. (2015). "Inter-subject variability effects on the primary stability of a short cementless femoral stem". In: *Journal of Biomechanics* 48.66, pp. 1032–1042.



- Baleani, Massimiliano, Luca Cristofolini, and Aldo Toni (2000). "Initial stability of a new hybrid fixation hip stem: Experimental measurement of implant–bone micromotion under torsional load in comparison with cemented and cementless stems". In: *Journal of Biomedical Materials Research* 50.44, pp. 605–615.
- Beck, Ryan T, Kenneth D Illingworth, and Khaled J Saleh (2012). "Review of periprosthetic osteolysis in total joint arthroplasty: An emphasis on host factors and future directions". In: *Journal of orthopaedic research : official publication of the Orthopaedic Research Society* 30.44, pp. 541–546.
- Bergmann, G et al. (2010a). "Erratum: Realistic loads for testing hip implants (Bio-Medical Materials and Engineering (2010) 20 (65-75))". In: *Bio-Medical Materials and Engineering* 20.66, p. 381.
- (2010b). "Realistic loads for testing hip implants". In: *Bio-Medical Materials and Engineering* 20.22, pp. 65–75.
- Bergmann, Georg et al. (2016). "Standardized loads acting in hip implants". In: *PloS One* 11.55, e0155612.
- Besl, P J and H D McKay (1992). "A method for registration of 3-D shapes". In: *IEEE Transactions on Pattern Analysis and Machine Intelligence* 14.22, pp. 239–256.
- Bieger, Ralf et al. (2012). "Primary stability and strain distribution of cementless hip stems as a function of implant design". In: *Clinical Biomechanics* 27.22, pp. 158–164.
- Bieger, Ralf et al. (2013). "Biomechanics of a short stem: In vitro primary stability and stress shielding of a conservative cementless hip stem." In: *Journal of orthopaedic research : official publication of the Orthopaedic Research Society* 31.88, pp. 1180–1186.
- Bieger, Ralf et al. (2016). "Primary stability of a shoulderless Zweymüller hip stem: a comparative in vitro micromotion study". In: *Journal of Orthopaedic Surgery and Research* 11.11, p. 500.
- Boas, F Edward and Dominik Fleischmann (2012). "CT artifacts: Causes and reduction techniques". In: *Imaging in Medicine* 4.22, pp. 229–240.
- Britton, J R, C G Lyons, and Patrick J Prendergast (2004). "Measurement of the Relative Motion Between an Implant and Bone under Cyclic Loading". In: *Strain* 40.44, pp. 193–202.
- Carlsson, Lars et al. (1986). "Osseointegration of titanium implants". In: *Acta Orthopaedica* 57.44, pp. 285–289.
- Conroy, Mark J et al. (2006). "High-resolution magnetic resonance flow imaging in a model of porous bone–implant interface". In: *Magnetic Resonance Imaging* 24.55, pp. 657–661.
- Cowin, Stephen C (1999). "Bone poroelasticity". In: *Journal of Biomechanics* 32.33, pp. 217–238.
- Currey, John D et al. (1995). "Effect of formaldehyde fixation on some mechanical properties of bovine bone". In: *Biomaterials* 16.1616, pp. 1267–1271.

- Davies, J E (2003). "Understanding peri-implant endosseous healing". In: *Journal of dental education* 67.88, pp. 932–949.
- Demey, Guillaume et al. (2011). "Does a Collar Improve the Immediate Stability of Uncemented Femoral Hip Stems in Total Hip Arthroplasty? A Bilateral Comparative Cadaver Study". In: *The Journal of Arthroplasty* 26.88, pp. 1549–1555.
- Diamond, S L (1999). "Engineering design of optimal strategies for blood clot dissolution". In: *Annual Review of Biomedical Engineering* 1.11, pp. 427–462.
- Donahue, T L Haut et al. (2003). "Mechanosensitivity of bone cells to oscillating fluid flow induced shear stress may be modulated by chemotransport". In: *Journal of Biomechanics* 36.99, pp. 1363–1371.
- Ebramzadeh, E et al. (2004). "Initial stability of cemented femoral stems as a function of surface finish, collar, and stem size". In: *The Journal of Bone and Joint Surgery. American Volume* 86A.11, pp. 106–115.
- Engl, Charles A et al. (1992). "Quantification of Implant Micromotion, Strain Shielding, and Bone Resorption With Porous-Coated Anatomic Medullary Locking Femoral Prostheses". In: *Clinical Orthopaedics and Related Research* 285.285, pp. 13–29.
- Enoksen, Cathrine H et al. (2014). "Initial stability of an uncemented femoral stem with modular necks. An experimental study in human cadaver femurs". In: *Clinical Biomechanics* 29.33, pp. 330–335.
- Ethgen, Olivier et al. (2004). "Health-Related Quality of Life in Total Hip and Total Knee Arthroplasty". In: *The Journal of Bone and Joint Surgery. American Volume* 86.55, pp. 963–974.
- Fahlgren, Anna et al. (2010). "Fluid pressure and flow as a cause of bone resorption." In: *Acta Orthopaedica* 81.44, pp. 508–516.
- Fahlgren, Anna, Lars Johansson, and Ulf Edlund (2012). "Direct ex vivo measurement of the fluid permeability of loose scar tissue". In: *Acta of Bioengineering and Biomechanics*.
- Ferrier, G M et al. (2000). "The effect of cyclic pressure on human monocyte-derived macrophages in vitro." In: *The Journal of bone and joint surgery. British volume* 82.55, pp. 755–759.
- Feyen, H and A J Shimmin (2014). "Is the length of the femoral component important in primary total hip replacement?" In: *The Bone and Joint Journal* 96-B.44, pp. 442–448.
- Fottner, Andreas et al. (2009). "Biomechanical evaluation of two types of short-stemmed hip prostheses compared to the trust plate prosthesis by three-dimensional measurement of micromotions". In: *Clinical Biomechanics* 24.55, pp. 429–434.
- Fottner, Andreas et al. (2011). "Biomechanical evaluation of different offset versions of a cementless hip prosthesis by 3-dimensional measurement of micromotions". In: *Clinical Biomechanics* 26.88, pp. 830–835.

- Gabarre, Sergio et al. (2016). "Comparative Analysis of the Biomechanical Behaviour of Two Cementless Short Stems for Hip Replacement: Linea Anatomic and Minihip". In: *PloS One* 11.77, e0158411.
- Geris, Liesbet et al. (2003). "Assessment of Mechanobiological Models for the Numerical Simulation of Tissue Differentiation around Immediately Loaded Implants". In: *Computer Methods in Biomechanics and Biomedical Engineering* 6.55, pp. 277–288.
- Geris, Liesbet et al. (2010). "Mechanical loading affects angiogenesis and osteogenesis in an in vivo bone chamber: a modeling study." In: *Tissue Engineering Part A* 16.1111, pp. 3353–3361.
- Glossop, John R and Sarah H Cartmell (2009). "Effect of fluid flow-induced shear stress on human mesenchymal stem cells: Differential gene expression of IL1B and MAP3K8 in MAPK signaling". In: *Gene Expression Patterns* 9.55, pp. 381–388.
- Gortchacow, Michael et al. (2011). "A new technique to measure micromotion distribution around a cementless femoral stem". In: *Journal of Biomechanics* 44.33, pp. 557–560.
- Gortchacow, Michael et al. (2012). "Simultaneous and multisite measure of micromotion, subsidence and gap to evaluate femoral stem stability". In: *Journal of Biomechanics* 45.77, pp. 1232–1238.
- Gortchacow, Michael, Alexandre Terrier, and Dominique P Pioletti (2013). "A Flow Sensing Model for Mesenchymal Stromal Cells Using Morphogen Dynamics". In: *Biophysical journal* 104.1010, pp. 2132–2136.
- Götze, Christian et al. (2002). "Primary stability in cementless femoral stems: custom-made versus conventional femoral prosthesis". In: *Clinical Biomechanics* 17.44, pp. 267–273.
- Govey, Peter M, Alayna E Loiselle, and Henry J Donahue (2013). "Biophysical Regulation of Stem Cell Differentiation". In: *Current Osteoporosis Reports* 11.22, pp. 83–91.
- Gruen, Thomas A, Gregory M McNeice, and Harlan C Amstutz (1979). "'Modes of Failure' of Cemented Stem-type Femoral Components". In: *Clinical Orthopaedics and Related Research* 141141, pp. 17–27.
- Guérin, Gaëtan, Dominique Ambard, and Pascal Swider (2009). "Cells, growth factors and bioactive surface properties in a mechanobiological model of implant healing". In: *Journal of Biomechanics* 42.1515, pp. 2555–2561.
- Gurkan, Umut Atakan and Ozan Akkus (2008). "The Mechanical Environment of Bone Marrow: A Review". In: *Annals of biomedical engineering* 36.1212, pp. 1978–1991.
- Hardy, D C R, P Frayssinet, and P E Delince (1999a). "Osteointegration of hydroxyapatite-coated stems of femoral prostheses". In: *European Journal of Orthopaedic Surgery and Traumatology* 9.22, pp. 75–81.
- Hardy, D C et al. (1999b). "Histopathology of a well-functioning hydroxyapatite-coated femoral prosthesis after 52 months." In: *Acta orthopaedica Belgica* 65.11, pp. 72–82.

- Hassanizadeh, S Majid and William G Gray (1987). "High velocity flow in porous media". In: *Transport in Porous Media* 2.66, pp. 521–531.
- Haudenschild, Anne K et al. (2009). "Pressure and distortion regulate human mesenchymal stem cell gene expression." In: *Annals of biomedical engineering* 37.33, pp. 492–502.
- Hauptfleisch, J et al. (2006). "The premature failure of the Charnley Elite-Plus stem - A confirmation of RSA predictions". In: *The Journal of bone and joint surgery. British volume* 88B.22, pp. 179–183.
- Hemmingsen, Mette et al. (2013). "The Role of Paracrine and Autocrine Signaling in the Early Phase of Adipogenic Differentiation of Adipose-derived Stem Cells". In: *PloS One* 8.55, e63638.
- Hendrix, R W et al. (1983). "Arthrography after total hip arthroplasty: a modified technique used in the diagnosis of pain." In: *Radiology* 148.33, pp. 647–652.
- Hooper, G J et al. (2009). "Revision following cemented and uncemented primary total hip replacement: a seven-year analysis from the New Zealand Joint Registry." In: *The Journal of bone and joint surgery. British volume* 91.44, pp. 451–458.
- Huiskes, Rik, W D Van Driel, and Patrick J Prendergast (1997). "A biomechanical regulatory model for periprosthetic fibrous-tissue differentiation". In: *Journal of Materials Science* 8.1212, pp. 785–788.
- Hutt, Jonathan et al. (2014). "The effect of a collar and surface finish on cemented femoral stems: A prospective randomised trial of four stem designs". In: *International Orthopaedics* 38.66, pp. 1131–1137.
- Isaksson, Hanna, Corrinus C van Donkelaar, and Keita Ito (2009). "Sensitivity of tissue differentiation and bone healing predictions to tissue properties". In: *Journal of Biomechanics* 42.55, pp. 555–564.
- Issa, Kimona and Michael A Mont (2013). "Total hip replacement: Mortality and risks". In: *The Lancet* 382.98989898, pp. 1074–1076.
- Jameson, S S et al. (2013). "Independent predictors of failure up to 7.5 years after 35 386 single-brand cementless total hip replacements". In: *The Bone and Joint Journal* 95-B.66, pp. 747–757.
- Jasty, M et al. (1997a). "In Vivo Skeletal Responses to Porous-Surfaced Implants Subjected to Small Induced Motions". In: *The Journal of Bone and Joint Surgery. American Volume* 79.55, pp. 707–714.
- Jasty, Murali et al. (1997b). "Enhanced stability of uncemented canine femoral components by bone ingrowth into the porous coatings". In: *The Journal of Arthroplasty* 12.11, pp. 106–113.
- Johansson, Lars et al. (2011). "Fluid-induced osteolysis: modelling and experiments." In: *Computer Methods in Biomechanics and Biomedical Engineering* 14.44, pp. 305–318.

- Johnson, M W et al. (1982). "Fluid flow in bone in vitro". In: *Journal of Biomechanics* 15.1111, pp. 881–885.
- Jurvelin, J S, M D Buschmann, and E B Hunziker (1997). "Optical and mechanical determination of poisson's ratio of adult bovine humeral articular cartilage". In: *Journal of Biomechanics* 30.33, pp. 235–241.
- Kampschulte, M et al. (2016). "Nano-Computed Tomography: Technique and Applications". In: *RöFo - Fortschritte auf dem Gebiet der Röntgenstrahlen und der bildgebenden Verfahren* 188.22, pp. 146–154.
- Kang, Q, YHH An, and R J Friedman (1997). "Effects of multiple freezing-thawing cycles on ultimate indentation load and stiffness of bovine cancellous bone". In: *American Journal of Veterinary Research* 58.1010, pp. 1171–1173.
- Kärrholm, J et al. (1994). "Does early micromotion of femoral stem prostheses matter? 4-7-year stereoradiographic follow-up of 84 cemented prostheses." In: *The Journal of bone and joint surgery. British volume* 76.66, pp. 912–917.
- Kassi, Jean-Pierre et al. (2005). "Stair climbing is more critical than walking in pre-clinical assessment of primary stability in cementless THA in vitro". In: *Journal of Biomechanics* 38.55, pp. 1143–1154.
- Keurentjes, J Christiaan et al. (2014). "Which Implant Should We Use for Primary Total Hip Replacement?" In: *Journal of Bone and Joint Surgery-American Volume* 96A, pp. 79–97.
- Khanuja, Harpal S et al. (2011). "Cementless femoral fixation in total hip arthroplasty." In: *The Journal of Bone and Joint Surgery. American Volume* 93.55, pp. 500–509.
- Khayeri, Hanifeh et al. (2009). "Corroboration of mechanobiological simulations of tissue differentiation in an in vivo bone chamber using a lattice-modeling approach". In: *Journal of orthopaedic research : official publication of the Orthopaedic Research Society* 27.1212, pp. 1659–1666.
- Kiviranta, Panu et al. (2006). "Collagen network primarily controls Poisson's ratio of bovine articular cartilage in compression". In: *Journal of orthopaedic research : official publication of the Orthopaedic Research Society* 24.44, pp. 690–699.
- Kohles, Sean S and Julie B Roberts (2002). "Linear Poroelastic Cancellous Bone Anisotropy: Trabecular Solid Elastic and Fluid Transport Properties". In: *Journal of Biomechanical Engineering* 124.55, p. 521.
- Kraaij, Gert et al. (2014). "Mechanical properties of human bone-implant interface tissue in aseptically loose hip implants". In: *Journal of the Mechanical Behavior of Biomedical Materials* 38, pp. 59–68.
- Krakovits, G (1996). "Which primary total hip replacement?" In: *The Journal of bone and joint surgery. British volume* 78B.33, p. 510.

- Kreke, Michelle R, William R Huckle, and Aaron S Goldstein (2005). "Fluid flow stimulates expression of osteopontin and bone sialoprotein by bone marrow stromal cells in a temporally dependent manner." In: *Bone* 36.66, pp. 1047–1055.
- Kynaston-Pearson, F et al. (2013). "Primary hip replacement prostheses and their evidence base: systematic review of literature". In: *BMJ* 347, f6956.
- Learmonth, Ian D, Claire Young, and Cecil Rorabeck (2007). "The operation of the century: total hip replacement". In: *The Lancet* 370.95979597, pp. 1508–1519.
- Leong, P L and E F Morgan (2008). "Measurement of fracture callus material properties via nanoindentation". In: *Acta Biomaterialia* 4.55, pp. 1569–1575.
- Leys, Christophe et al. (2013). "Detecting outliers: Do not use standard deviation around the mean, use absolute deviation around the median". In: *Journal of Experimental Social Psychology* 49.44, pp. 764–766.
- Linde, Frank and Hans Christian Florian Sørensen (1993). "The effect of different storage methods on the mechanical properties of trabecular bone". In: *Journal of Biomechanics* 26.1010, pp. 1249–1252.
- MacQueen, L, Y Sun, and Craig A Simmons (2013). "Mesenchymal stem cell mechanobiology and emerging experimental platforms". In: *Journal of The Royal Society Interface* 10.8484, p. 20130179.
- Mai, Kenny T et al. (2010). "Cementless Femoral Fixation in Total Hip Arthroplasty". In: *Am J Orthop*.
- Malfroy Camine, Valérie et al. (2016). "Full-field measurement of micromotion around a cementless femoral stem using micro-CT imaging and radiopaque markers". In: *Journal of Biomechanics*.
- Mandell, Jay A et al. (2004). "A conical-collared intramedullary stem can improve stress transfer and limit micromotion". In: *Clinical Biomechanics* 19.77, pp. 695–703.
- Mann, Kenneth A et al. (2012). "Interface Micromotion of Uncemented Femoral Components from Postmortem Retrieved Total Hip Replacements". In: *The Journal of Arthroplasty* 27.22, pp. 238–245.
- Mann, Kenneth A and Mark A Miller (2014). "Fluid-structure interactions in micro-interlocked regions of the cement-bone interface". In: *Computer Methods in Biomechanics and Biomedical Engineering* 17.1616, pp. 1809–1820.
- Matthews, J B et al. (2000a). "Comparison of the response of primary human peripheral blood mononuclear phagocytes from different donors to challenge with model polyethylene particles of ..." In: *Biomaterials* 21.20, pp. 2033–2044.
- Matthews, J B et al. (2000b). "Evaluation of the response of primary human peripheral blood mononuclear phagocytes to challenge with in vitro generated clinically relevant



- UHMWPE particles of known size and dose.” In: *Journal of Biomedical Materials Research* 52.22, pp. 296–307.
- Meding, John B et al. (1997). “Comparison of collared and collarless femoral components in primary uncemented total hip arthroplasty”. In: *The Journal of Arthroplasty* 12.33, pp. 273–280.
- Meulen, Marjolein C H van der and Rik Huiskes (2002). “Why mechanobiology?” In: *Journal of Biomechanics* 35.44, pp. 401–414.
- Mjöberg, Bengt (1994). “Theories of wear and loosening in hip prostheses: Wear-induced loosening vs loosening-induced wear-a review”. In: *Acta Orthopaedica* 65.33, pp. 361–371.
- Moerman, Astrid et al. (2016). “Structural and mechanical characterisation of the periprosthetic tissue surrounding loosened hip prostheses. An explorative study.” In: *Journal of the Mechanical Behavior of Biomedical Materials* 62, pp. 456–467.
- Monti, Luisa, Luca Cristofolini, and Marco Viceconti (1999). “Methods for Quantitative Analysis of the Primary Stability in Uncemented Hip Prostheses”. In: *Artificial Organs* 23.99, pp. 851–859.
- Nadorf, J et al. (2014). “Fixation of the shorter cementless GTS<sup>TM</sup> stem: biomechanical comparison between a conventional and an innovative implant design.” In: *Archives of orthopaedic and trauma surgery* 134.55, pp. 719–726.
- Nahirnyak, Volodymyr M, Suk Wang Yoon, and Christy K Holland (2006). “Acousto-mechanical and thermal properties of clotted blood”. In: *Journal of the Acoustical Society of America* 119.66, pp. 3766–3772.
- Nam, Denis, Mathias P G Bostrom, and Anna Fahlgren (2013). “Emerging Ideas: Instability-induced Periprosthetic Osteolysis Is Not Dependent on the Fibrous Tissue Interface”. In: *Clinical Orthopaedics and Related Research* 471.66, pp. 1758–1762.
- National Joint Registry for England, Wales, Northern Ireland and the Isle of Man (2015). “13th Annual Report”. In:
- Noble, P C et al. (1988). “The Anatomic Basis of Femoral Component Design”. In: *Clinical Orthopaedics and Related Research* 235.235, pp. 148–165.
- Öhman, Caroline et al. (2008). “The effects of embalming using a 4 compressive mechanical properties of human cortical bone”. In: *Clinical Biomechanics* 23.1010, pp. 1294–1298.
- Ollivere, B et al. (2012). “Current concepts in osteolysis”. In: *The Journal of bone and joint surgery. British volume* 94 B.11, pp. 10–15.
- Ong, Kevin L et al. (2010). “Risk of Subsequent Revision after Primary and Revision Total Joint Arthroplasty”. In: *Clinical Orthopaedics and Related Research* 468.1111, pp. 3070–3076.
- Østbyhaug, Per Olav et al. (2010). “Primary stability of custom and anatomical uncemented femoral stems”. In: *Clinical Biomechanics* 25.44, pp. 318–324.

- Pabinger, C and A Geissler (2014). "Utilization rates of hip arthroplasty in OECD countries." In: *Osteoarthritis and cartilage* 22.66, pp. 734–741.
- Pancanti, Alberto, Marek Bernakiewicz, and Marco Viceconti (2003). "The primary stability of a cementless stem varies between subjects as much as between activities". In: *Journal of Biomechanics* 36.66, pp. 777–785.
- Pedersen, A B et al. (2014). "Association between fixation technique and revision risk in total hip arthroplasty patients younger than 55 years of age. Results from the Nordic Arthroplasty Register Association." In: *Osteoarthritis and cartilage / OARS, Osteoarthritis Research Society* 22.55, pp. 659–667.
- Pettersen, Sune H, Tina S Wik, and Bjørn Skallerud (2009). "Subject specific finite element analysis of implant stability for a cementless femoral stem". In: *Clinical Biomechanics* 24.66, pp. 480–487.
- Pilliar, R M, J M Lee, and C Maniopoulos (1986). "Observations on the Effect of Movement on Bone Ingrowth into Porous-Surfaced Implants". In: *Clinical Orthopaedics and Related Research* 208208, pp. 108–113.
- Ploeg, Bas van der et al. (2011). "Toward a more realistic prediction of peri-prosthetic micro-motions". In: *Journal of Orthopaedic Research* 30.77, pp. 1147–1154.
- Podichetty, Jagdeep T and Sundararajan V Madihally (2014). "Modeling of porous scaffold deformation induced by medium perfusion". In: *Journal of Biomedical Materials Research Part B-Applied Biomaterials* 102.44, pp. 737–748.
- Prendergast, Patrick J and Rik Huiskes (1996). "Finite element analysis of fibrous tissue morphogenesis - A study of the osteogenic index with a biphasic approach". In: *Mechanics of Composite Materials* 32.22, pp. 144–150.
- Prendergast, Patrick J, Rik Huiskes, and Kjeld Søballe (1997). "Biophysical stimuli on cells during tissue differentiation at implant interfaces". In: *Journal of Biomechanics* 30.66, pp. 539–548.
- Raghavendra, Sangeetha, Marjorie C Wood, and Thomas D Taylor (2005). "Early wound healing around endosseous implants: a review of the literature." In: *The International journal of oral and maxillofacial implants* 20.33, pp. 425–431.
- Reggiani, B et al. (2007). "Predicting the subject-specific primary stability of cementless implants during pre-operative planning: Preliminary validation of subject-specific finite-element models". In: *Journal of Biomechanics* 40.1111, pp. 2552–2558.
- Reggiani, Barbara et al. (2008). "Sensitivity of the Primary Stability of a Cementless Hip Stem to Its Position and Orientation". In: *Artificial Organs* 32.77, pp. 555–560.
- Reimeringer, M and N Nuño (2016). "The influence of contact ratio and its location on the primary stability of cementless total hip arthroplasty: A finite element analysis". In: *Journal of Biomechanics* 49.77, pp. 1064–1070.



- Roberts, Bryant C, Egon Perilli, and Karen J Reynolds (2014). "Application of the digital volume correlation technique for the measurement of displacement and strain fields in bone: A literature review". In: *Journal of Biomechanics* 47.55, pp. 923–934.
- Robertsson, O et al. (1997). "Intracapsular pressure and loosening of hip prostheses. Preoperative measurements in 18 hips." In: *Acta Orthopaedica Scandinavica* 68.33, pp. 231–234.
- Roy, N et al. (2002). "3M Capital hip arthroplasty - 3-8-year follow-up of 208 primary hip replacements". In: *Acta Orthopaedica Scandinavica* 73.44, pp. 400–402.
- Sebaa, N et al. (2006). "Ultrasonic characterization of human cancellous bone using the Biot theory: Inverse problem". In: *The Journal of the Acoustical Society of America* 120.44, pp. 1816–1824.
- Sharp, Lindsay A, Yong W Lee, and Aaron S Goldstein (2009). "Effect of low-frequency pulsatile flow on expression of osteoblastic genes by bone marrow stromal cells". In: *Annals of biomedical engineering* 37.33, pp. 445–453.
- Simmons, Craig A, Shaker A Meguid, and Robert M Pilliar (2001a). "Differences in osseointegration rate due to implant surface geometry can be explained by local tissue strains". In: 19.22, pp. 187–194.
- Simmons, Craig A, S A Meguid, and R M Pilliar (2001b). "Mechanical regulation of localized and appositional bone formation around bone-interfacing implants." In: *Journal of Biomedical Materials Research* 55.11, pp. 63–71.
- Smit, Theo H, Jacques M Huyghe, and Stephen C Cowin (2002). "Estimation of the poroelastic parameters of cortical bone." In: *Journal of Biomechanics* 35.66, pp. 829–835.
- Søballe, Kjeld et al. (1992). "Tissue ingrowth into titanium and hydroxyapatite-coated implants during stable and unstable mechanical conditions". In: *Journal of Orthopaedic Research* 10.22, pp. 285–299.
- Søballe, Kjeld et al. (2009). "Hydroxyapatite coating modifies implant membrane formation". In: *Acta Orthopaedica Scandinavica* 63.22, pp. 128–140.
- Stefan, Unger, Blauth Michael, and Schmoelz Werner (2010). "Effects of three different preservation methods on the mechanical properties of human and bovine cortical bone". In: *Bone* 47.66, pp. 1048–1053.
- Steward, Andrew J and Daniel J Kelly (2014). "Mechanical regulation of mesenchymal stem cell differentiation". In: *Journal of Anatomy* 227.66, pp. 717–731.
- Stolberg, Sarah and Kara E McCloskey (2009). "Can shear stress direct stem cell fate?" In: *Biotechnology Progress* 25.11, pp. 10–19.
- Su, E P and R L Barrack (2013). "Cementless femoral fixation: not all stems are created equally". In: *The Bone and Joint Journal* 95-B.1111, pp. 53–56.

- Sukjamsri, Chamaiporn et al. (2015). "Digital volume correlation and micro-CT: An in-vitro technique for measuring full-field interface micromotion around polyethylene implants". In: *Journal of Biomechanics* 48.1212, pp. 3447–3454.
- Sundfeldt, Mikael et al. (2002). "Effect of submicron polyethylene particles on an osseointegrated implant: an experimental study with a rabbit patello-femoral prosthesis." In: *Acta Orthopaedica Scandinavica* 73.44, pp. 416–424.
- Sundfeldt, Mikael et al. (2006). "Aseptic loosening, not only a question of wear: A review of different theories". In: *Acta Orthopaedica* 77.22, pp. 177–197.
- Swider, Pascal et al. (2011). "Sensitivity analysis of periprosthetic healing to cell migration, growth factor and post-operative gap using a mechanobiological model". In: *Computer Methods in Biomechanics and Biomedical Engineering* 14.99, pp. 763–771.
- Tarala, M et al. (2010). "Experimental versus computational analysis of micromotions at the implant–bone interface". In: *Proceedings of the Institution of Mechanical Engineers, Part H: Journal of Engineering in Medicine* 225.11, pp. 8–15.
- Taylor, Mark, Rebecca Bryan, and Francis Galloway (2013). "Accounting for patient variability in finite element analysis of the intact and implanted hip and knee: a review." In: *International Journal for Numerical Methods in Biomedical Engineering* 29.22, pp. 273–292.
- Taylor, Mark and Patrick J Prendergast (2015). "Four decades of finite element analysis of orthopaedic devices: Where are we now and what are the opportunities?" In: *Journal of Biomechanics* 48.55, pp. 767–778.
- Terheyden, Hendrik et al. (2011). "Osseointegration - communication of cells". In: *Clinical Oral Implants Research* 23.1010, pp. 1127–1135.
- Thomas, Kevin A et al. (1987). "The effect of surface macrotecture and hydroxylapatite coating on the mechanical strengths and histologic profiles of titanium implant materials". In: 21.1212, pp. 1395–1414.
- Thompson, M S et al. (2010). "In vitro models for bone mechanobiology: applications in bone regeneration and tissue engineering". In: *Proceedings of the Institution of Mechanical Engineers, Part H: Journal of Engineering in Medicine* 224, pp. 1533–1541.
- Uccelli, Antonio, Lorenzo Moretta, and Vito Pistoia (2008). "Mesenchymal stem cells in health and disease". In: *Nature Reviews Immunology* 8.99, pp. 726–736.
- Vanhegan, I S et al. (2012). "A financial analysis of revision hip arthroplasty". In: *The Journal of bone and joint surgery. British volume* 94-B.55, pp. 619–623.
- Viceconti, Marco et al. (2000). "Large-sliding contact elements accurately predict levels of bone–implant micromotion relevant to osseointegration". In: *Journal of Biomechanics* 33.1212, pp. 1611–1618.
- Viceconti, Marco et al. (2006). "Primary stability of an anatomical cementless hip stem: A statistical analysis". In: *Journal of Biomechanics* 39.77, pp. 1169–1179.

- Vidalain, Jean Pierre (2010). "Twenty-year results of the cementless Corail stem". In: *International Orthopaedics* 35.22, pp. 189–194.
- Vis, Harm M Van der et al. (1998a). "Fluid pressure causes bone resorption in a rabbit model of prosthetic loosening." In: *Clinical Orthopaedics and Related Research* 350350, pp. 201–208.
- Vis, Harm M Van der et al. (1998b). "Short periods of oscillating fluid pressure directed at a titanium-bone interface in rabbits lead to bone lysis". In: *Acta Orthopaedica Scandinavica* 69.11, pp. 5–10.
- Wagner, Diane R et al. (2008). "Hydrostatic pressure enhances chondrogenic differentiation of human bone marrow stromal cells in osteochondrogenic medium." In: *Annals of biomedical engineering* 36.55, pp. 813–820.
- Wang, S and J M Tarbell (2000). "Effect of Fluid Flow on Smooth Muscle Cells in a 3-Dimensional Collagen Gel Model". In: *Arteriosclerosis, Thrombosis, and Vascular Biology* 20.1010, pp. 2220–2225.
- Willert, Hans Georg, Manfred Semlitsch, and Leonard F Peltier (1996). "Tissue Reactions to Plastic and Metallic Wear Products of Joint Endoprostheses." In: *Clinical Orthopaedics and Related Research* 333, p. 4.
- Wolff, Julius (2010). "The classic: on the inner architecture of bones and its importance for bone growth. 1870." In: *Clinical orthopaedics and related research* 468.44, pp. 1056–1065.
- Wyatt, Michael et al. (2014). "Survival outcomes of cemented compared to uncemented stems in primary total hip replacement". In: *World Journal of Orthopedics* 5.55, p. 591.
- Yourek, Gregory et al. (2010). "Shear stress induces osteogenic differentiation of human mesenchymal stem cells". In: *Regenerative Medicine* 5.55, pp. 713–724.
- Zadpoor, Amir A and Harrie Weinans (2015). "Patient-specific bone modeling and analysis: The role of integration and automation in clinical adoption". In: *Journal of Biomechanics* 48.55, pp. 750–760.



# Curriculum Vitae



# Valérie Malfroy Camine

Research Engineer in Biomechanics, PhD

## PROFILE

---

A biomedical engineer completing a PhD degree in December 2016, with strong analytical thinking and creativity. I have experience in developing novel mechanical tests for orthopedic implants. Now seeking to contribute my experience, skills and expertise to a multi-disciplinary R&D team.

## PROFESSIONAL EXPERIENCE

---

2012 – 2016

### Research Engineer in Hip Biomechanics

Ecole Polytechnique Fédérale de Lausanne (EPFL), Switzerland

- PhD thesis in the Laboratory of Biomechanical Orthopedics (<http://lbo.epfl.ch/>). Developed and optimized **mechanical tests, finite element (FE) models, and biological assays** to characterize the bone-implant interface of femoral components in total hip replacement.
- **Published as a first author and co-authored 4 peer-reviewed scientific articles**, and gave >10 **oral presentations** at international conferences to a public of both engineers and surgeons.
- **Teaching** assistant for finite element modeling and biomechanics courses, and **supervised** 6 students during their master or semester projects.
- **Responsible** for **IT purchases** and for the operation of the **micro-CT scanner** of the lab (**training** of users, creation of **standard protocols and procedures**, regular **maintenance** of the equipment).
- Collaborated with a **multi-disciplinary team** composed of researchers, engineers, life scientists, and clinicians.
- Was **awarded** a 20kCHF research grant by the Swisslife Jubiläumsstiftung.

2011 – 2012

### Research Assistant in Shoulder Biomechanics

Ecole Polytechnique Fédérale de Lausanne (EPFL), Switzerland

- MSc thesis in Biomechanical Orthopedics.
- Implemented **optimization algorithms** in **FORTRAN** user subroutines in **Abaqus** for muscle force estimation in a **FE model** of the shoulder, resulting in significant time gain to run the model.
- Co-authored 2 publications in peer-reviewed journals.

2009 – 2012

### IT Helpdesk Technician

Ecole Polytechnique Fédérale de Lausanne (EPFL), Switzerland

- Provided 1st level **IT support** via phone/email to all IT users of EPFL and updated the **support documentation**.



## CONTACT DETAILS

---

Valérie MALFROY CAMINE

Avenue du Tir-Fédéral 12

1022 Chavannes-près-Renens

Switzerland

+41 77 459 31 68

[valeriemalfroycamine@gmail.com](mailto:valeriemalfroycamine@gmail.com)



<http://ch.linkedin.com/in/valeriemalfroycamine>

## SKILLS

---

### Technical

- Micro-CT imaging
- Image processing
- Finite element modeling
- Mechanical testing
- Computer assisted design
- Cell culture
- Immunocytochemistry
- Fluorescence microscopy
- qRT-PCR
- Mechanobiology
- Microfluidics
- Microfabrication basics (cleanroom, photolithography)

### Programming

- C++
- Fortran
- Tcl scripting

### Softwares

- Matlab
- Amira
- Image J
- Abaqus
- Comsol
- Solidworks
- Adobe Illustrator

- Developed strong **listening, communication** and **conflict management** skills.
- **Trained** new technicians and organized **work schedules** for a team of more than 30 people.

2008 – 2009

#### Quality Control Summer Intern

Merial (Sanofi), Lyon, France

- Edited **batch release certificates** for vaccines.
- Maintained **compliance** with all company and industry **policies and procedures**.

## EDUCATION

---

2012 – 2016

#### PhD in Mechanics

Ecole Polytechnique Fédérale de Lausanne (EPFL), Switzerland

2006 – 2012

#### MSc in Bioengineering, minor in Biomedical Technologies

Ecole Polytechnique Fédérale de Lausanne (EPFL), Switzerland

- *Summa cum laude*, distinction for GPA > 5.5/6.
- **Class representative** and **head of communication** of the life sciences student's association, and volunteer for several campus events (scientific conferences, science festivals, fundraising events).
- **Mentored** new students through the coaching association.

## ACADEMIC PROJECTS

---

2012 – 2016

#### PhD Thesis

My objective was to extend a technique based on micro-CT imaging to measure micromotion of metallic hip implants. I **developed and tested an experimental setup and an analysis software** to measure micromotion **with a similar accuracy and much higher coverage** than traditional methods. This could potentially lead to the validation of pre-clinical testing or pre-operative planning tools to **improve the lifetime of orthopedic implants**.

2011 – 2012

#### MSc Thesis

The goal of the project was to estimate muscle forces in a numerical model of the shoulder. **In a very short timeframe**, I successfully implemented in the FE software two algorithms based on EMG measurements and on mathematical **optimization techniques** to estimate muscle forces. The model was **then applied to a clinical situation** to study the effects of muscle deficiencies after shoulder replacement.

## LANGUAGES

---

**French:** Native, C2

**English:** Fluent, C1

**German:** Good, B2 (KMK Stufe II)

**Spanish:** Good, B2

## INTERESTS

---

Scientific illustration

Science outreach

Maker culture

Swing dancing

## PERSONAL DETAILS

---

**Birthdate:** 15 Jan 1989

**Nationality:** French

**Civil state:** Single, no children

# LIST OF PUBLICATIONS

## JOURNAL ARTICLES

- Malfroy Camine, V., Terrier, A. & Pioletti, D. (2016)** – Micromotion-induced peri-prosthetic fluid flow around a cementless femoral stem – *To be Submitted*.
- Malfroy Camine, V., Rüdiger, H. A., Pioletti, D. & Terrier, A. (2016)** – Effect of a collar on subsidence and local micromotion of cementless femoral stems – *Submitted to Clinical Orthopedics and Related Research*.
- Malfroy Camine, V., Rüdiger, H. A., Pioletti, D. & Terrier, A. (2016)** – Full-field measurement of micromotion around a cementless femoral stem using micro-CT imaging and radiopaque markers - *Journal of Biomechanics*.
- Nassajian Moghadam, M., Abdel-Sayed, P., Malfroy Camine, V. & Pioletti, D. (2014)** - Impact of synovial fluid flow on temperature regulation in knee cartilage - *Journal of Biomechanics*.
- Engelhardt, C., Malfroy Camine, V., Ingram, D., Mühlhaupt, P., Farron, A., Pioletti, D. & Terrier, A. (2014)** - Comparison of an EMG-based and a stress-based method to predict shoulder muscle forces - *Computer Methods in Biomechanics and Biomedical Engineering*.
- Terrier, A., Larrea, X., Malfroy Camine, V., Pioletti, D.P. & Farron, A. (2013)**. Importance of the subscapularis muscle after total shoulder arthroplasty. *Clinical Biomechanics*.

## CONFERENCE PROCEEDINGS

- Malfroy Camine, V., Rüdiger, H. A., Pioletti, D. & Terrier, A. (2015)** - Distribution of gap and micromotion during compressive loading around a cementless femoral stem - *Computer Methods in Biomechanics and Biomedical Engineering., Proceedings of the 40th Congress of the Société de Biomécanique, 28.10 – 30.10.2015, Paris, France - (Podium Talk)*
- Malfroy Camine, V., Pioletti, D. & Terrier, A. (2014)** - A model for micromotion-induced fluid flow at the bone-implant interface - *Computer Methods in Biomechanics and Biomedical Engineering., Proceedings of the 39th Congress of the Société de Biomécanique, 27.08 – 29.08.2014, Valenciennes, France - (Podium Talk)*

## CONFERENCE ABSTRACTS

- Malfroy Camine, V., Rüdiger, H., Pioletti, D. & Terrier, A.** - The effect of a collar on cementless femoral stems primary stability: an experimental cadaveric study – *22nd Congress of the European Society of Biomechanics, 10.07 – 13.07.2015, Lyon, France - (Podium Talk)*
- Malfroy Camine, V., Rüdiger, H., A., Pioletti, D. & Terrier, A.** - Micro-CT-based measurement of local micromotion around a straight cementless femoral stem during compressive and torsional loading – *62nd Annual Meeting of the Orthopedic Research Society, 5.03 – 8.03.2016, Orlando, USA - (Poster Presentation)*
- Malfroy Camine, V., Rüdiger, H., A., Pioletti, D. & Terrier, A.** - Micromotion-induced fluid flow at the bone-implant interface around a straight cementless femoral stem – *62nd Annual Meeting of the Orthopedic Research Society, 5.03 – 8.03.2016, Orlando, USA - (Poster Presentation)*
- Malfroy Camine, V., Rüdiger, H., Pioletti, D. & Terrier, A.** - Micro-CT based measurement of micromotion around femoral stems in compression and torsion - *13th International Symposium Computer Methods in Biomechanics and Biomedical Engineering., 1.09 – 5.09.2015, Montreal, Canada - (Podium Talk)*
- Malfroy Camine, V., Rüdiger, H., Pioletti, D. & Terrier, A.** - Complete distribution of micromotion measured around a cementless femoral stem – *21st Congress of the European Society of Biomechanics, 5.07 – 8.07.2015, Prague, Czech Republic - (Podium Talk)*
- Malfroy Camine, V., Rüdiger, H., Pioletti, D. & Terrier, A.** - In vitro measurement of micromotion around an uncemented fully coated femoral stem – *75th Congress of the Swiss Society of Orthopedics and Traumatology, 24.06 – 26.06.2015, Basel, Switzerland - (Podium Talk)*
- Malfroy Camine, V., Rüdiger, H., A., Pioletti, D. & Terrier, A.** - Evaluating the initial stability of cementless femoral stems: an *in vitro* method to obtain the distribution of interfacial micromotion and gap around the whole stem during loading – *61st Annual Meeting of the Orthopedic Research Society, 28.03 – 31.03.2015, Las Vegas, USA - (Poster Presentation)*
- Malfroy Camine, V., Rüdiger, H., Pioletti, D. & Terrier, A.** - Micromotion-induced fluid flow within the granulation tissue surrounding the femoral stem after total hip arthroplasty - *12th International Symposium Computer Methods in Biomechanics and Biomedical Engineering., 13.10 – 15.10.2014, Amsterdam, The Netherlands - (Podium Talk)*
- Malfroy Camine, V., Parvex, V., Rüdiger, H., A., Pioletti, D. & Terrier, A.** - Bone-implant gap and micromotion around cementless femoral stems: *in vitro* measurement during compression and torsion - *60th Annual Meeting of the Orthopedic Research Society, 15.03 – 18.03.2014, New Orleans, USA - (Poster Presentation)*
- Malfroy Camine, V., Rüdiger, H., Bauduin, P., Pioletti, D. & Terrier, A.** - Multisite measure of micromotion around a cementless femoral stem in compression and torsion - *V International Conference on Computational Bioengineering, 11.09 – 13.09.2013, Leuven, Belgium - (Podium Talk)*
- Engelhardt, C., Malfroy Camine, V., Ingram, D., Mühlhaupt, P., Farron, A., Pioletti, D. & Terrier, A.** - Comparison of muscle force estimation methods to predict humeral head translation after total shoulder arthroplasty - *V International Conference on Computational Bioengineering, 11.09 – 13.09.2013, Leuven, Belgium - (Poster Presentation)*
- Malfroy Camine, V., Rüdiger, H., Bauduin, P., Pioletti, D. & Terrier, A.** - Local micromotion around a cementless hip stem measured in compression and torsion - *19th Congress of the European Society of Biomechanics, 25.06 – 28.08.2013, Patras, Greece - (Podium Talk)*
- Engelhardt, C., Malfroy Camine, V., Ingram, D., Mühlhaupt, P., Farron, A., Pioletti, D. & Terrier, A.** - Comparison of two methods to predict forces in deficient rotator cuff muscles after total shoulder arthroplasty - *19th Congress of the European Society of Biomechanics, 25.06 – 28.08.2013, Patras, Greece - (Podium Talk)*



**Malfroy Camine, V., Rüdiger, H., Bauduin, P., Pioletti, D. & Terrier, A.** - Micromotion, subsidence and gap at the stem-femur interface after THA: a cadaveric study - *73rd Congress of the Swiss Society of Orthopedics and Traumatology, 26.06 - 28-06.2013, Lausanne, Switzerland* - (Podium Talk)